mtwardowski@fau.edu
http://www.fau.edu/hboi/ocean_optics

Light Scattering in Water

Mike Twardowski

Harbor Branch Oceanographic Institute

Ft. Pierce, FL

Background

BS	Major: Biology; Minor: Physics, Music – Trinity University, TX	1992
PhD	Oceanography – University of Rhode Island (Percy Donaghay)	1998
Postdoc	Environmental Optics Fellowship – Oregon State University (Ron Zaneveld)	1998-1999

CURRENT POSITIONS

Professor, *Harbor Branch Oceanographic Institute, FAU*	2015-present
Affiliate Professor, *Ocean Engineering, FAU*	2017-present
Associate Director, *NOAA Cooperative Institute, HBOI*	2018-present
President, *Sunstone Scientific LLC*	2017-present
President, *Environmental Optics Consulting LLC*	2016-present
Program Lead, Maritime Sensing, *I-SENSE, FAU*	2016-present
Senior Engineer, *SEACORP Inc.*	2015-present

FORMER POSITION

Director of Research and Vice President, *WET Labs, Inc.*	2005-2015

- Ocean optics research, basic science
- Sensor development in ocean optics
- NASA PACE Science Team

“Lex Groovius”

Radiative Transfer in the Ocean

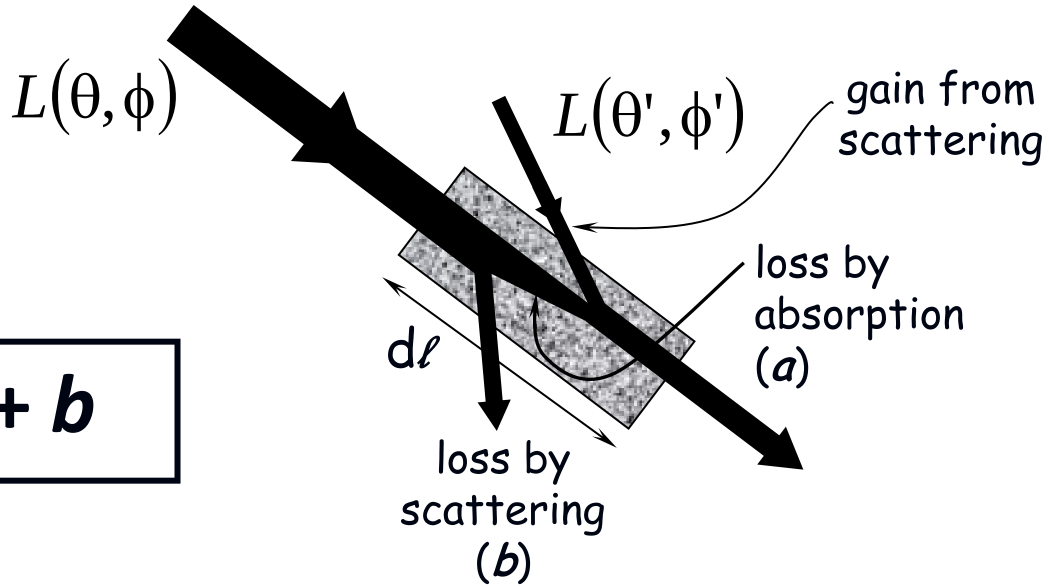

$$\boxed{c \equiv a + b}$$

<u>Inherent Optical Properties (IOPs)</u>
Depend only on substances in water
[Attenuation (c), Absorption (a), Scattering, (b), and related subfractions]

<u>Apparent Optical Properties (AOPs)</u>
Depend on substances in water AND *ambient light field*
[Reflectance (R), Diffuse attenuation (K), and related parameters]

Volume Scattering Function (VSF) defined

$$\beta(\theta) = \frac{dI(\theta)}{EdV} = \frac{W \cdot sr^{-1}}{W \cdot m^{-2} \cdot m^{3}} = m^{-1} \cdot sr^{-1}$$

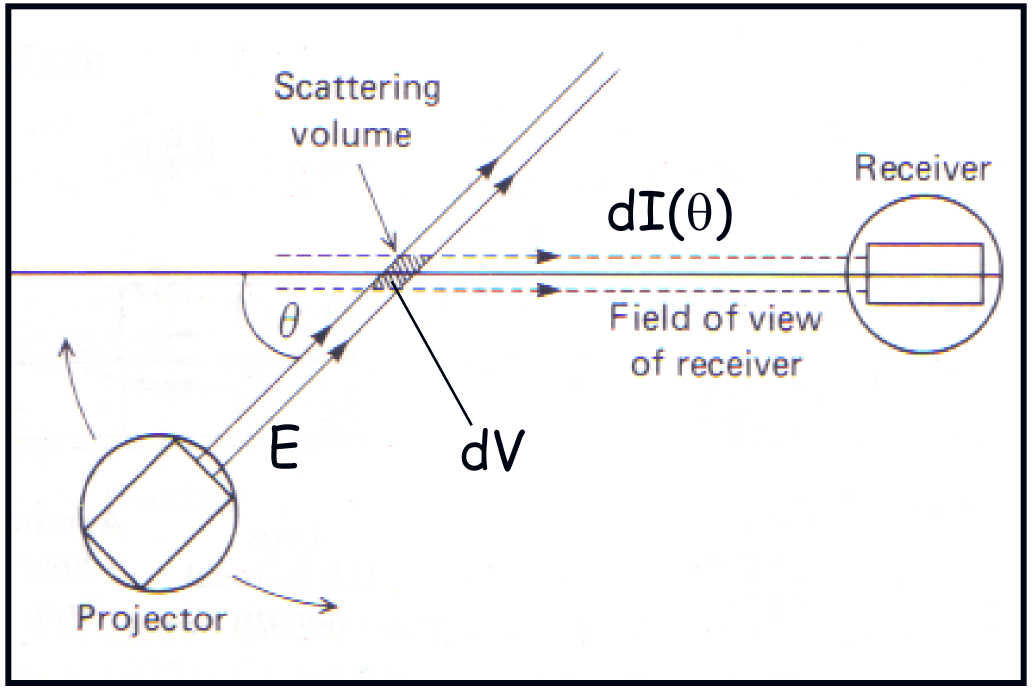

dI(θ) radiant flux in direction dθ ($W\ sr^{-1}$)

dV elemental volume (m^3)

E incident irradiance ($W\ m^{-2}$)

Typical VSF

*Log Scale ~10^7 Dynamic range

*Very steeply forward peaked

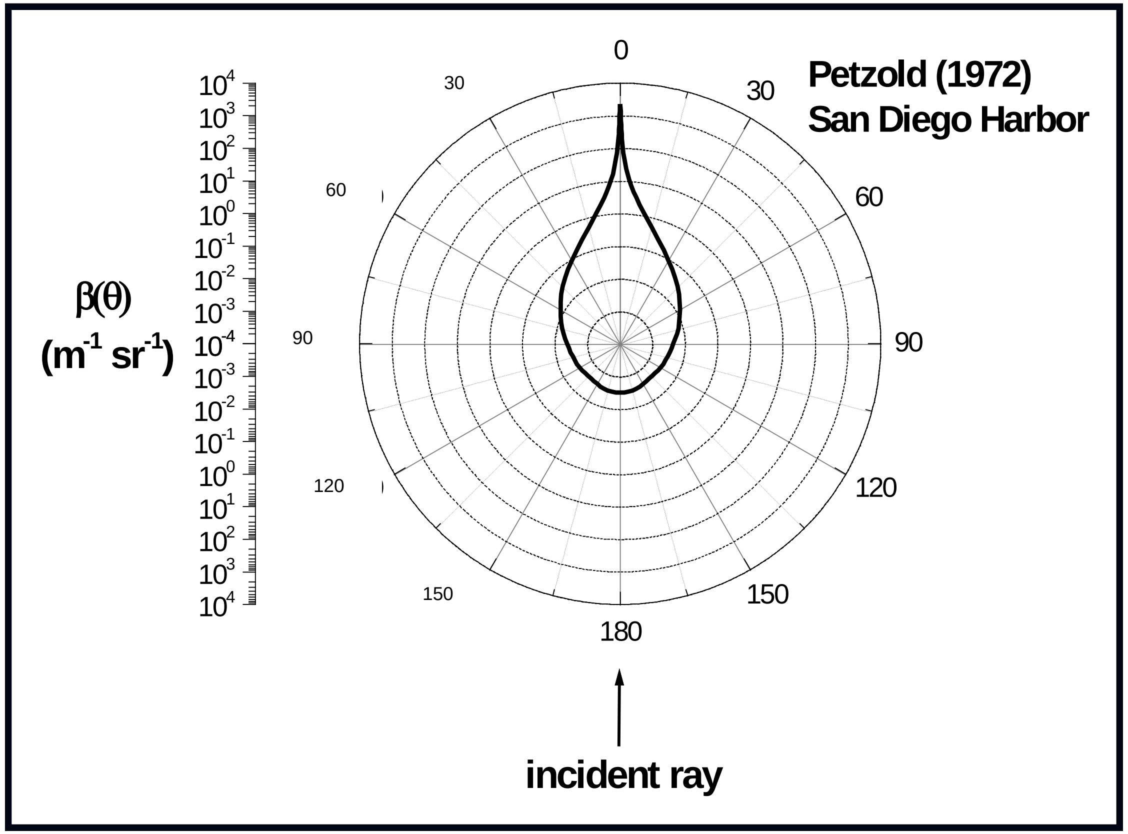

Scripps Pier, 2008

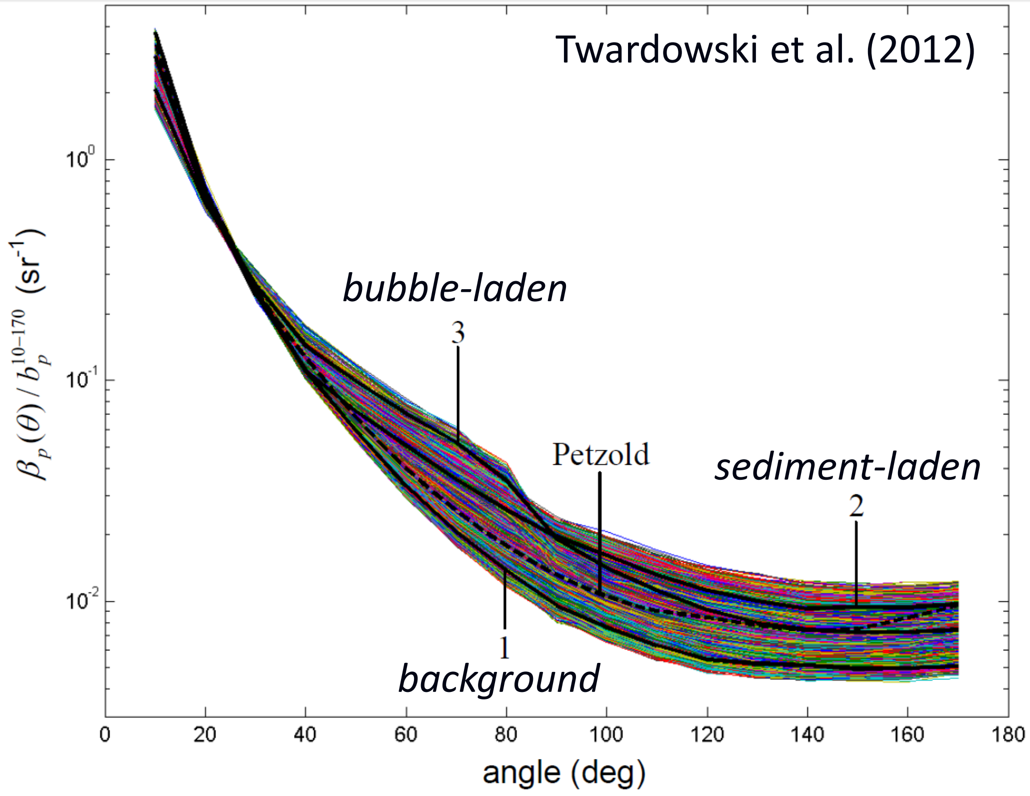

Typically, only ~0.3-3% of scattering (b) is backscattering (b_b)
(however, in clear waters, b_w can increase this %)

VSF integration to obtain *b*

Remember…

$$b = 2\pi \int_0^{\pi} \sin(\theta)\beta(\theta)d\theta$$

Assuming azimuthal symmetry

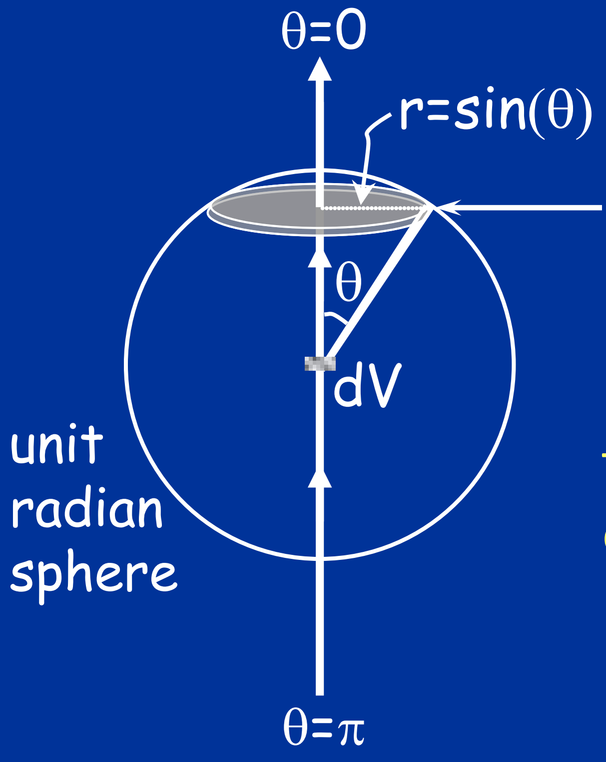

perimeter = $2\pi r$

solid angle, $d\omega = 2\pi r\, d\theta = \underline{2\pi \sin(\theta) d\theta}$ (sr)

The $2\pi\sin(\theta)$ effectively "weights" contribution of β to b

The contribution of β to b is zero at $\theta=0$ and $\theta=\pi$, even though β is nonzero

Scattering components

Can partition with respect to constituent components…, e.g.:

$$b_t(\lambda) = b_w(\lambda) + b_p(\lambda)$$ Units m^{-1}

Also with respect to angular distribution:

$$b_x = 2\pi \int_i^j \sin(\theta)\beta(\theta)d\theta$$

<u>Total scattering</u>
set $x = t$
$[i, j] = [0, \pi]$

<u>Forward scattering</u>
set $x = f$
$[i, j] = [0, \pi/2]$

<u>Backscattering</u>
set $x = b$
$[i, j] = [\pi/2, \pi]$

Other scattering properties

Phase function:

$$\tilde{\beta}(\theta) = \frac{\beta(\theta)}{b}$$ Units (sr^{-1})

Asymmetry parameter (mean cosine):

$$g = \langle \cos(\theta) \rangle = 2\pi \int_0^{\pi} \tilde{\beta}(\theta)\cos(\theta)\sin(\theta)d\theta$$

If symmetric around 90°, g = 0

If highly skewed g → 1

VSF Measurement Considerations

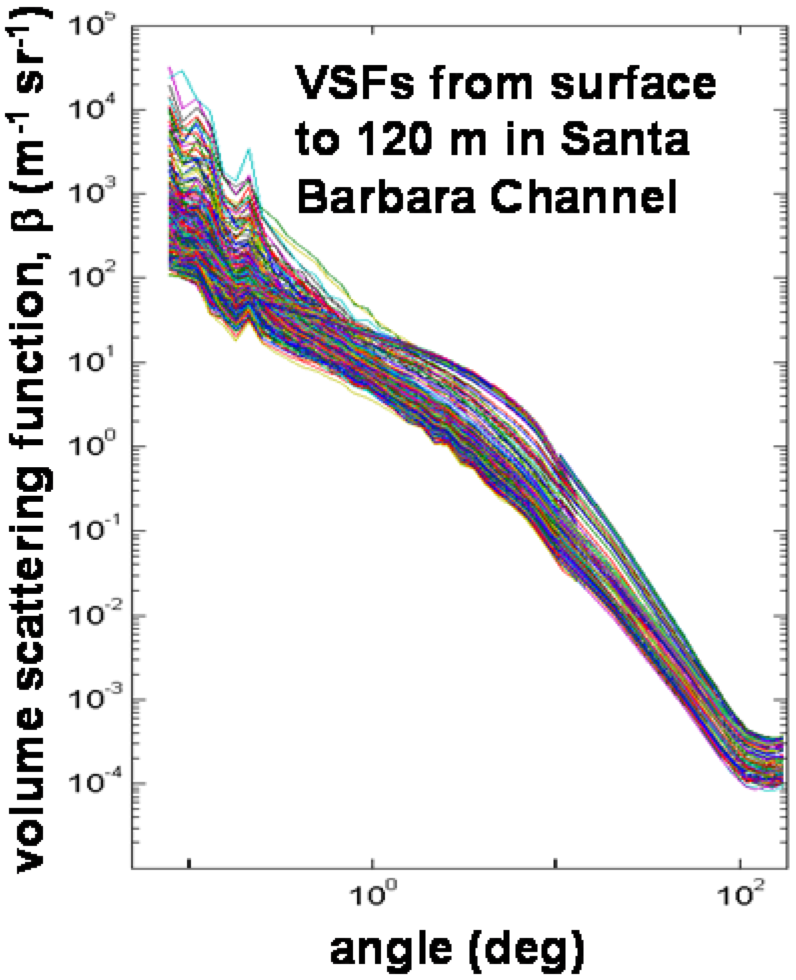

- 6+ orders of magnitude variation in intensity from the near-forward to backward in single VSF
- several orders of magnitude natural dynamic range in intensity at any single angle
- rapid temporal variability in particle fields in surface waters
- rejecting ambient light is challenging at surface, particularly for low scattering signals in the backward
- calibration without absolute "standard"

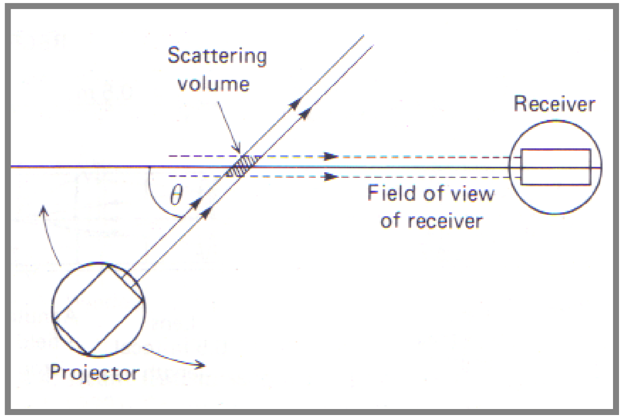

Measuring the VSF: MASCOT (HBOI)

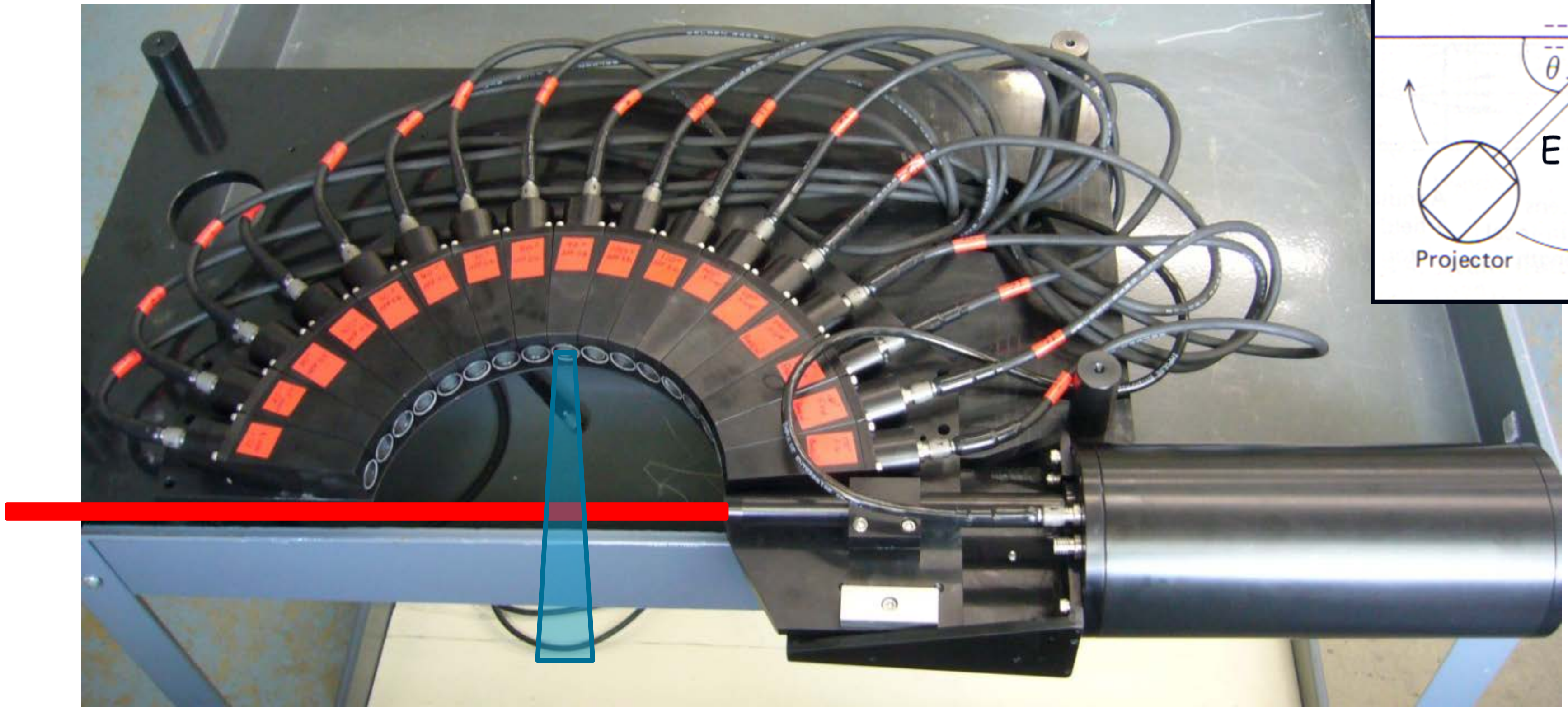

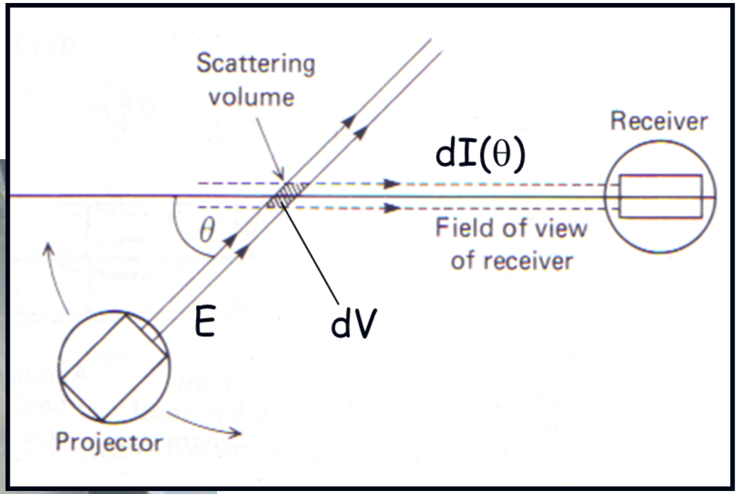

- Measures VSF from 10°(10°)170°
- 0.8-5° detector FOVs
- 20 Hz sampling rate
- Wedge depolarizer on source

LISST-100X (Sequoia)

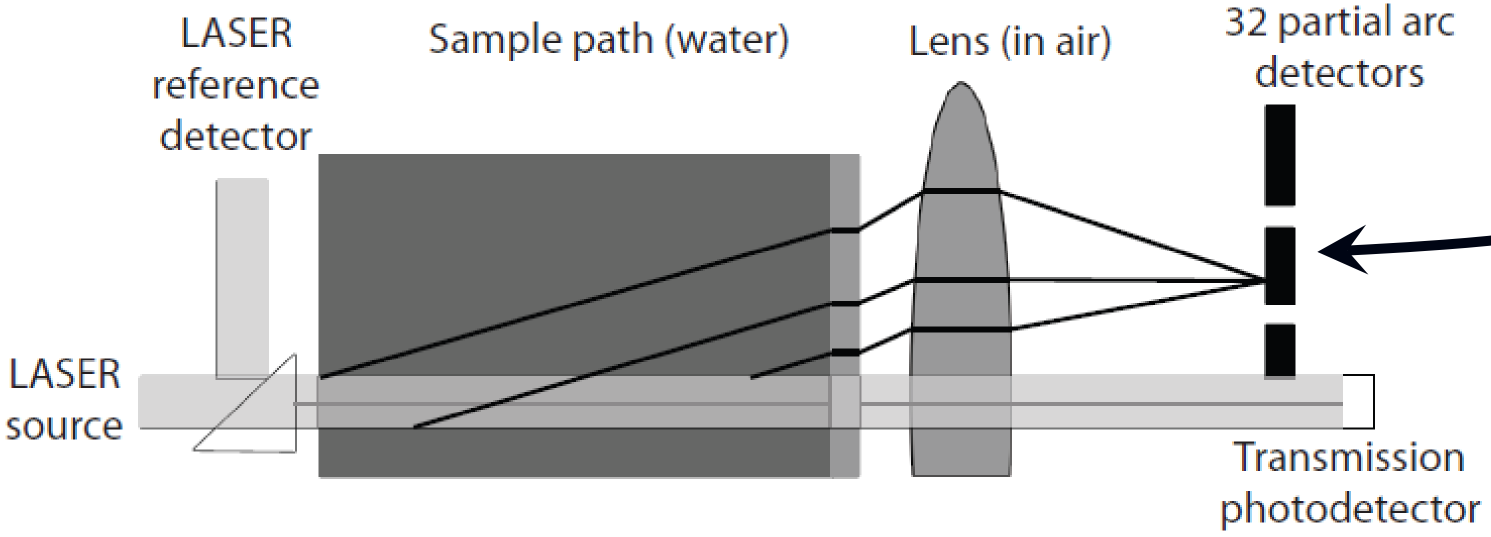

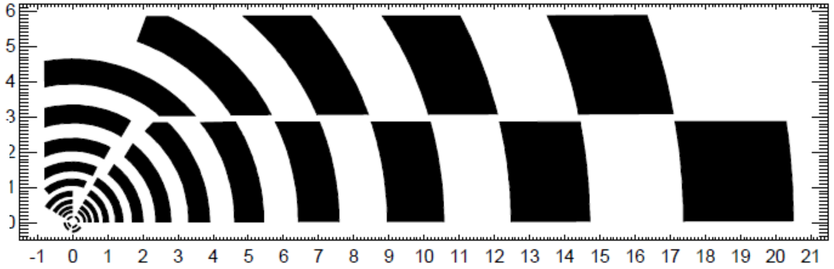

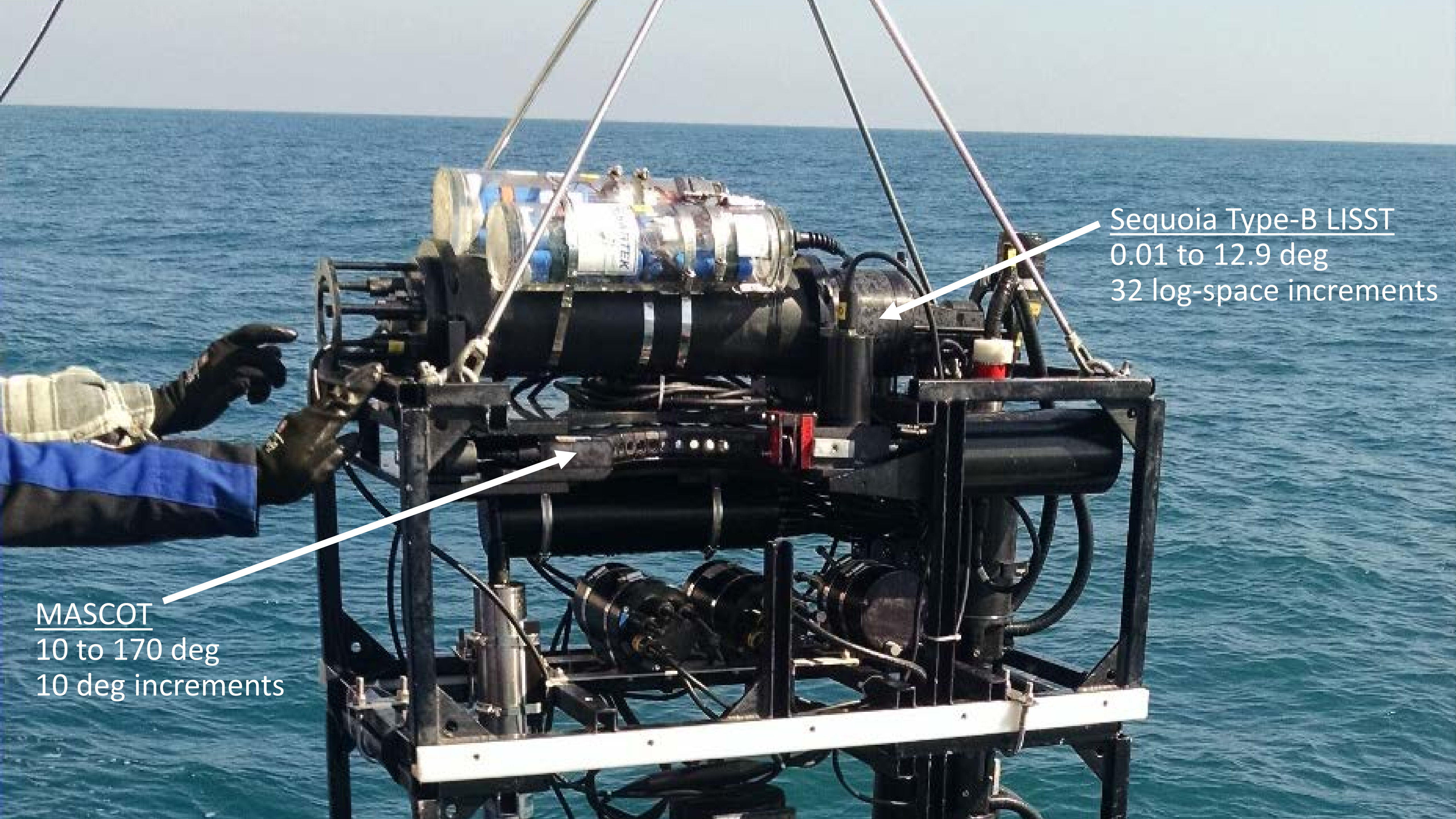
Sequoia Type-B LISST
0.01 to 12.9 deg
32 log-space increments
MASCOT
10 to 170 deg
10 deg increments

VSF profile data

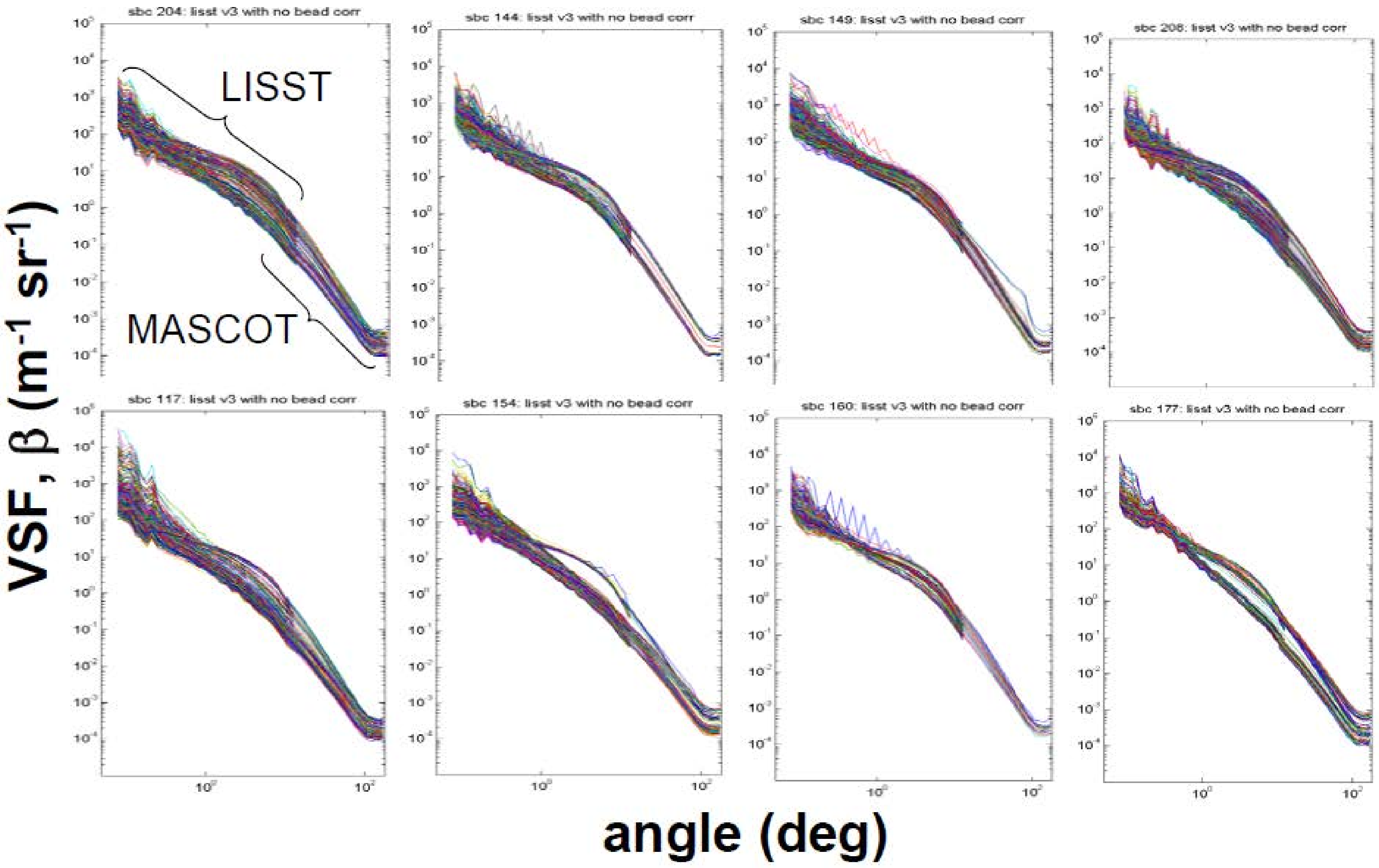

Integrating the VSF: test closure

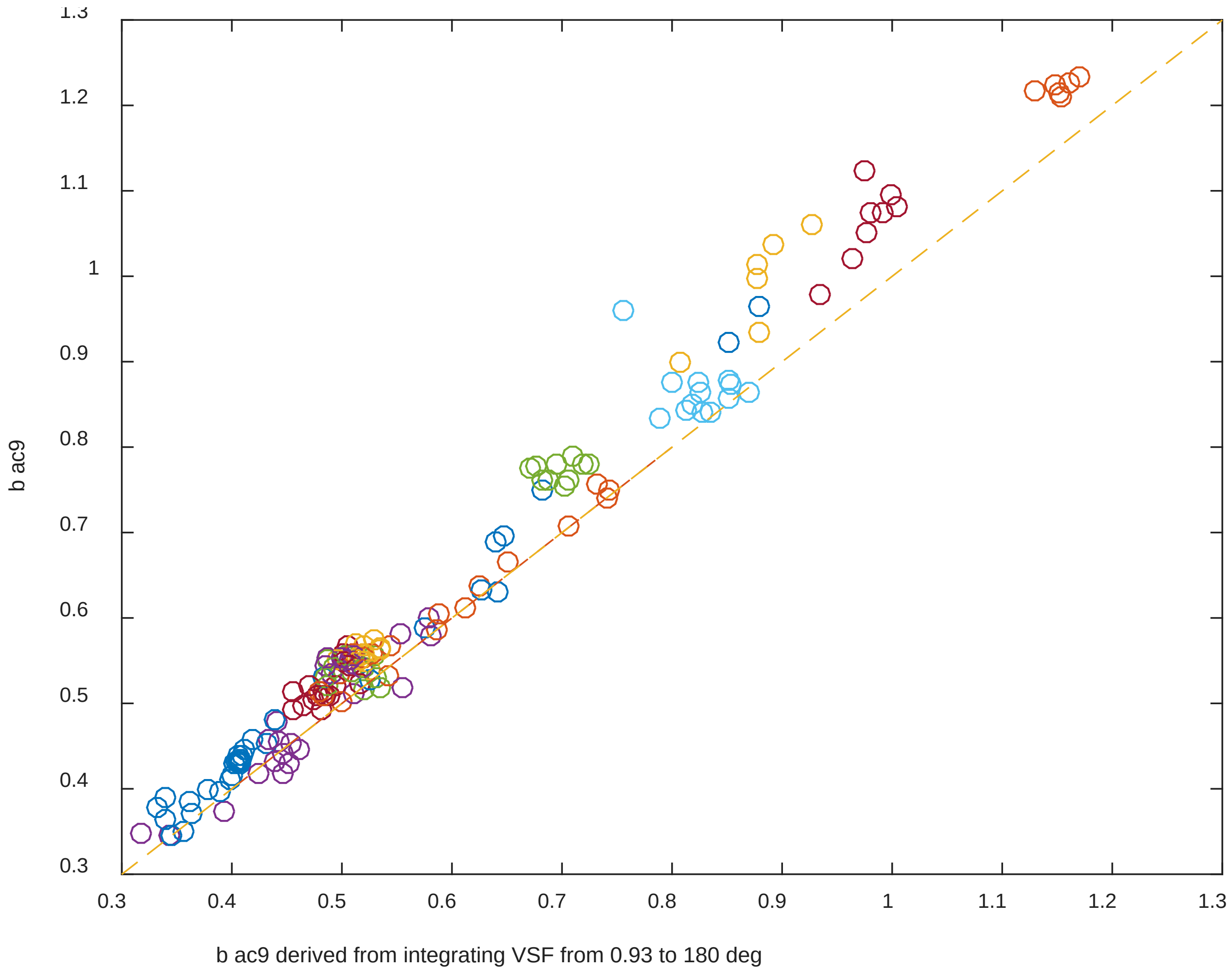

$$b_x = 2\pi \int_i^j \sin(\theta)\beta(\theta)d\theta$$

Cumulative scattering contribution

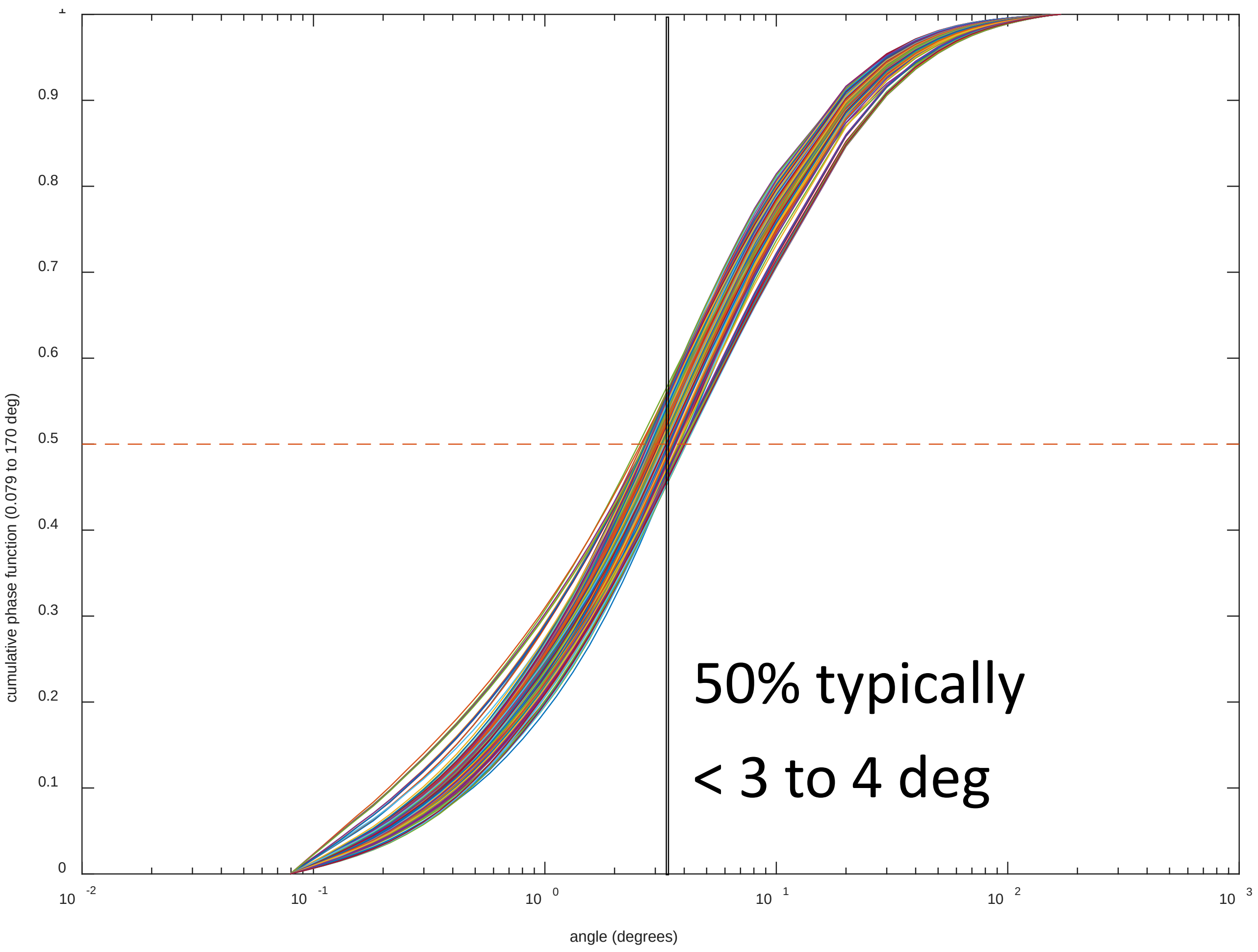

$$\frac{b_x = 2\pi \int_i^j \sin(\theta)\beta(\theta)\,d\theta}{b}$$

Analytical modeling: Beardsley-Zaneveld (1969)

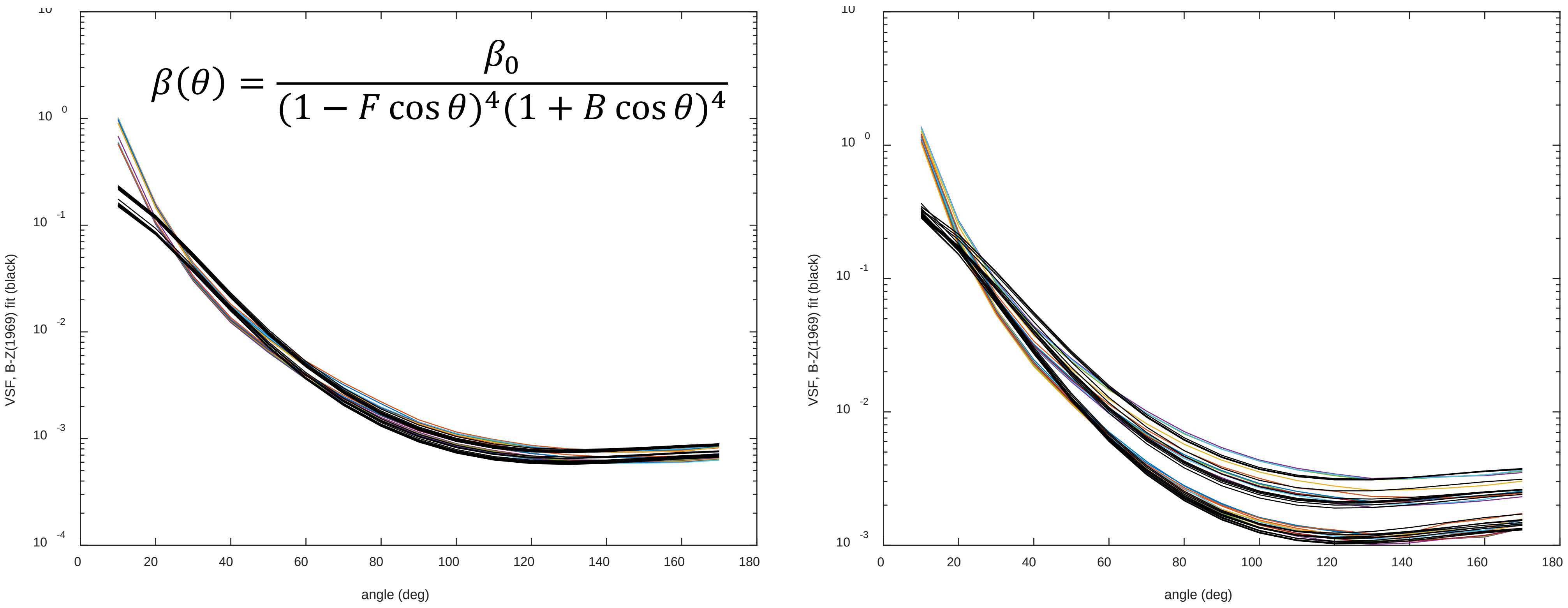

Excellent fitting algorithm in backward

(as noted by Balch et al. and others)

Analytical modeling: fitted Kattawar-Haltrin 2-term, 1-parameter Henyey-Greenstein

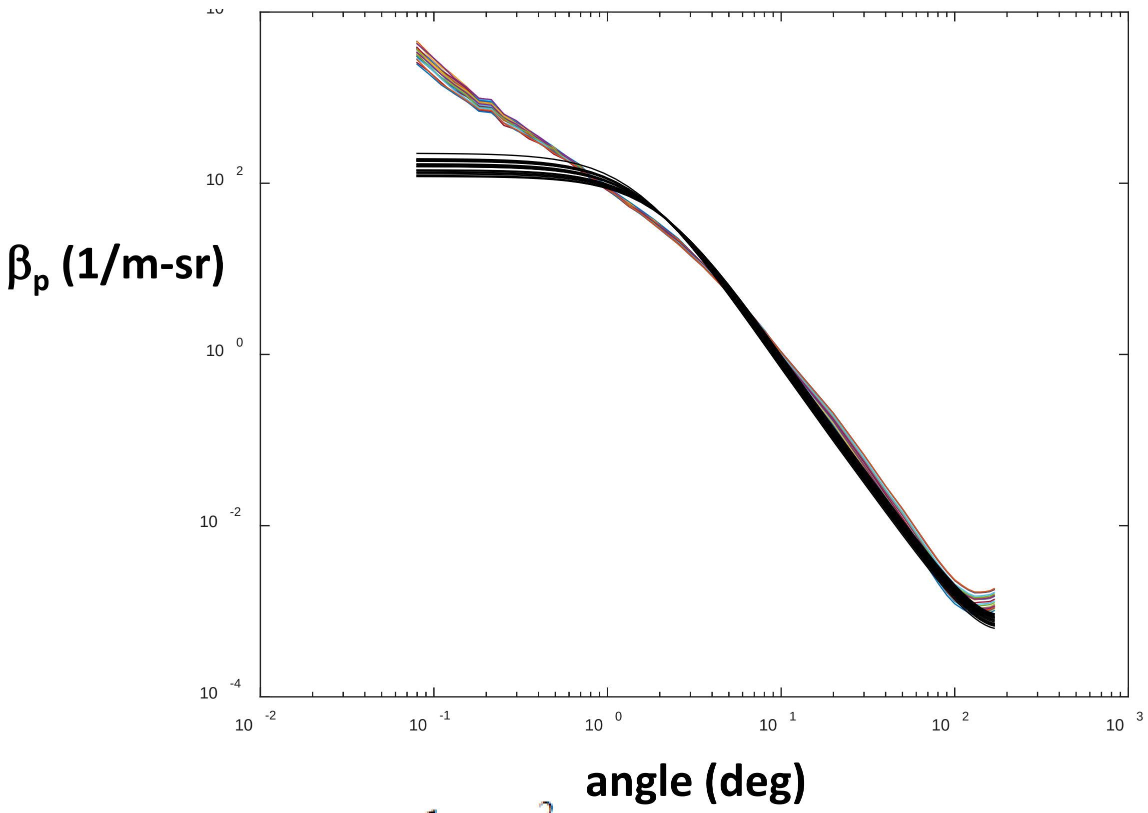

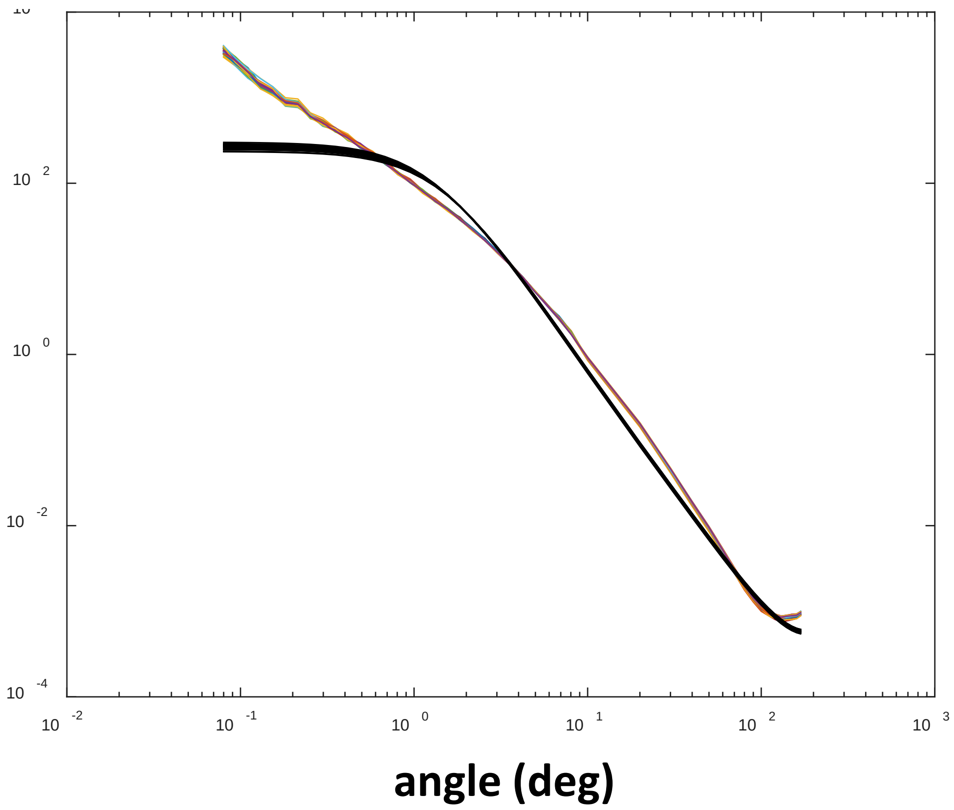

$$p_{HG}(\mu, g) = \frac{1-g^2}{\left(1-2g\mu+g^2\right)^{3/2}}, \quad \mu = \cos\vartheta,$$

$$p_{TTHG}(\mu, \alpha, g, h) = \alpha\, p_{HG}(\mu, g) + (1-\alpha)\, p_{HG}(\mu, -h)$$

$$0 \le \alpha, g, h \le 1.$$

h(g) and α(g)

Analytical modeling: fitted Kopelevich

Fit 2 basis vectors recommended by Kopelevich (1983)

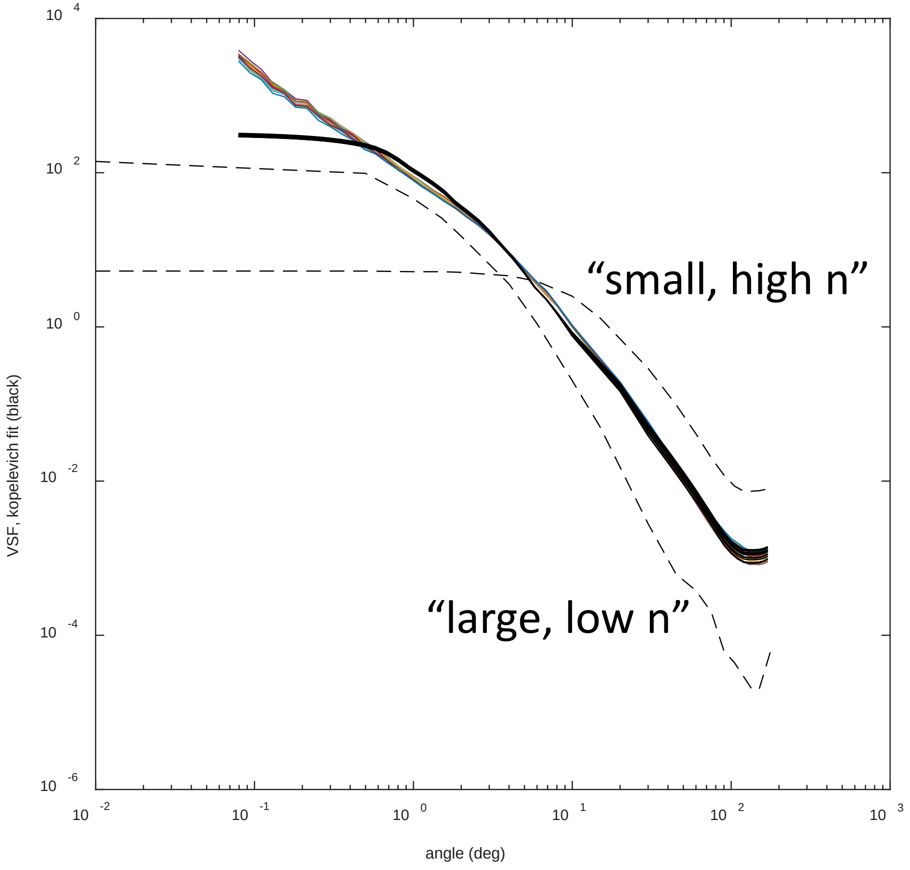

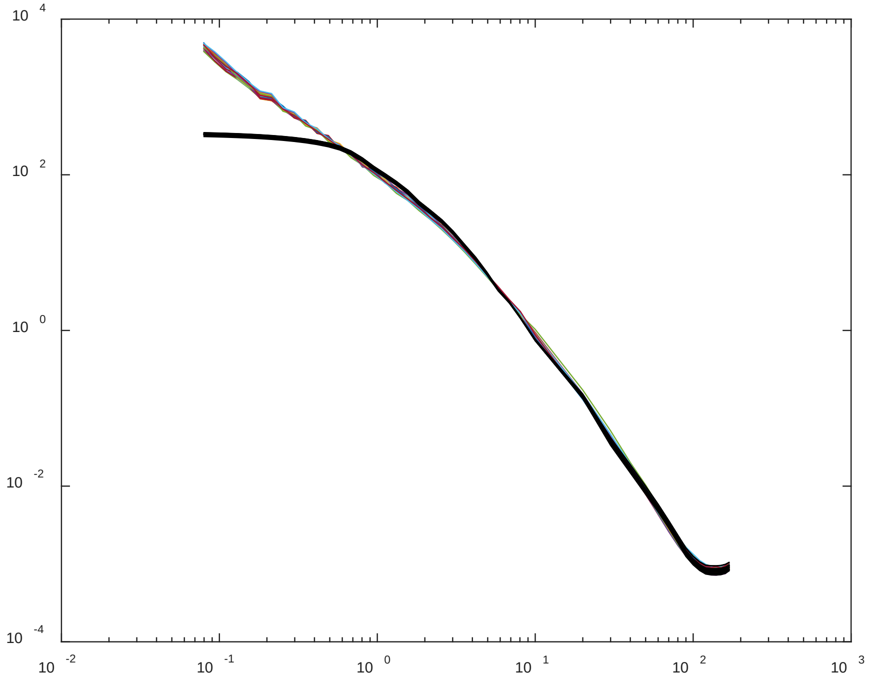

Very good results > ~0.6 deg

(as noted by Berthon et al. 2007)

Analytical modeling: fitted Kopelevich

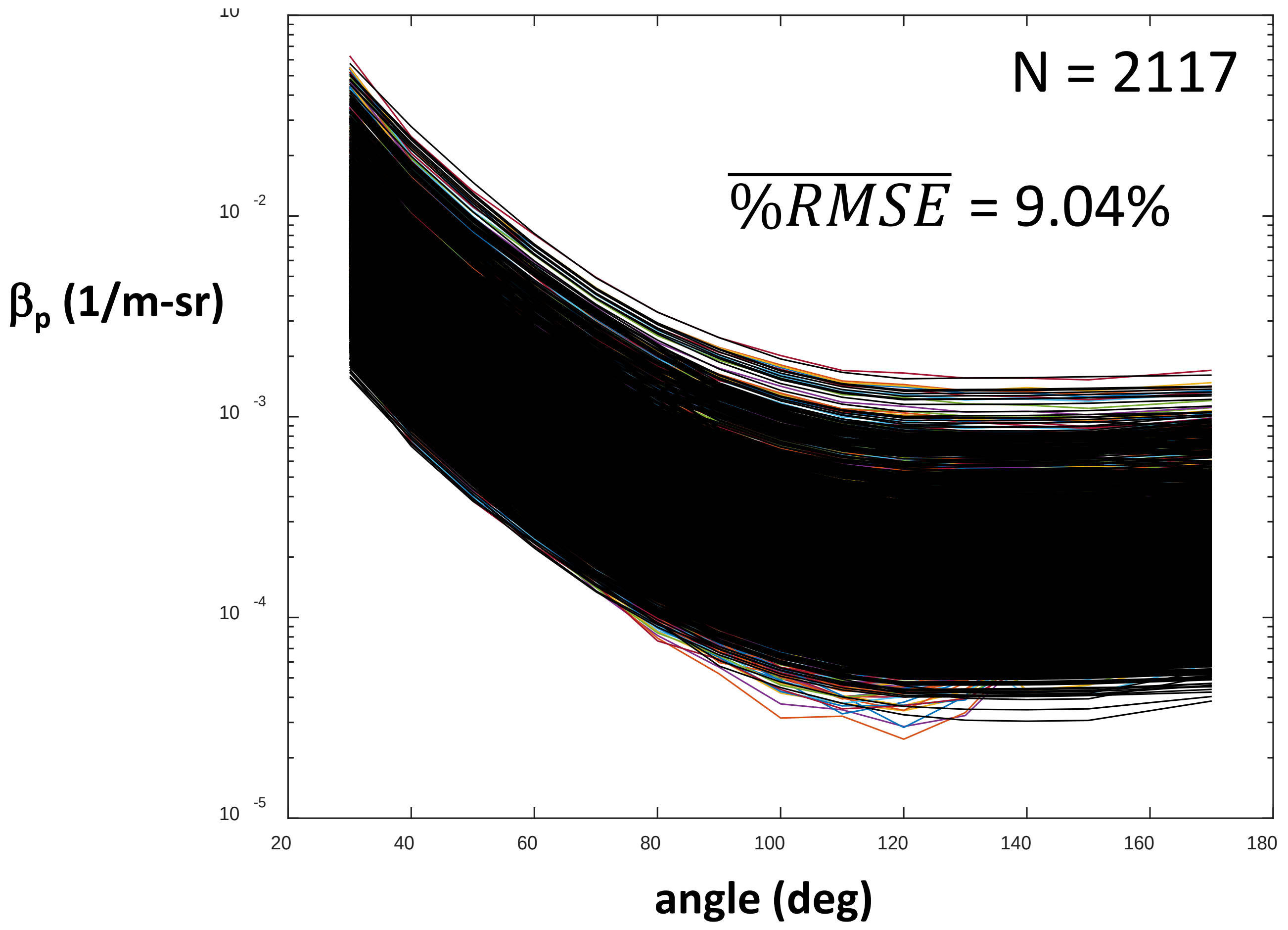

SABOR

NW Atlantic 08/2014

>10 deg only

Analytical modeling: fitted Fournier-Forand (1994, 1999)

see Jonasz and Fournier (2007, with erratum)

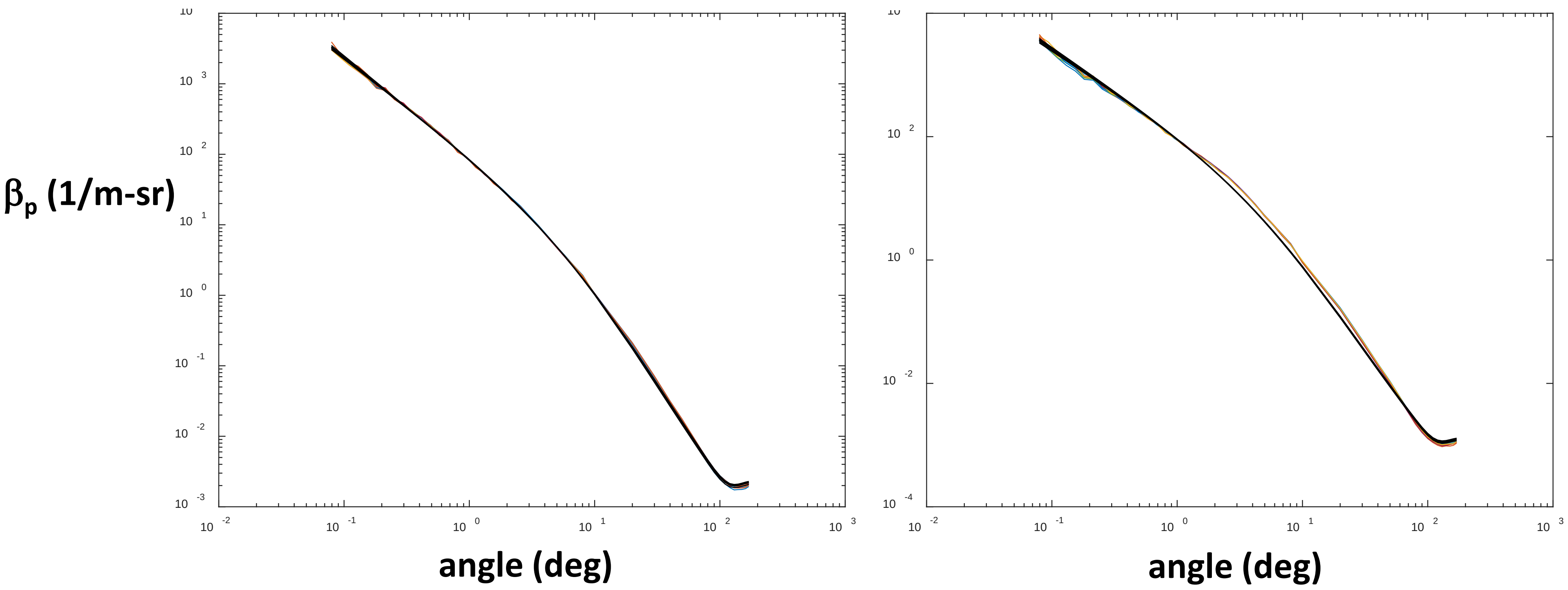

Excellent fits for entire angular range (0.079 to 180 deg)

Cluster analysis

After

Moore et al. (2009, 2014, 2015)

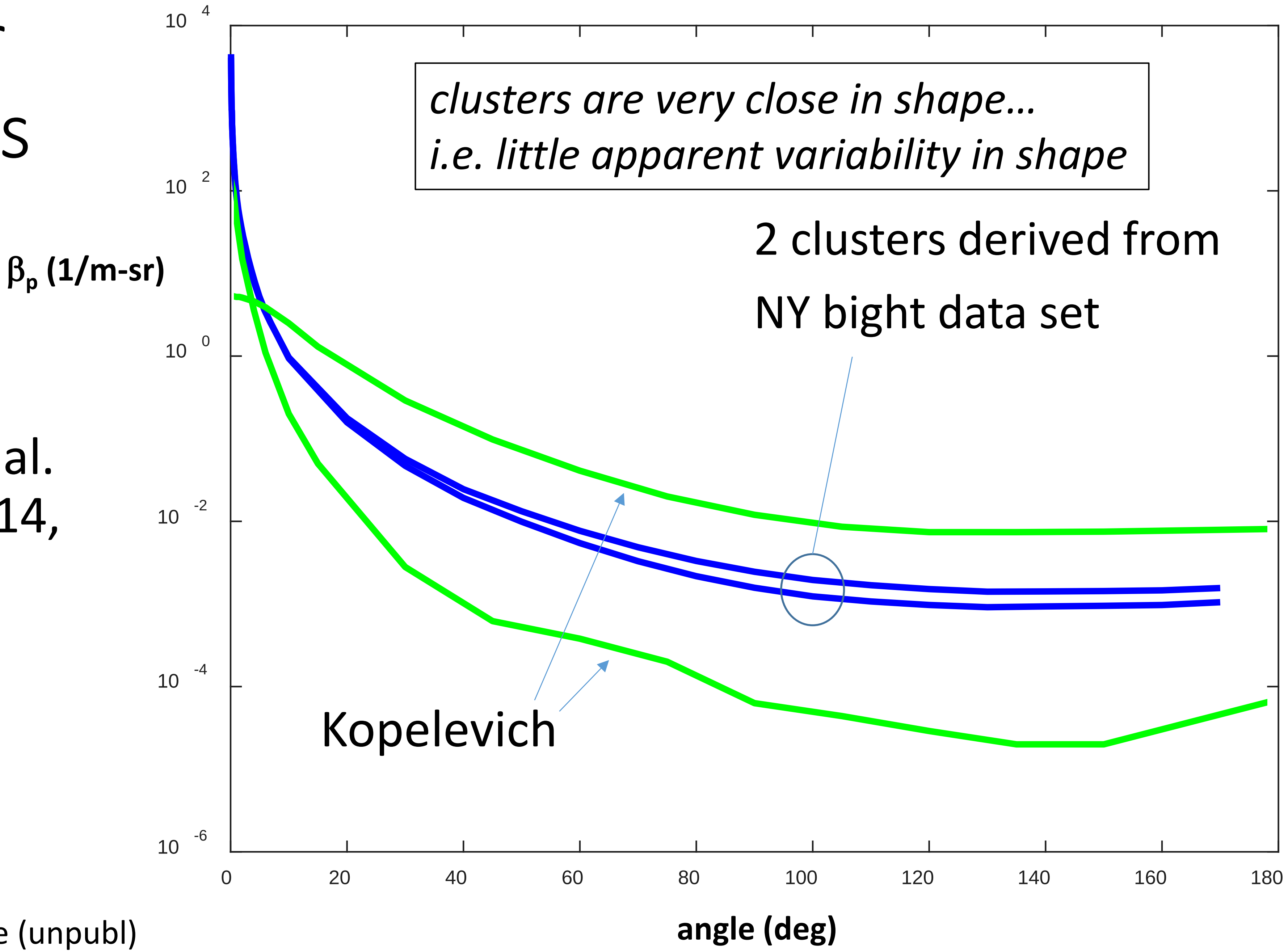

Twardowski and Moore (unpubl)

Fitting 2 clusters from NY Bight 11/2007

NY Bight 07/2008

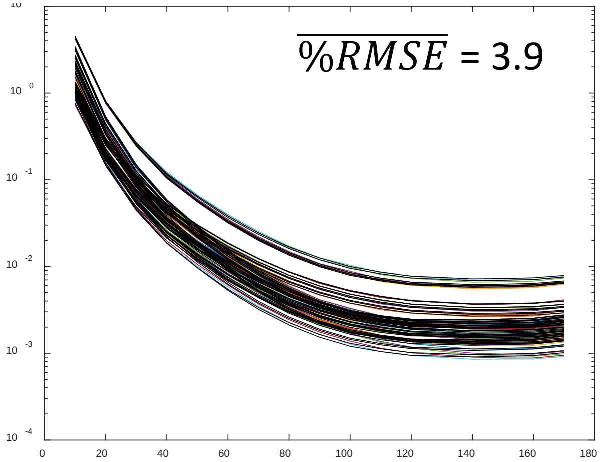

San Diego 01/2008

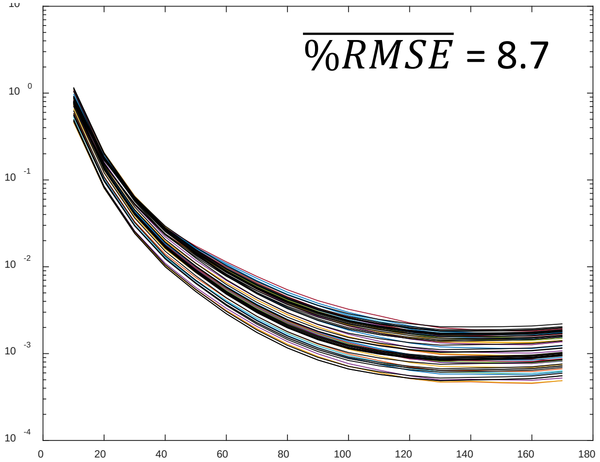

Lake Erie 08/2014

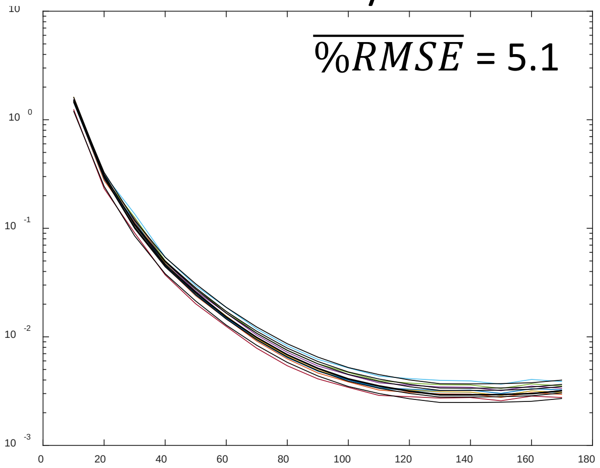

NW Atlantic 08/2014

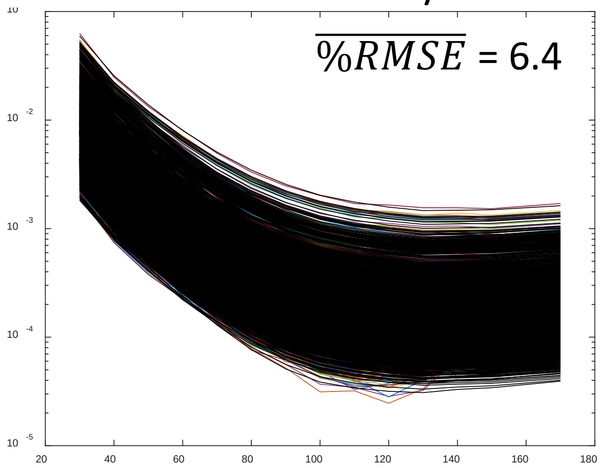

Ligurian Sea 10/2008

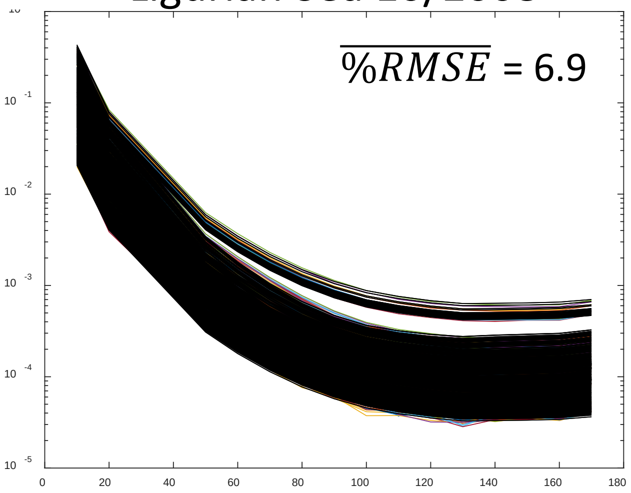

NY Bight 11/2007

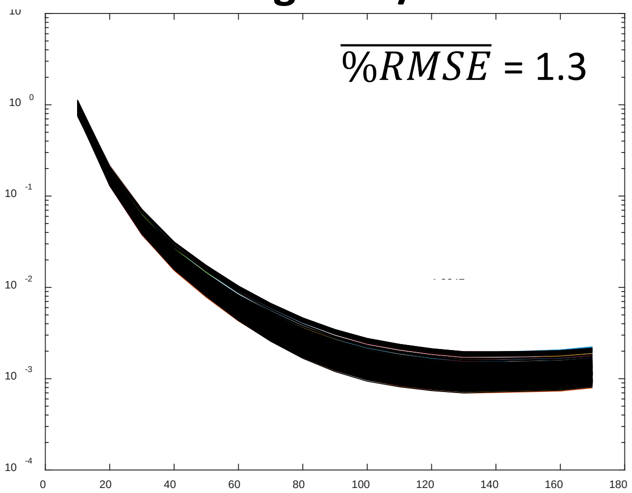

Hawaii 09/2009

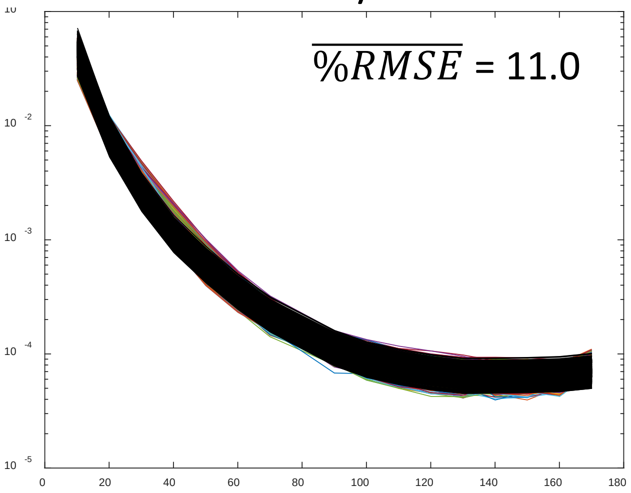

>10 deg only

Backward phase function (i.e., VSF shape)

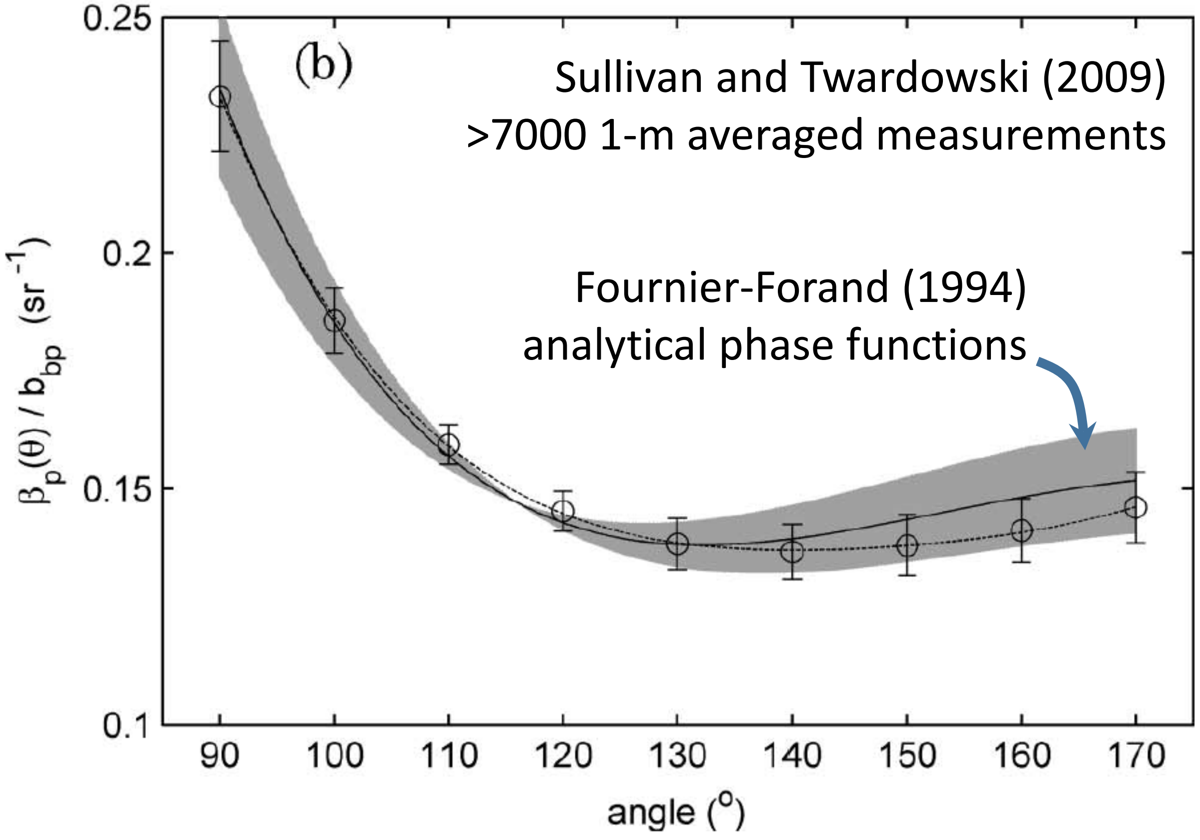

<u>*Remarkably consistent shape…*</u>

Important implications for ocean color remote sensing

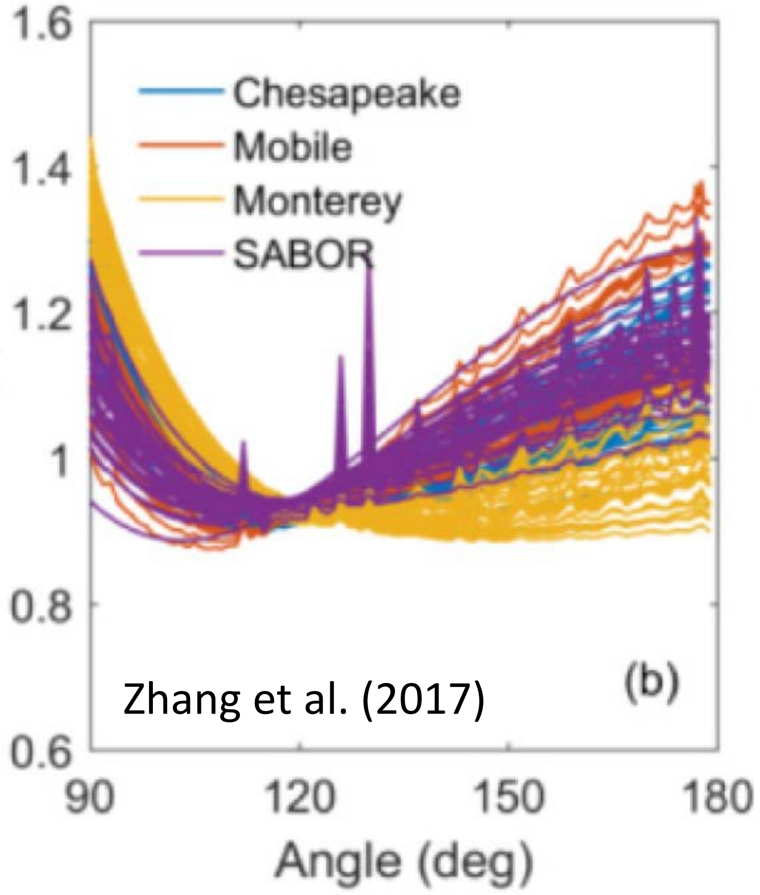

However, some inconsistency in current literature…

Constant backward VSF shape appears realistic…

Tonizzo et al. (2017) val data set

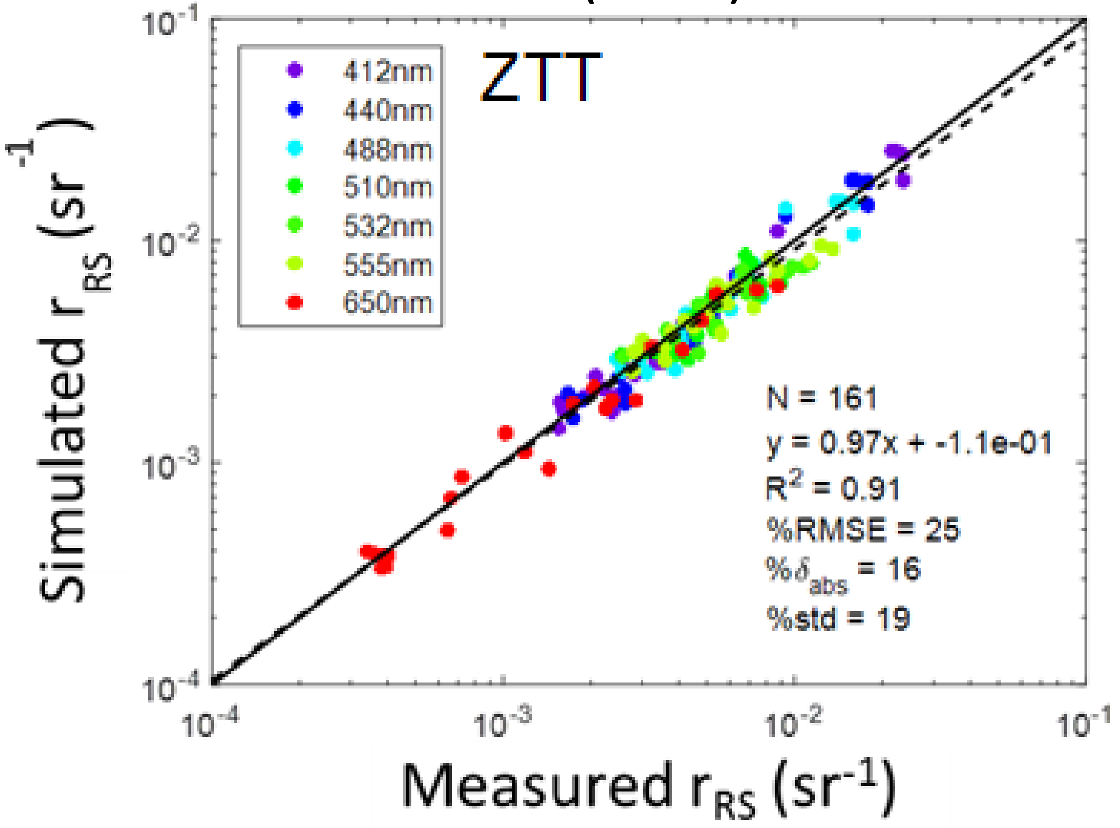

Radiative transfer simulations assuming constant backward VSF shape

Results are equivalent to simulations using measured VSFs

Twardowski and Tonizzo (in review)

Measuring the VSF: WET Labs ECOs

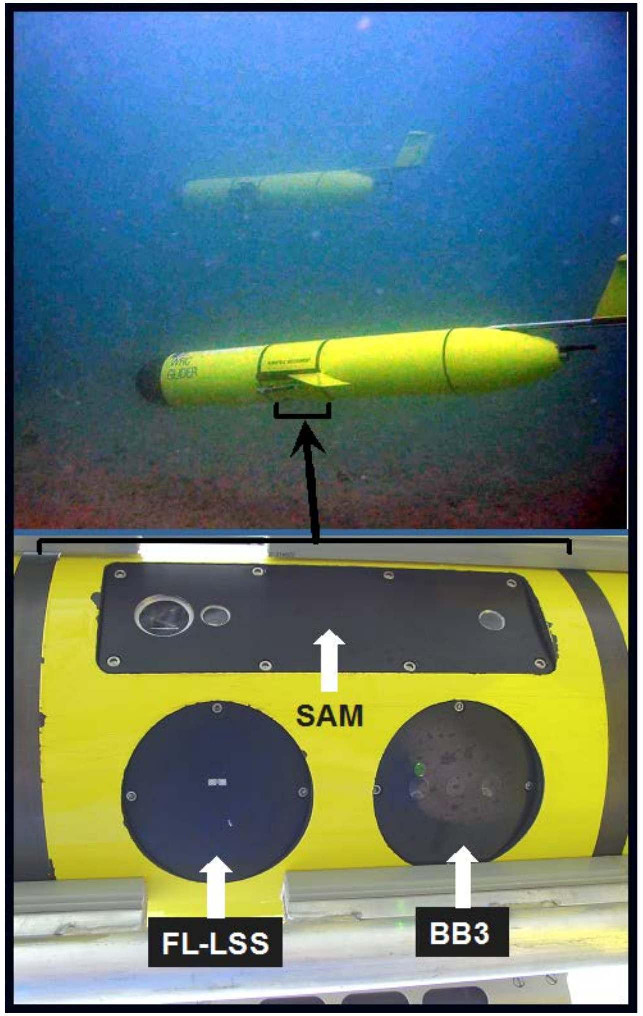

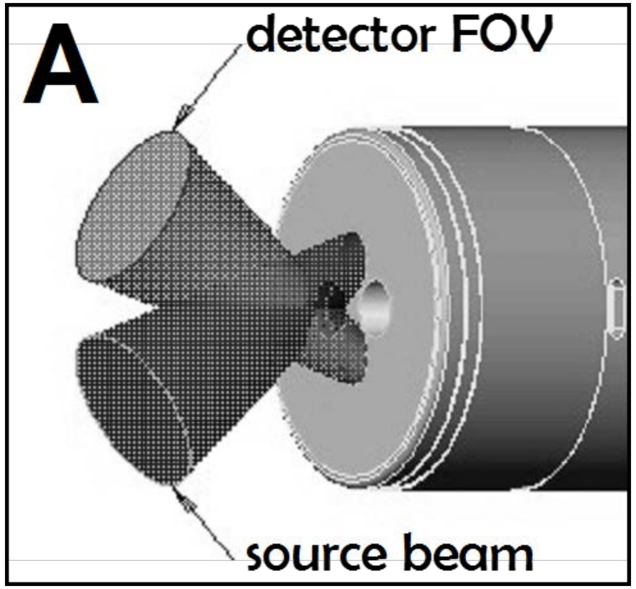

Measuring the VSF: IMO-SC6

In-situ Marine Optics

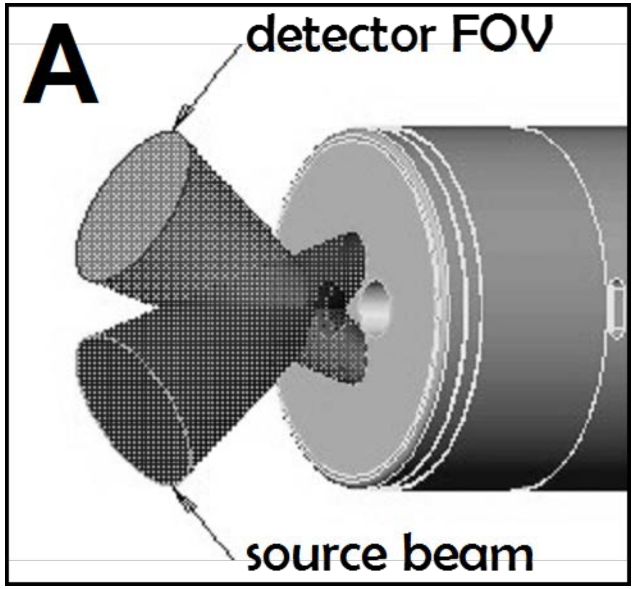

6 wavelengths, centroid angle ~120 deg

LISST-VSF (Sequoia)

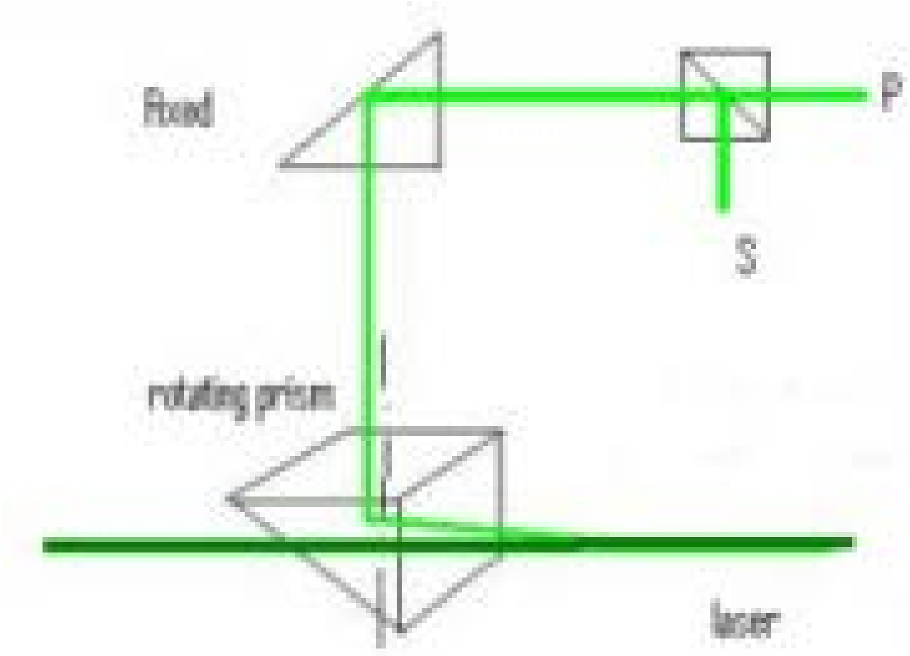

I-VSF
Helmholtz-Zentrum Geesthacht (HZG)

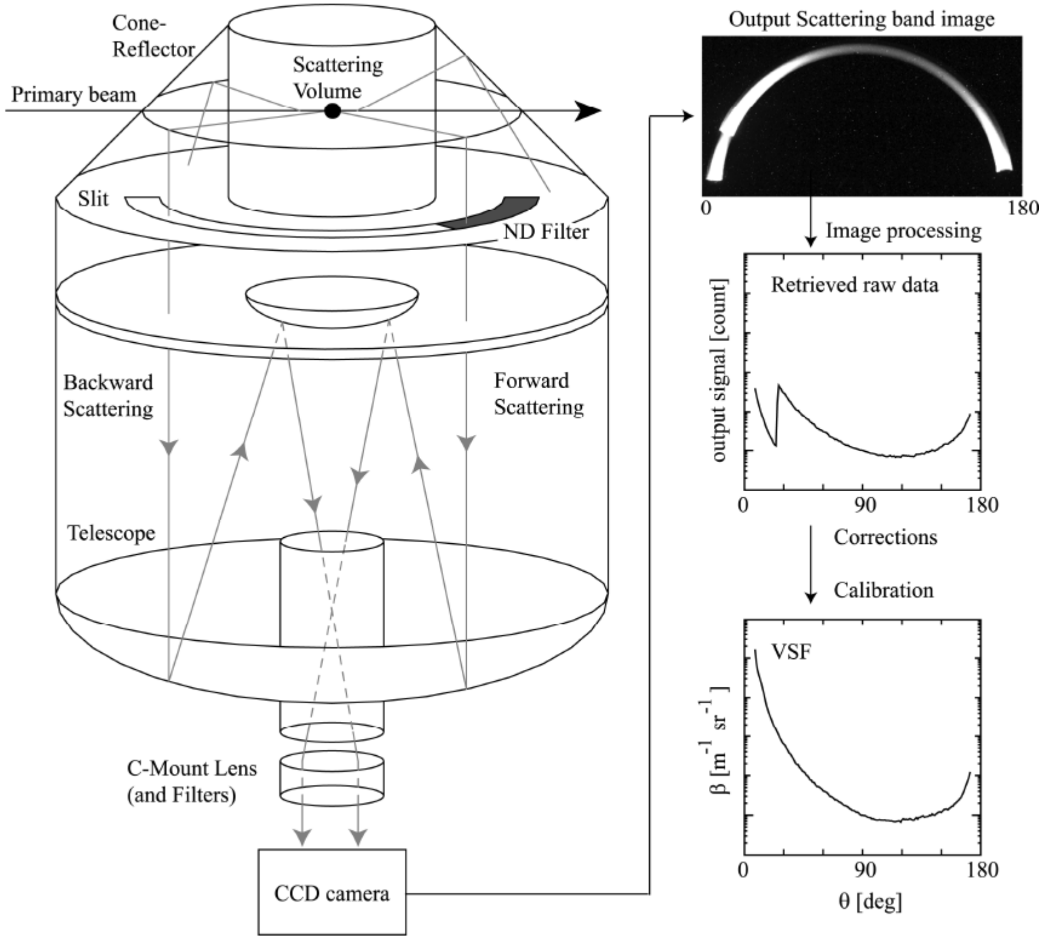

Tan et al. (2013)

Measuring the VSF: MVSM

(Marine Hydrophysical Institute, Academy of Sciences of the Ukraine)

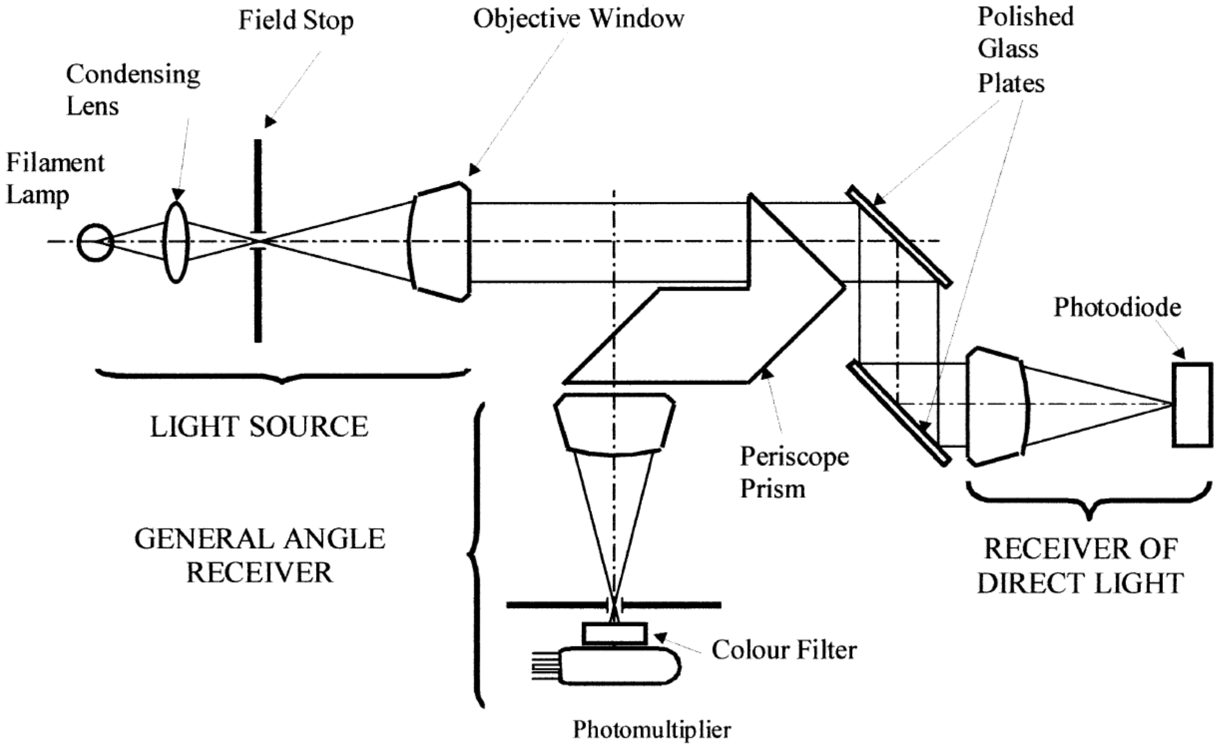

Lee and Lewis (2003)

POLVSM (LOV)

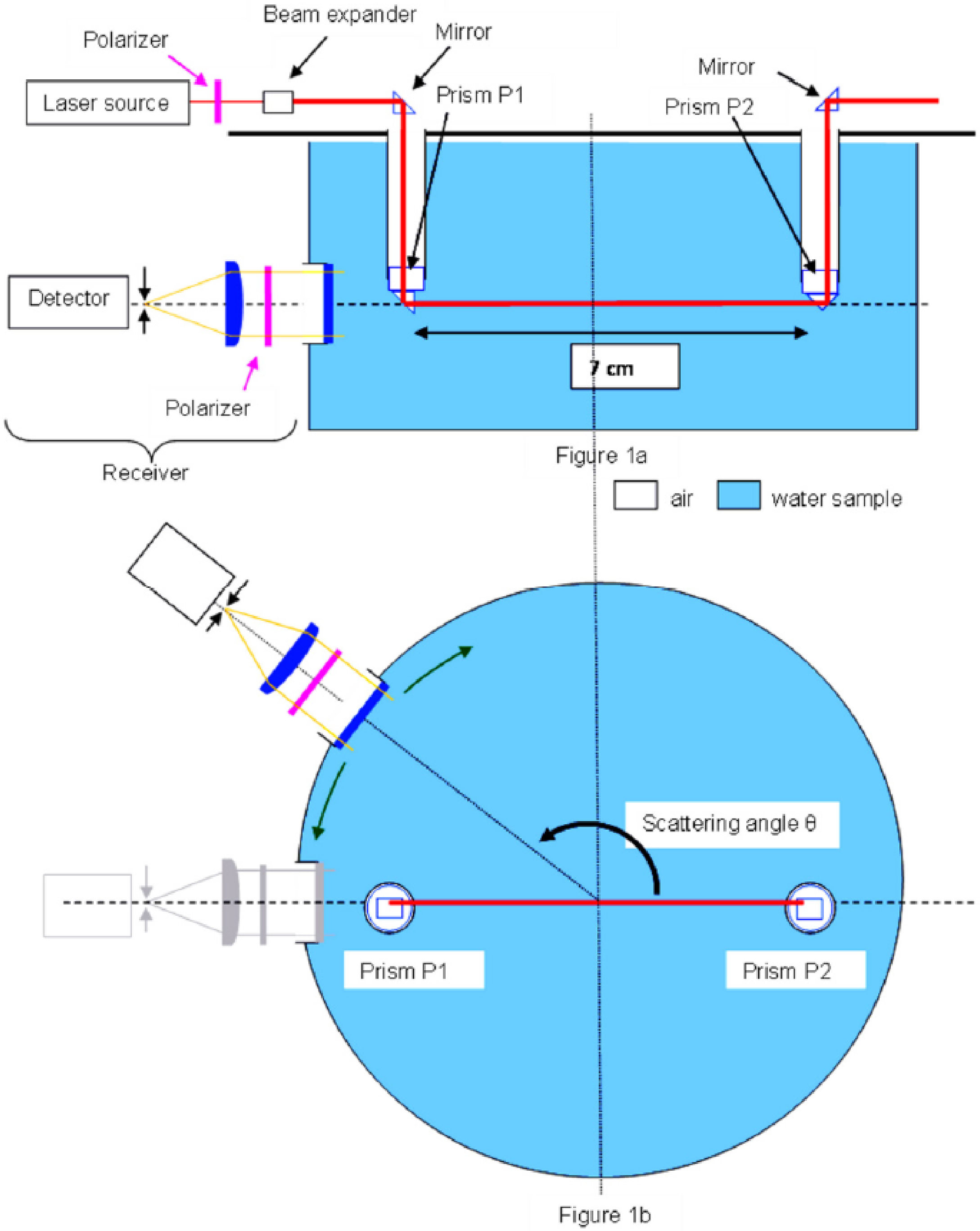

Chami et al. (2014)
Harmel et al. (2015)

BI-200 Goniometer (Brookhaven)

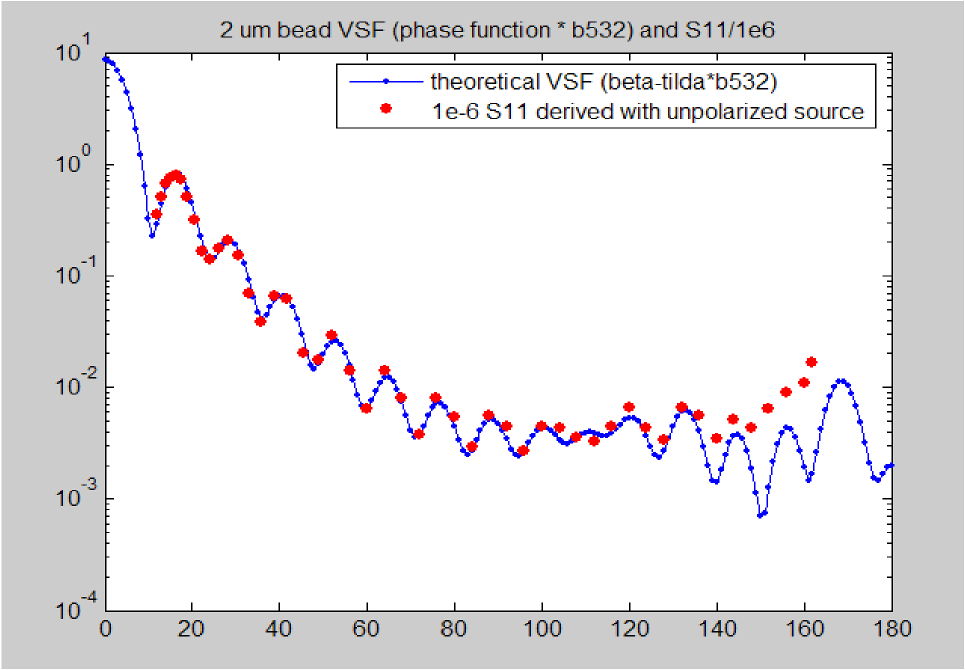

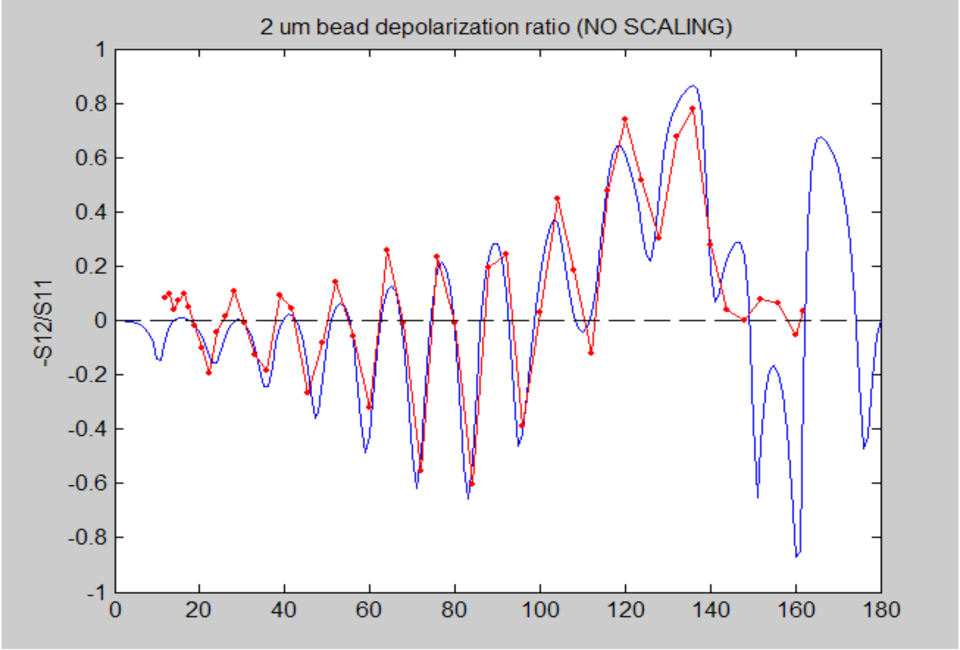

Near $\beta(180)$, coherent scattering

Phases interact in a constructive way to enhance scattering near 180 deg

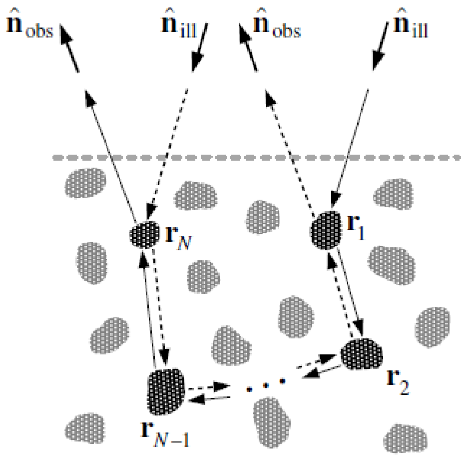

Figure 3.3. Schematic explanation of coherent backscattering.

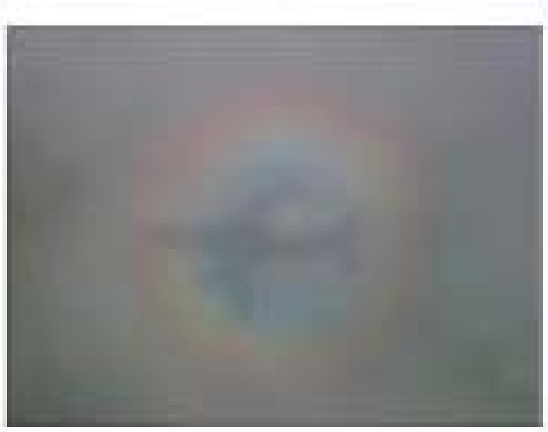

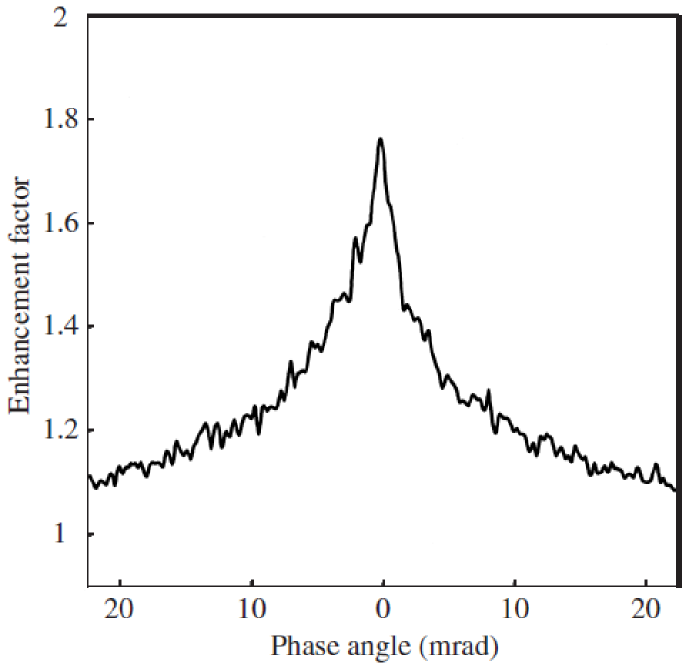

Figure 3.5. Angular profile of the coherent backscattering peak produced by a 1500-µm-thick slab of 9.6 vol% of 0.215-µm-diameter polystyrene spheres suspended in water. The slab was illuminated by a linearly polarized laser beam ($\lambda_1 = 633$ nm) incident normally to the slab surface. The scattering plane (i.e., the plane through the vectors $\hat{\mathbf{n}}_{ill}$ and $\hat{\mathbf{n}}_{obs}$, Fig. 3.3) was fixed in such a way that the electric vector of the incident beam vibrated in this plane. The detector measured the component of the backscattered intensity polarized parallel to the scattering plane. The curve shows the profile of the backscattered intensity normalized by the intensity of the incoherent background as a function of the phase angle. The latter is defined as the angle between the vectors $\hat{\mathbf{n}}_{obs}$ and $-\hat{\mathbf{n}}_{ill}$. (After van Albada *et al.* 1987.)

Mishchenko et al. 2002

“Turbidity” ? “NTU” measurements…?

- Typically a measurement of scattering ~90° but many sensors use angles > 90°
- Spectral characteristics vary (“white light,” 880 nm, etc.)
- Angular weighting ($\Delta\theta$) varies
- Calibrated to formazin particles (phase function looks nothing like that of the real ocean)

<u>So what does this mean?</u>

Virtually every turbidity measurement, and NTU, is different.

Turbidity is not “water clarity” (*c* is best for estimating this).

Signal may be correlated with backscattering.

Polarized scattering

VSF — V, H linear polarization — particle orientation

$$\begin{pmatrix} I_s \\ Q_s \\ U_s \\ V_s \end{pmatrix} = \frac{1}{k^2 r^2} \begin{pmatrix} S_{11} & S_{12} & \boxed{S_{13} \quad S_{14}} \\ S_{21} & S_{22} & S_{23} \quad S_{24} \\ S_{31} & S_{32} & S_{33} \quad S_{34} \\ S_{41} & S_{42} & S_{43} \quad S_{44} \end{pmatrix} \begin{pmatrix} I_i \\ Q_i \\ U_i \\ V_i \end{pmatrix}$$

total intensity

$\oplus$

$\otimes$

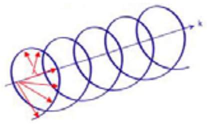

Stokes vector describing intensity and polarization of incident beam

SCATTERED BEAM

particle nonsphericity

INCIDENT BEAM

(θ, λ)

Mueller matrix
(for a “scattering event”)

Every element has wavelength and angular dependencies

Mueller matrix: Voss and Fry (1984)

All normalized to S11

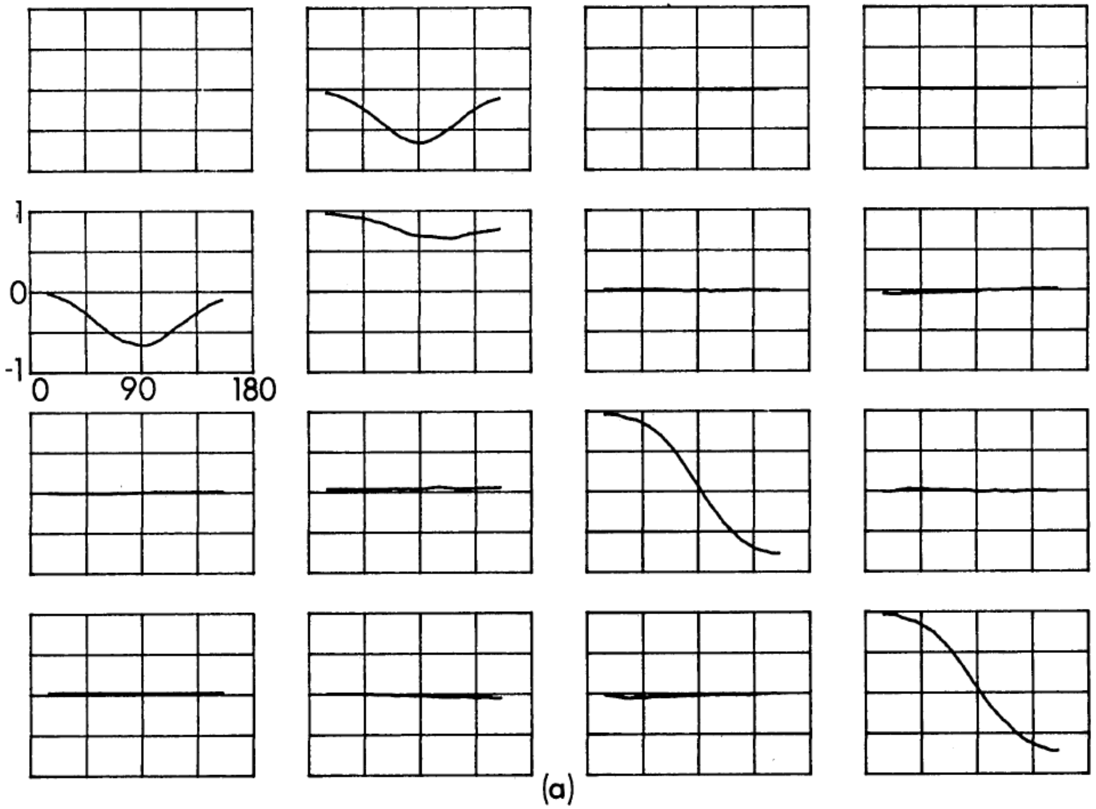

Modeled for very small particles (Rayleigh)

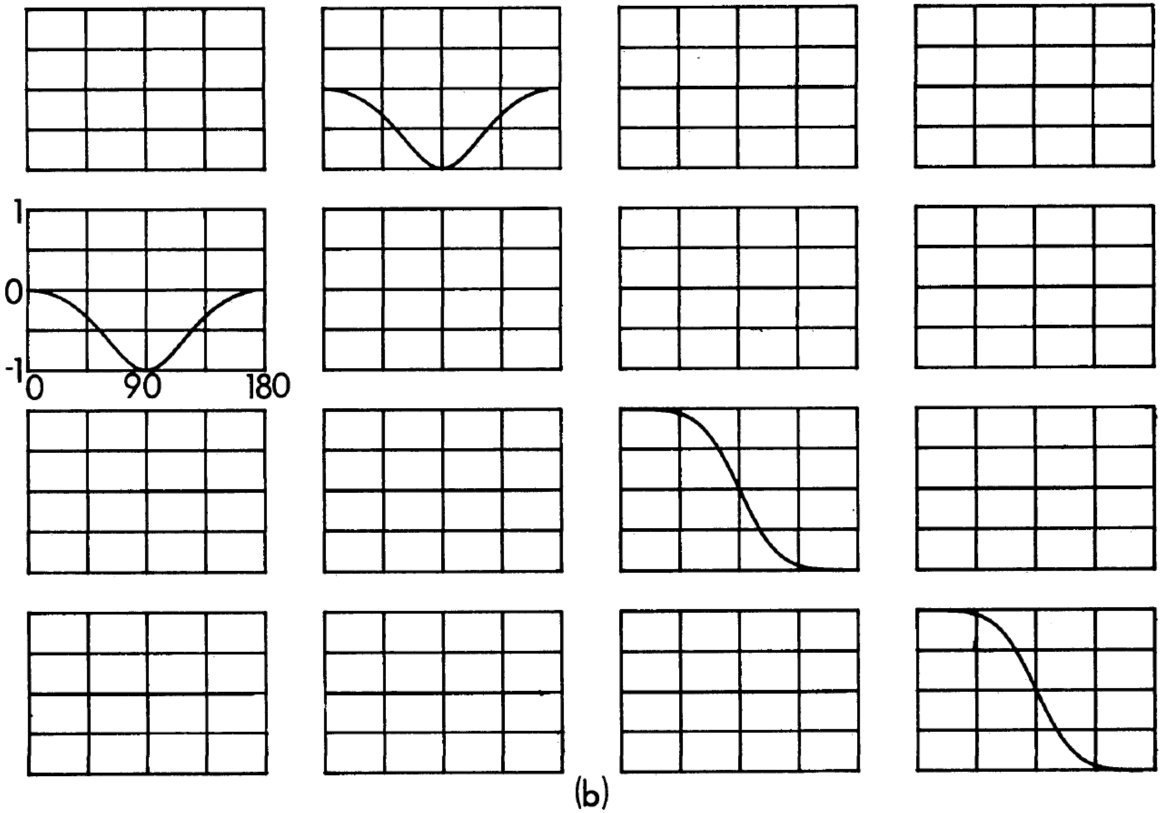

Averaged from Atlantic and Pacific Oceans

> 60 samples

Polarization: Measuring the Mueller matrix

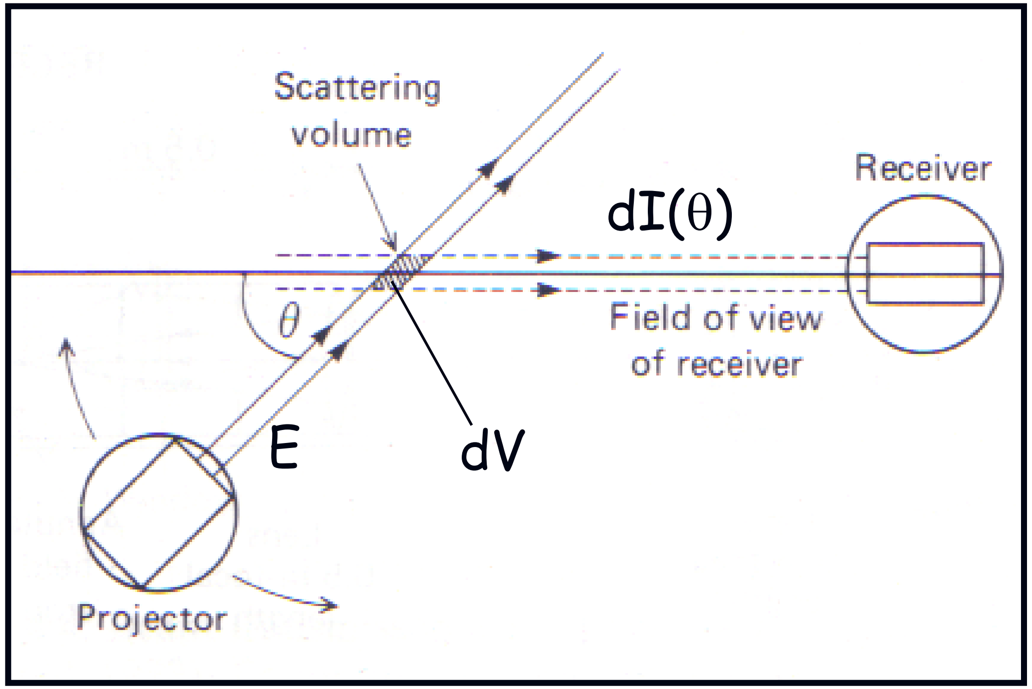

Bohren and Huffman 1983

Table 13.1 Combinations of Scattering Matrix Elements That Result from Measurements with a Polarizer P_s Forward of the Scattering Medium and an Analyzer A_s aft[a]

U	U	S_{11}	$P_\perp$	U	$\frac{1}{2}(S_{11} - S_{12})$
U	$A_\parallel$	$\frac{1}{2}(S_{11} + S_{21})$	$P_\perp$	$A_\parallel$	$\frac{1}{4}(S_{11} - S_{12} + S_{21} - S_{22})$
U	$A_\perp$	$\frac{1}{2}(S_{11} - S_{21})$	$P_\perp$	$A_\perp$	$\frac{1}{4}(S_{11} - S_{12} - S_{21} + S_{22})$
U	A_+	$\frac{1}{2}(S_{11} + S_{31})$	$P_\perp$	A_+	$\frac{1}{4}(S_{11} - S_{12} + S_{31} - S_{32})$
U	A_-	$\frac{1}{2}(S_{11} - S_{31})$	$P_\perp$	A_-	$\frac{1}{4}(S_{11} - S_{12} - S_{31} + S_{32})$
U	A_R	$\frac{1}{2}(S_{11} - S_{41})$	$P_\perp$	A_R	$\frac{1}{4}(S_{11} - S_{12} - S_{41} + S_{42})$
U	A_L	$\frac{1}{2}(S_{11} + S_{41})$	$P_\perp$	A_L	$\frac{1}{4}(S_{11} - S_{12} + S_{41} - S_{42})$
$P_\parallel$	U	$\frac{1}{2}(S_{11} + S_{12})$	P_+	U	$\frac{1}{2}(S_{11} + S_{13})$
$P_\parallel$	$A_\parallel$	$\frac{1}{4}(S_{11} + S_{12} + S_{21} + S_{22})$	P_+	$A_\parallel$	$\frac{1}{4}(S_{11} + S_{13} + S_{21} + S_{23})$
$P_\parallel$	$A_\perp$	$\frac{1}{4}(S_{11} + S_{12} - S_{21} - S_{22})$	P_+	$A_\perp$	$\frac{1}{4}(S_{11} + S_{13} - S_{21} - S_{23})$
$P_\parallel$	A_+	$\frac{1}{4}(S_{11} + S_{12} + S_{31} + S_{32})$	P_+	A_+	$\frac{1}{4}(S_{11} + S_{13} + S_{31} + S_{33})$
$P_\parallel$	A_-	$\frac{1}{4}(S_{11} + S_{12} - S_{31} - S_{32})$	P_+	A_-	$\frac{1}{4}(S_{11} + S_{13} - S_{31} - S_{33})$
$P_\parallel$	A_R	$\frac{1}{4}(S_{11} + S_{12} - S_{41} - S_{42})$	P_+	A_R	$\frac{1}{4}(S_{11} + S_{13} - S_{41} - S_{43})$
$P_\parallel$	A_L	$\frac{1}{4}(S_{11} + S_{12} + S_{41} + S_{42})$	P_+	A_L	$\frac{1}{4}(S_{11} + S_{13} + S_{41} + S_{43})$
P_-	U	$\frac{1}{2}(S_{11} - S_{13})$	P_L	U	$\frac{1}{2}(S_{11} - S_{14})$
P_-	$A_\parallel$	$\frac{1}{4}(S_{11} - S_{13} + S_{21} - S_{23})$	P_L	$A_\parallel$	$\frac{1}{4}(S_{11} - S_{14} + S_{21} - S_{24})$
P_-	$A_\perp$	$\frac{1}{4}(S_{11} - S_{13} - S_{21} + S_{23})$	P_L	$A_\perp$	$\frac{1}{4}(S_{11} - S_{14} - S_{21} + S_{24})$
P_-	A_+	$\frac{1}{4}(S_{11} - S_{13} + S_{31} - S_{33})$	P_L	A_+	$\frac{1}{4}(S_{11} - S_{14} + S_{31} - S_{34})$
P_-	A_-	$\frac{1}{4}(S_{11} - S_{13} - S_{31} + S_{33})$	P_L	A_-	$\frac{1}{4}(S_{11} - S_{14} - S_{31} + S_{34})$
P_-	A_R	$\frac{1}{4}(S_{11} - S_{13} - S_{41} + S_{43})$	P_L	A_R	$\frac{1}{4}(S_{11} - S_{14} - S_{41} + S_{44})$
P_-	A_L	$\frac{1}{4}(S_{11} - S_{13} + S_{41} - S_{43})$	P_L	A_L	$\frac{1}{4}(S_{11} - S_{14} + S_{41} - S_{44})$
P_R	U	$\frac{1}{2}(S_{11} + S_{14})$			
P_R	$A_\parallel$	$\frac{1}{4}(S_{11} + S_{14} + S_{21} + S_{24})$			
P_R	$A_\perp$	$\frac{1}{4}(S_{11} + S_{14} - S_{21} - S_{24})$			
P_R	A_+	$\frac{1}{4}(S_{11} + S_{14} + S_{31} + S_{34})$			
P_R	A_-	$\frac{1}{4}(S_{11} + S_{14} - S_{31} - S_{34})$			
P_R	A_R	$\frac{1}{4}(S_{11} + S_{14} - S_{41} - S_{44})$			
P_R	A_L	$\frac{1}{4}(S_{11} + S_{14} + S_{41} + S_{44})$			

$= S_{12}$ for sphere goniometer

$\frac{S_{12}}{S_{11}}$ = degree of linear polar

$\boxed{\text{See p. 65}}$ and p. 112

$S_{21} = S_{12}$, $S_{11} = S_{22}$ for sp

[a] U indicates the absence of a polarizer or analyzer.

Voss and Fry (1984): Mueller matrix

MASCOT: POLMOD

<u>Degree of Linear Polarization</u>

DoLP = -S12 / S11
= -(H-V)/(H+V)

H = ½(S11 + S12)
V = ½(S11 – S12)

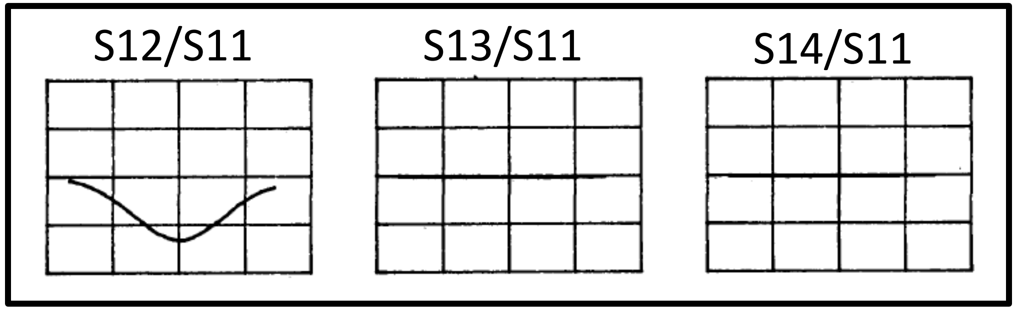

<u>4 positions</u>

1 - OPEN

2 - DARK

3 - H ⟷

4 - V ↕

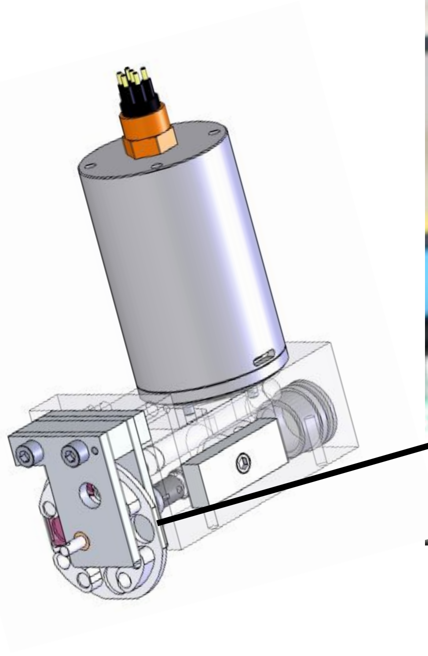

Measuring polarization

linear	*oblique linear*	*circular*
<u>Measuring S12</u>	<u>Measuring S13</u>	<u>Measuring S14</u>
H = ½(S11 + S12) V = ½(S11 – S12)	O_+ = ½(S11 + S13) O_- = ½(S11 – S13)	R = ½(S11 + S14) L = ½(S11 – S14)
-S12 / S11 = -(H-V)/(H+V)	-S13 / S11 = $\dfrac{-(O_+ - O_-)}{(O_+ + O_-)}$	-S14 / S11 = -(R-L)/(R+L)
S12 = H-V *and* S11 = H+V	S13 = $O_+ - O_-$ *and* S11 = $O_+ + O_-$	S14 = R-L *and* S11 = R+L

- *however, there are transmission losses due to the filters (~90% T)*
- *ratiometric values are fine, as transmission factors cancel*

“true” S11 = (H + V)/T (*where T = 0.9*)

S11 can be validated with direct open path measurement

Curaçao, 2012: single vertical profile

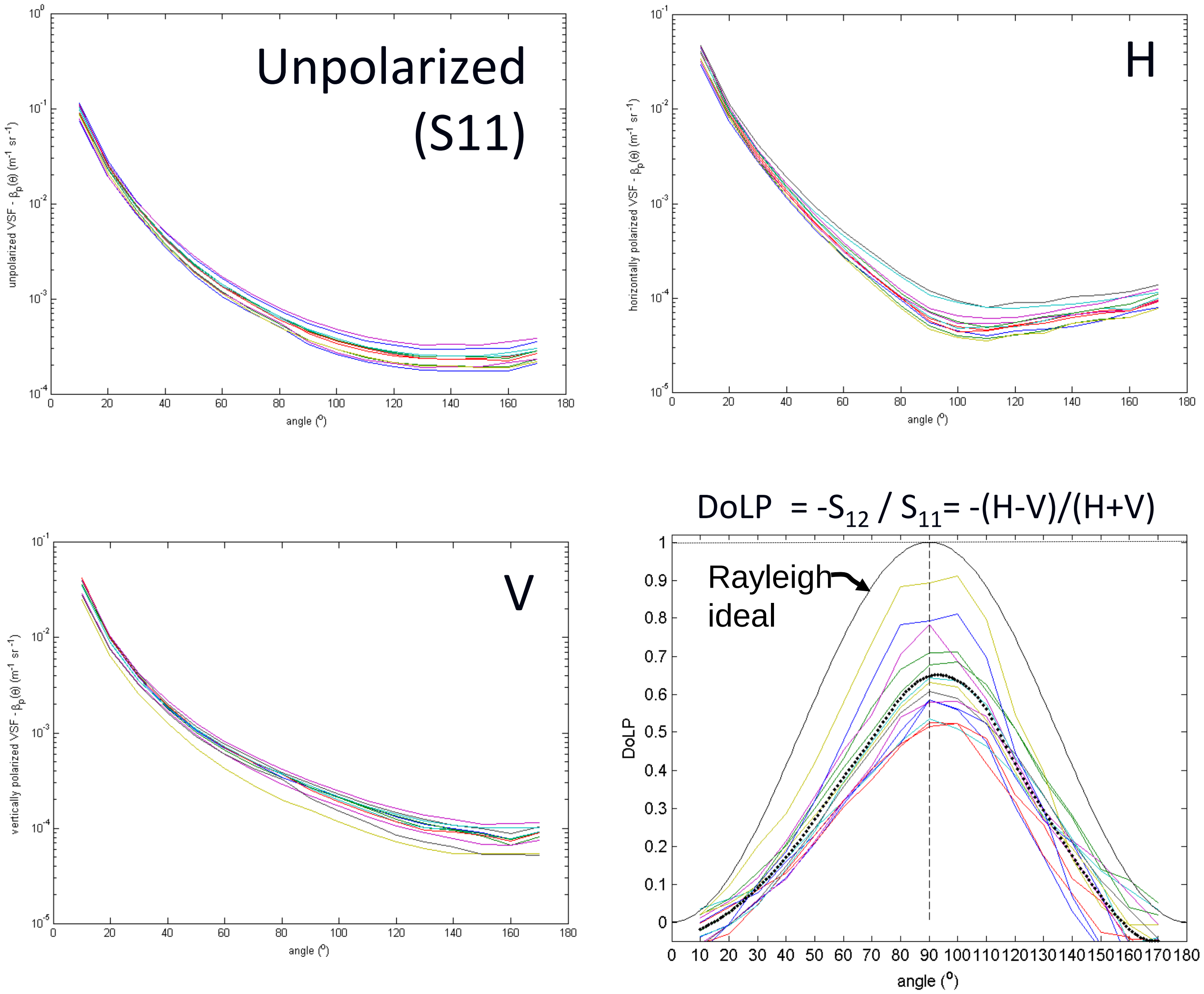

Cruise locations with MASCOT polarization measurements (since 2008)

- Ligurian Sea (S13 and S14 also)
- NY bight
- Santa Barbara Channel
- Gulf of Mexico
- Port Aransas, TX
- Florida Keys (2X)
- Curacao
- East Sound, WA
- Florida, Indian lagoon
- N. Lake Michigan

Polarized scattering measurements

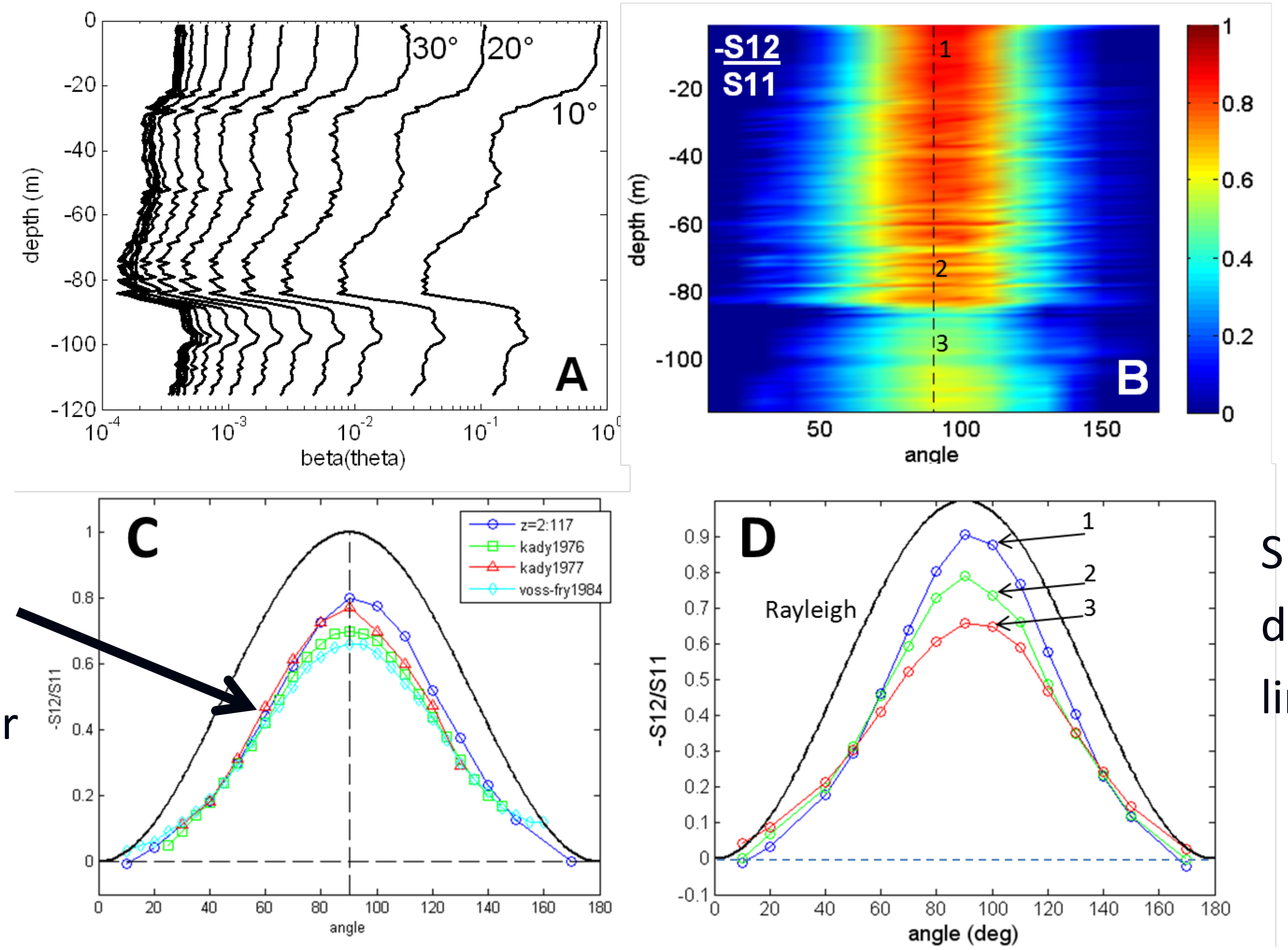

There are only 3 other measurements of S12/S11 for ocean water in the literature!

S12/S11: degree of linear polarization

Santa Barbara Channel, September 2008

Lorenz-Mie 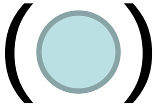

asymmetric hexahedra 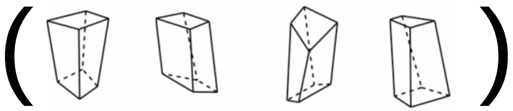

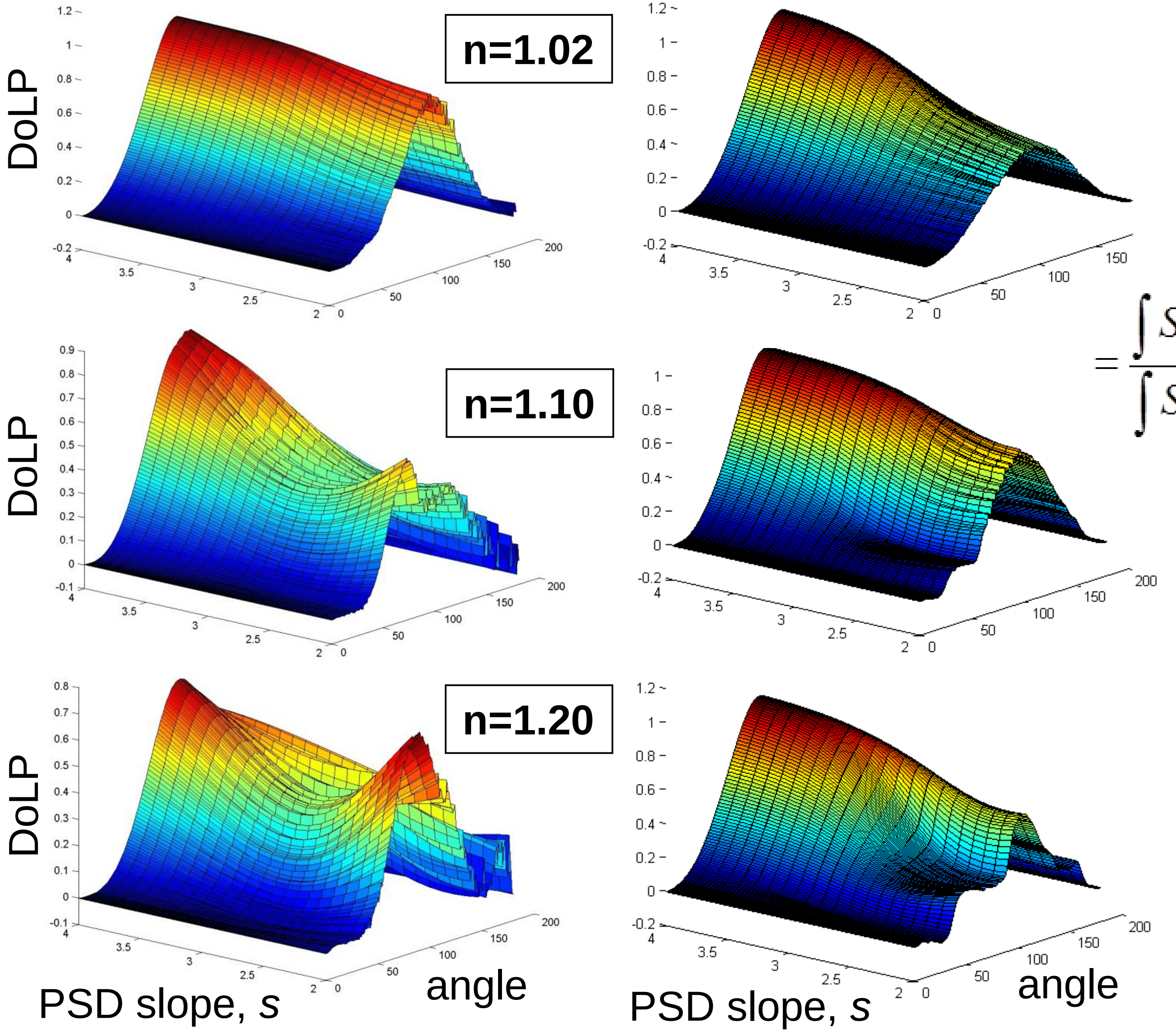

$$DoLP_{pop} = \frac{\overline{S12(\theta)}}{\overline{S11(\theta)}}$$

$$= \frac{\int S12(D,n,\theta,\lambda)F(D)dD}{\int S11(D,n,\theta,\lambda)F(D)dD}$$

$$F(D) = \frac{dN}{dD} = AD^{-s}$$

Twardowski, unpubl

Degree of Linear Polarization

asymmetric hexahedra

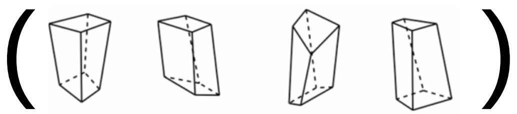

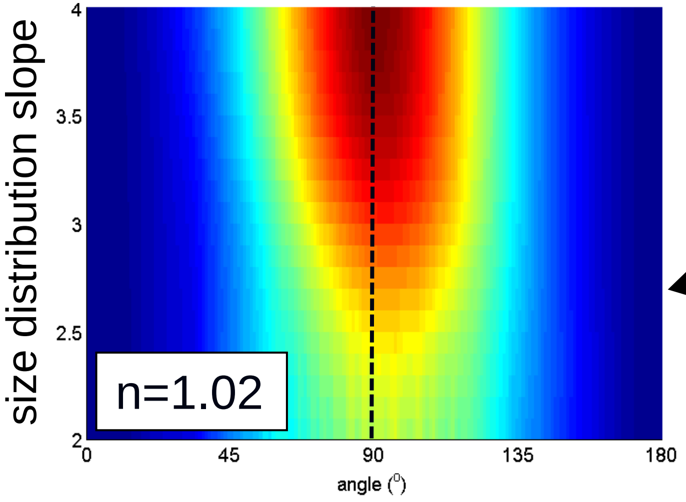

another view

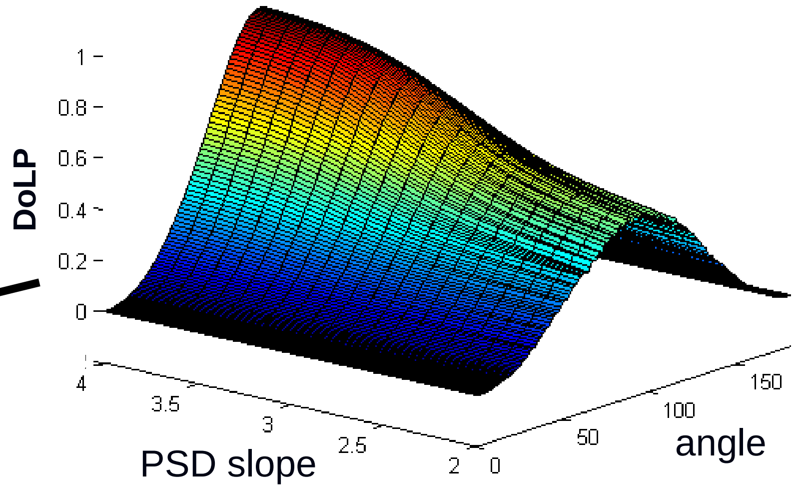

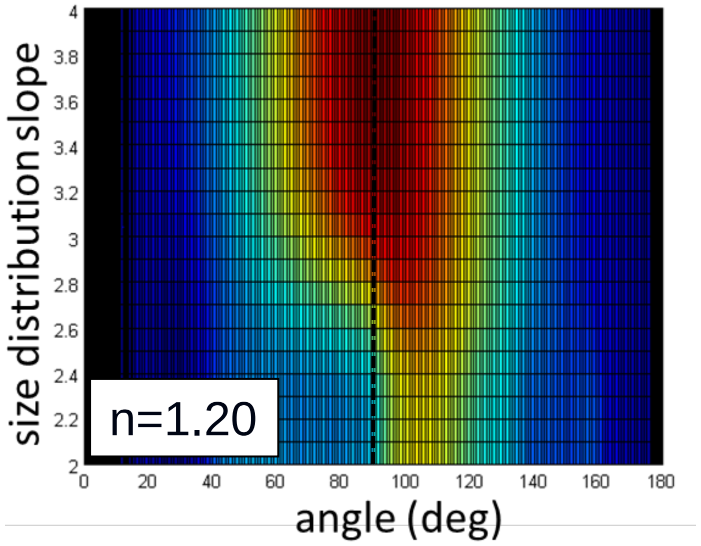

- **Increasing nonsphericity** lowers DoLP and shifts the DoLP peak to larger angles
- **Increasing refractive index** lowers DoLP, particularly for populations with relatively flat size distributions
- **As size distributions become increasingly flat**, the DoLP decreases and the maximum shifts to larger angles

Twardowski, unpubl

Polarized scattering

phytoplankton species

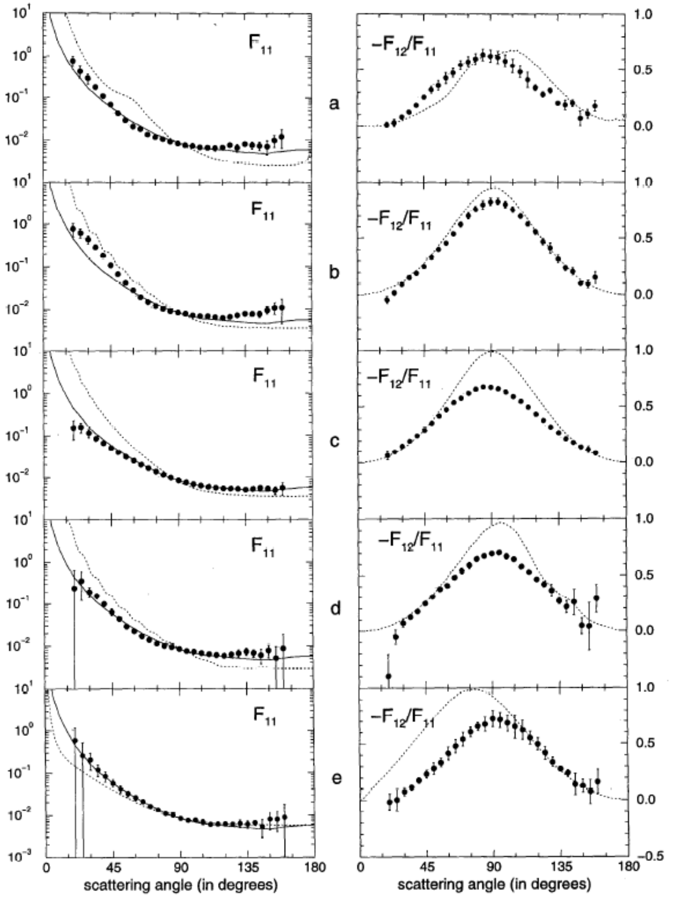

Fig. 6. The measured scattering functions, F_{11}, and ratios $-F_{12}/F_{11}$ are shown in the left and right panels, respectively (filled circles) for (a) *Microcystis aeruginosa* without gas vacuoles, (b) *Microcystis aeruginosa* with gas vacuoles, (c) *Microcystis* sp., (d) *Phaeocystis*, and (e) *Volvox aureus*. Also plotted are the scattering function for San Diego Harbor (solid, left panels) and the results of Mie calculations (dashed, left and right panels). The $F_{11}(\theta)$ functions are scaled at 90° to the scattering function of San Diego Harbor. Errors are smaller than symbols if no error bar is indicated.

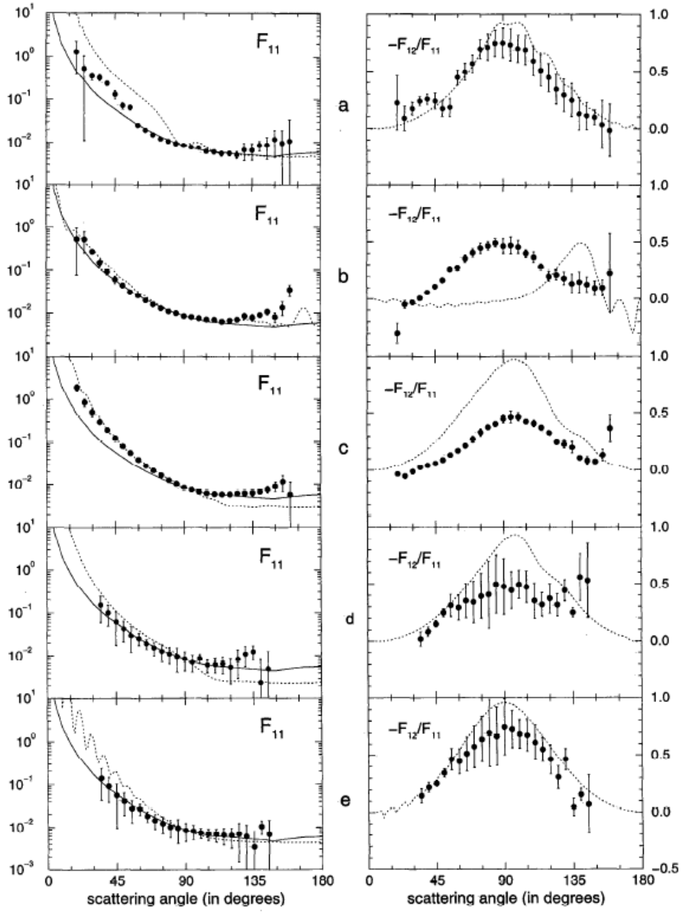

Fig. 8. Same as Fig. 6 for (a) *Astrionella formosa*, (b) *Selenastrum capricornutum*, (c) *Phaeodactylum*, (d) *Emiliania huxleyi* with coccoliths, and (e) *Emiliania huxleyi* without coccoliths.

sediment samples

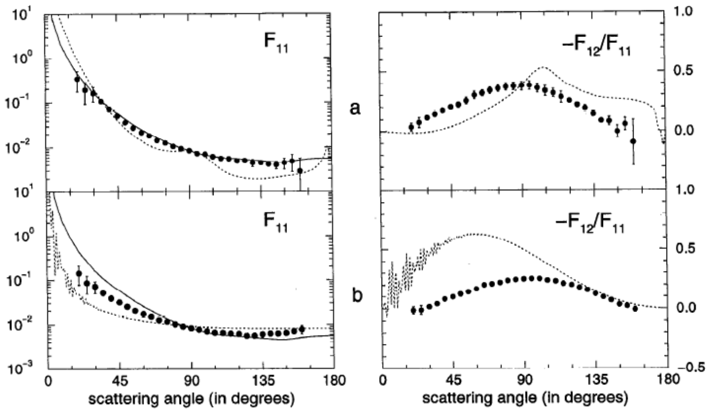

Fig. 9. Same as Fig. 6 for (a) Westerschelde silt with diameters ranging between 3 and 5 μm, and (b) Westerschelde silt with diameters ranging between 5 and 12 μm.

Included reflection corrections

Volten et al. (1998)

Interpreting polarized scattering

The angular and spectral characteristics of the Mueller scattering matrix parameters are a function of several properties of the particle population, including:

- Refractive index composition
- Size distribution
- Particle shape
- Particle orientation

Much to be done!

Scattering components

- Pure seawater (molecular)
- Turbulence (i.e., refractive index discontinuities)
- Particles
- Bubbles

Scattering by pure seawater – most literature pre~2006

VSF of water using Mor…)

$\beta_w(\theta,\lambda,S,T=20°C)=1.38(\lambda/500nm$ … $.3S/37)10^{-4}\ (1+\cos^2\theta(1-\delta)/(1+\delta))$

(where depola… tio, δ = 0.09)

NOT THE BEST VALUES

-Computed from Ei… oluchowsky theory

-The term 1.3… nm)$^{-4.32}$ describes $\beta(90)$ and was obtained by a fit to M… computed results

-The term (1+0.3S/37) is from Morel’s experimental data with 37 ppt seawater

Scattering by pure seawater, literature ~2007-2008

VSF of water using Buiteveld et al. (1994) and
Morel's salinity term:

(reviewed in Twardowski et

-Also uses Einstein-Smoluchowsky theory, b ated constants, mostly derived from experimental data from the 197

-The "famous" -4.32 exponent for s tering of water is now -4.14 because of a reformulation of the refra of water and the isothermal compressibility of water

-The depolarization ratio 51 after Farinato and Rowell (1974)

- **<u>this is a critica</u>** **<u>certainty</u> – needs further work**

NOT THE BEST VALUES

Scattering by pure seawater (current)

Zhang and Hu (2009); Zhang et al. (2009)

Review: Zhang (2012)

-Also uses Einstein-Smoluchowsky theory, but uses density derivative for refractive index fluctuations with updated constants – more accurate than approximation with pressure derivative

-The depolarization ratio used is 0.039, also after Farinato and Rowell (1974)

- **this is a critical area of uncertainty – needs further work**

These are currently considered the most accurate values (probably ±2-4%) but rigorous experimental verification is still needed

Agrees well with experimental work of Morel (1968)

For backscattering by seawater, divide b_w by 2.

Scattering by pure seawater

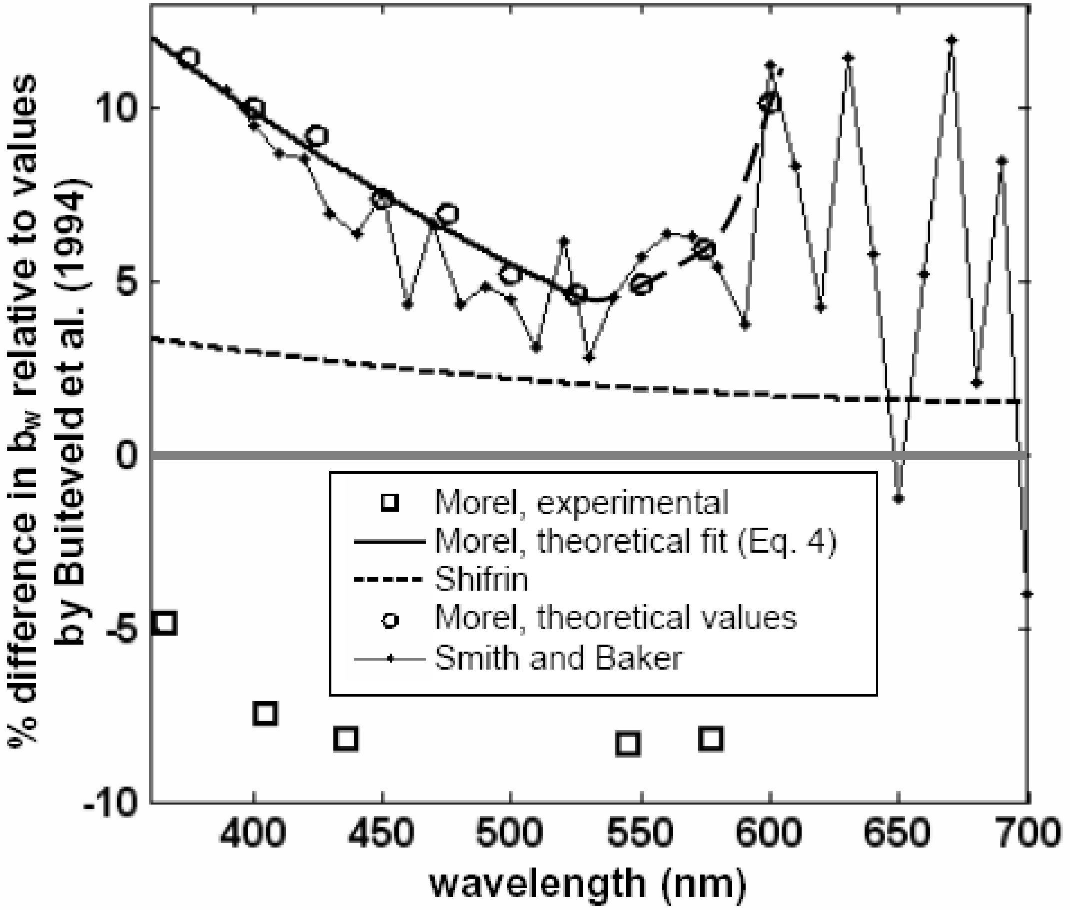

Backscattering by seawater can be 90+% of total b_b in the very clear ocean.
Accuracy is very important if we are interested in b_{bp}

$$\text{Morel}: b_w = 3.50\left(\frac{\lambda}{450}\right)^{-4.32} 10^{-3}\,\mathrm{m}^{-1},$$

$$\text{Shifrin}: b_w = 1.49\left(\frac{\lambda}{546}\right)^{-4.17} 10^{-3}\,\mathrm{m}^{-1}$$

Twardowski et al. 2007

Scattering by pure seawater

So. Pacific gyre – 2004

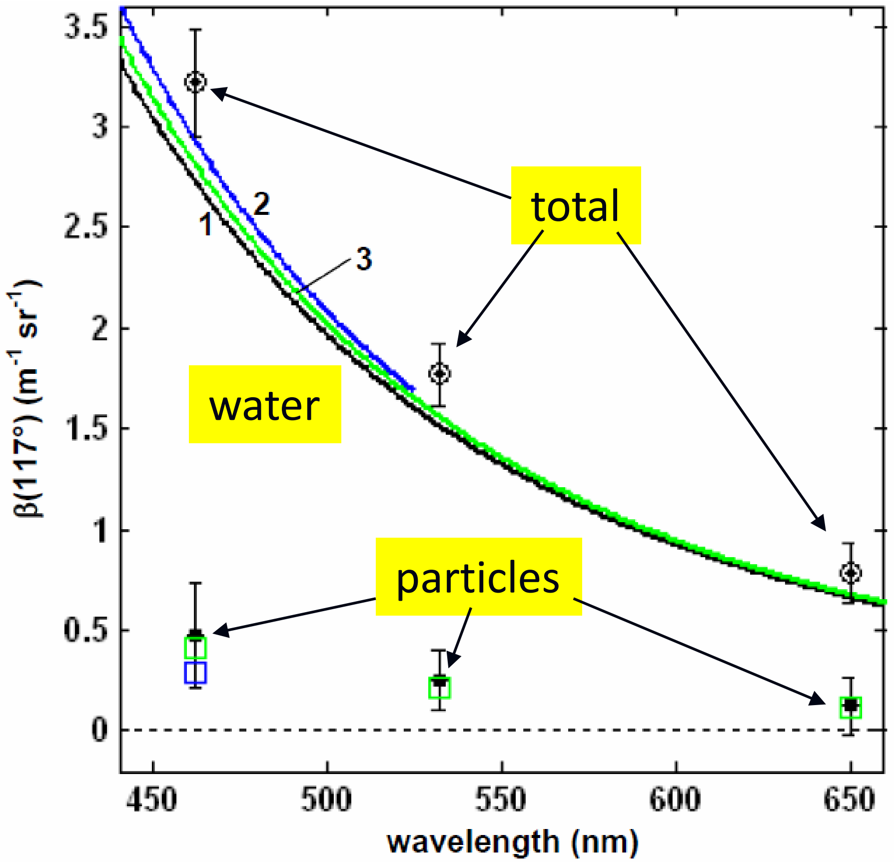

Backscattering by seawater can be 90+% of total b_b in the very clear ocean. *Accuracy is very important if we are interested in b_{bp}*

$$\text{Morel}: b_w = 3.50 \left(\frac{\lambda}{450}\right)^{-4.32} 10^{-3}\,\mathrm{m}^{-1},$$

$$\text{Shifrin}: b_w = 1.49 \left(\frac{\lambda}{546}\right)^{-4.17} 10^{-3}\,\mathrm{m}^{-1}$$

Twardowski et al. 2007

Turbulence (refractive index discontinuities)

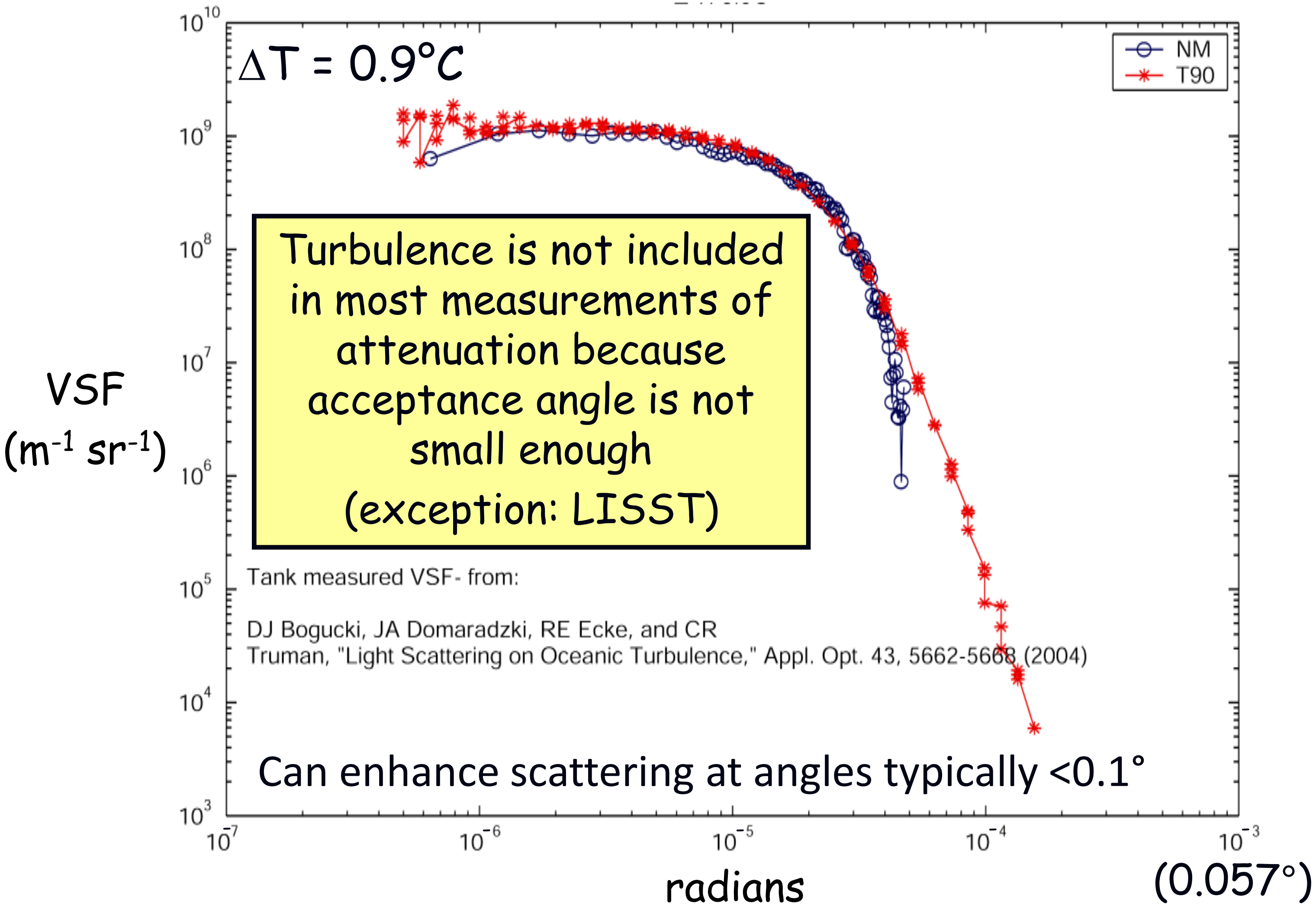

Turbulence measurement with LISST-100X

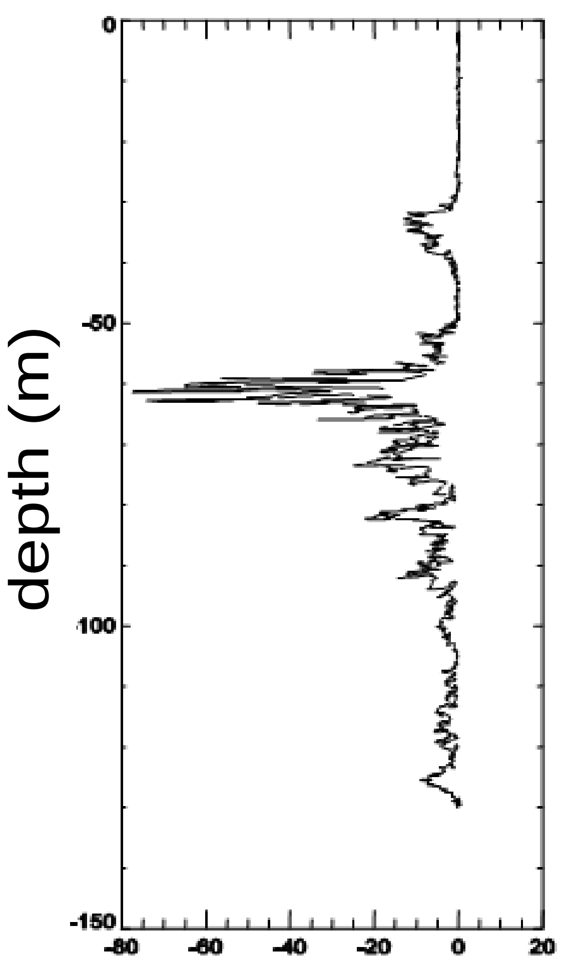

dn/dt
from T&S

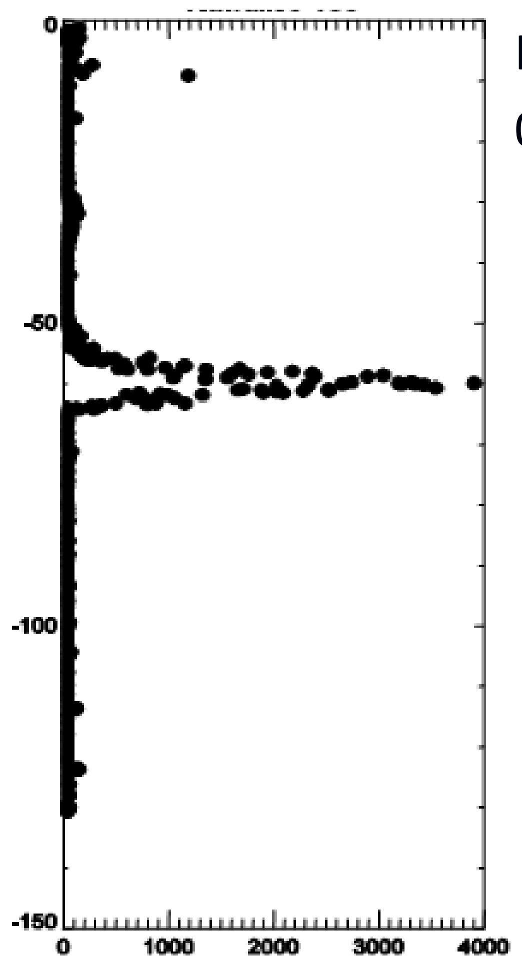

turbulence indicator
from LISST VSF

Hawaii
09/2009

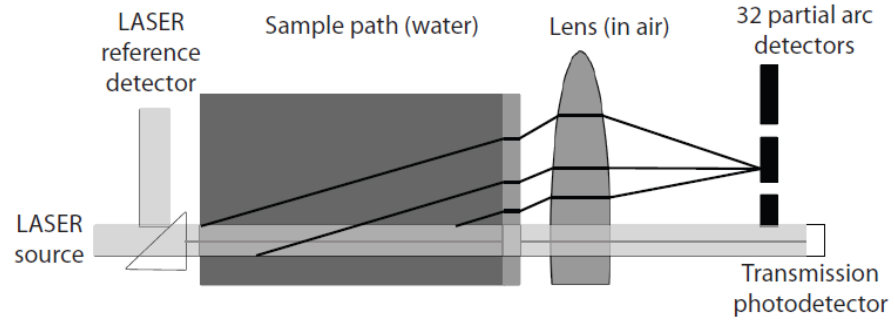

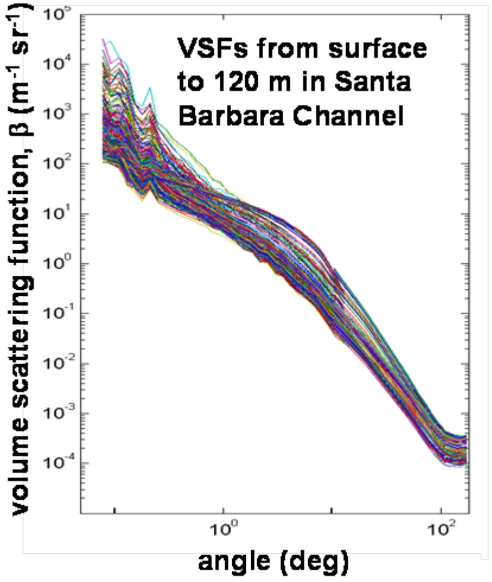

Slivkoff and Twardowski, unpub

Particle scattering

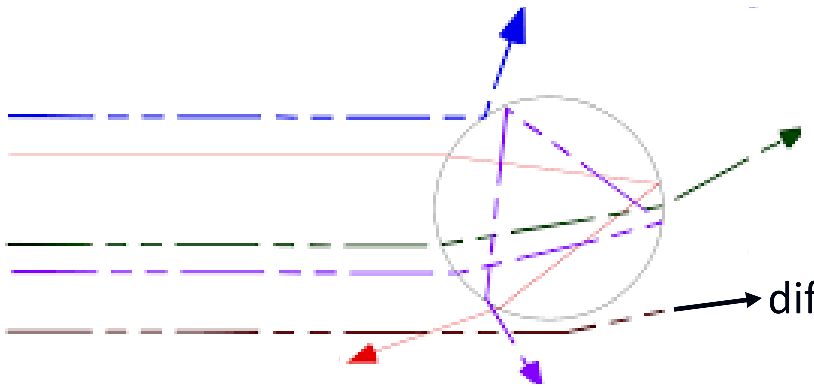

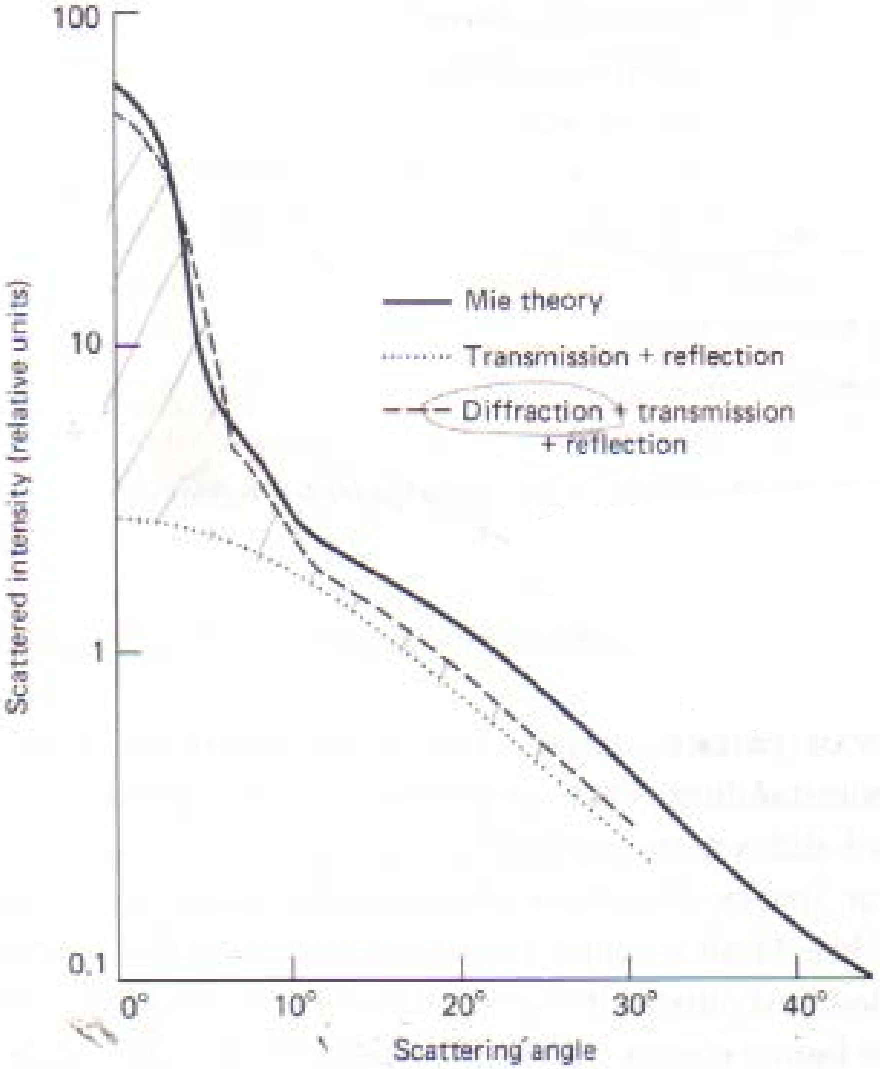

Fig. 4.1. Angular distribution of scattered intensity from transparent spheres calculated from Mie theory (Ashley & Cobb, 1958) or on the basis of transmission and reflection, or diffraction, transmission and reflection (Hodkinson & Greenleaves, 1963). The particles have a refractive index (relative to the surrounding medium) of 1.20, and have diameters 5–12 times the wavelength of the light. After Hodkinson & Greenleaves (1963).

Kirk 1994

"…our present-day interpretation and detailed understanding of major sources of backscattering and its variability in the ocean are uncertain and controversial."

Stramski, D., E. Boss, D. Bogucki, and K. J. Voss, 2004. The role of seawater constituents in light backscattering in the ocean. Progress in Oceanography, 61(1), 27-55.

The Enigma of Phytoplankton Backscattering…

Modeling phytoplankton as homogeneous spheres results in backscattering levels too low (only a few percent contribution) to be consistent with their influence on remote sensing reflectance (R_{RS}).

Stramski and Kiefer 1991; Stramski et al. 2001

Testing the “Complex Particle” Hypothesis

Thalassiosira weissflogii

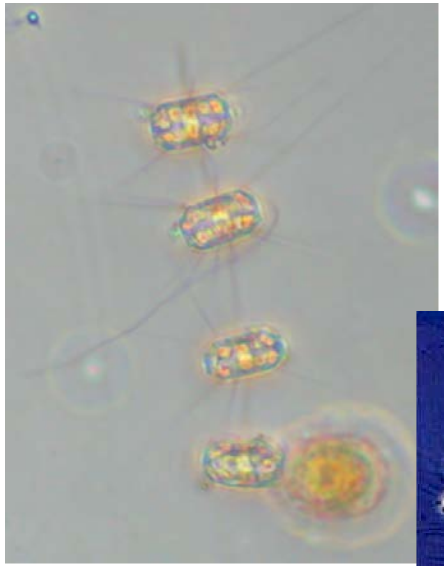

~25 μm diameter

Gyrodinium instriatum

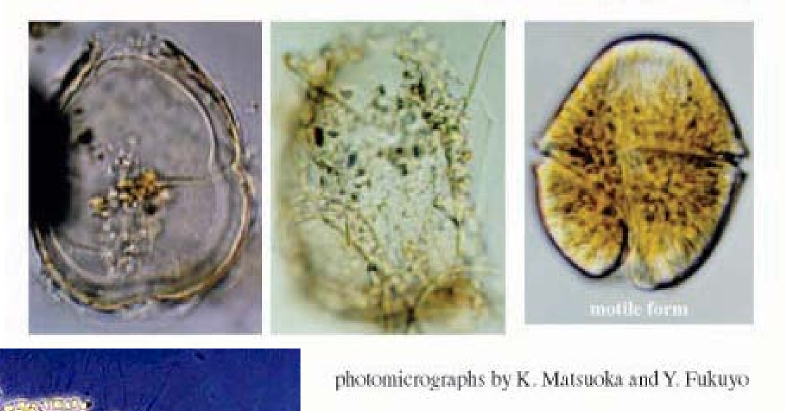

~50 mm diameter

~10 μm cell diameter
Up to 1 mm colonies

Chaetoceros socialis

The background in cultures is important

Background (<10 μm fraction) in culture experiments

	Thalassiosira	C. socialis	Gyrodinium
Fraction bbp	41%	53%	73%
bbp/bp	0.004	0.035	0.034

<u>Background is usually not considered in scattering measurements in phytoplankton cultures</u>

Twardowski, Sullivan, McFarland (unpubl)

Phytoplankton scattering: measurements and modeling

b_{bp}/b_p

	Measured	Mie theory	Coated Mie theory
Thalassiosira cells	**0.013**	0.006	0.013
Gyrodinium cells	**0.006**	0.003	0.007
C. socialis cells	**0.004**	0.0006	0.0237
C. socialis [1]cell Q_{bb} [2]colony Q_b	**0.004**	0.004	

Twardowski, Sullivan, McFarland (unpubl)

Imaging Particle Backscattering

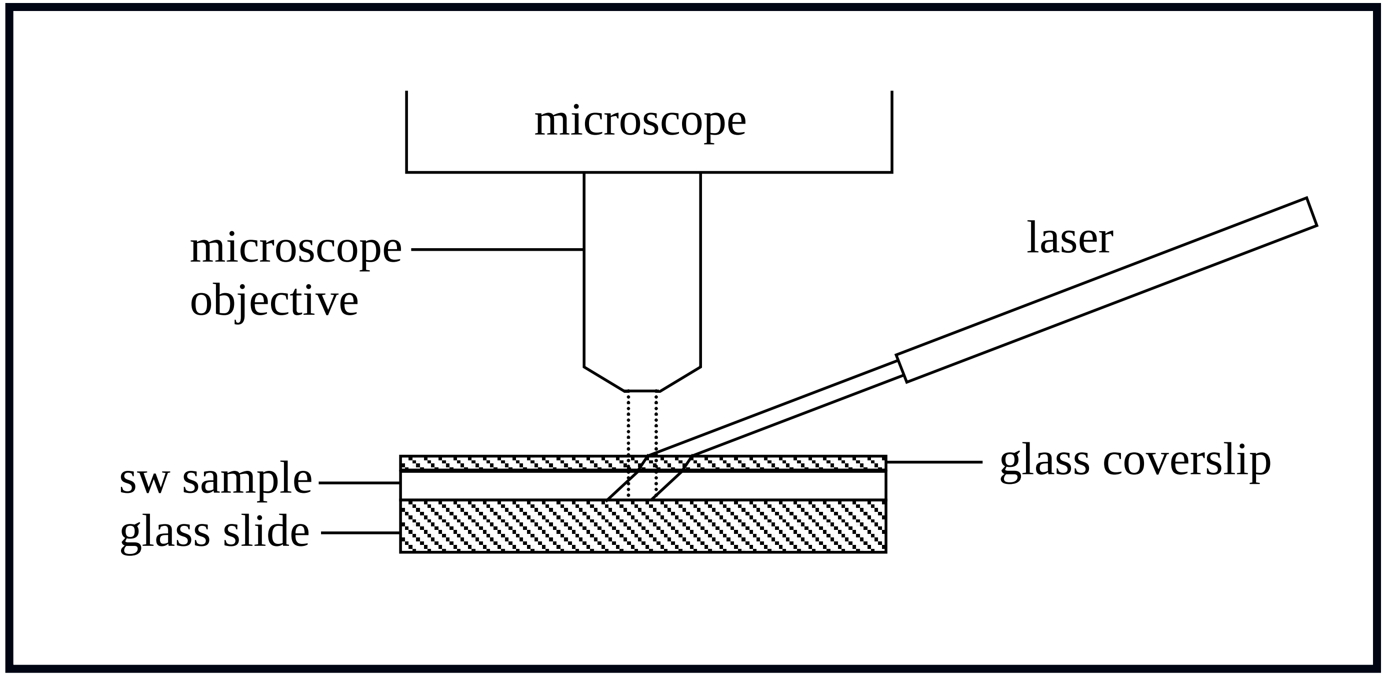

Backscattering imaged at ~140°

Twardowski, Sullivan, McFarland (unpubl)

Imaging Particle Backscattering

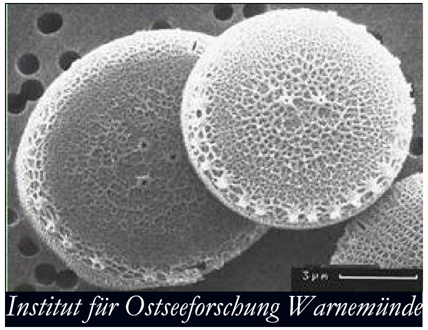

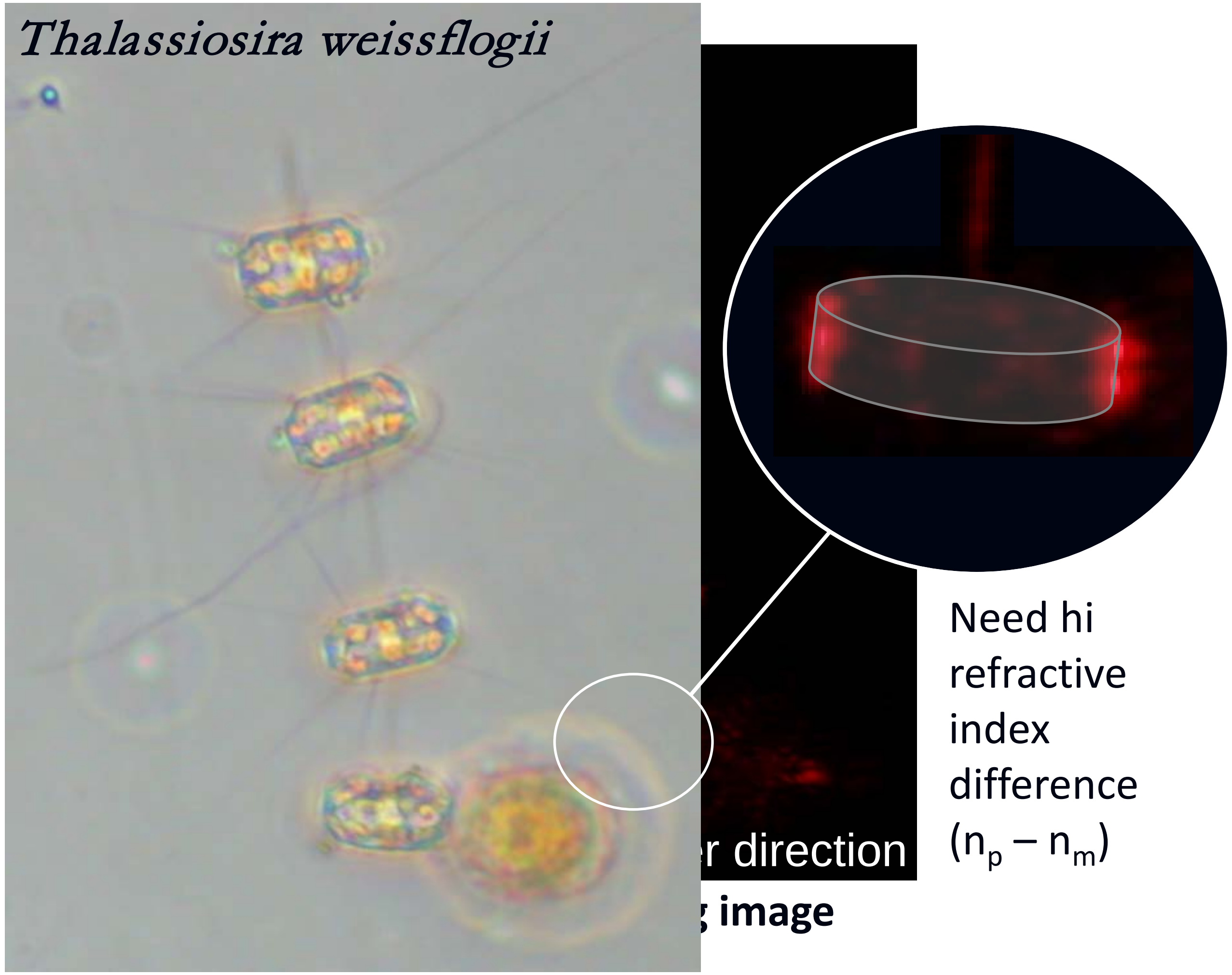

Need hi refractive index difference ($n_p - n_m$)

Twardowski, Sullivan, McFarland (unpubl)

Backscattering ratio and chlorophyll

Gulf of California

9 locations around the coastal US

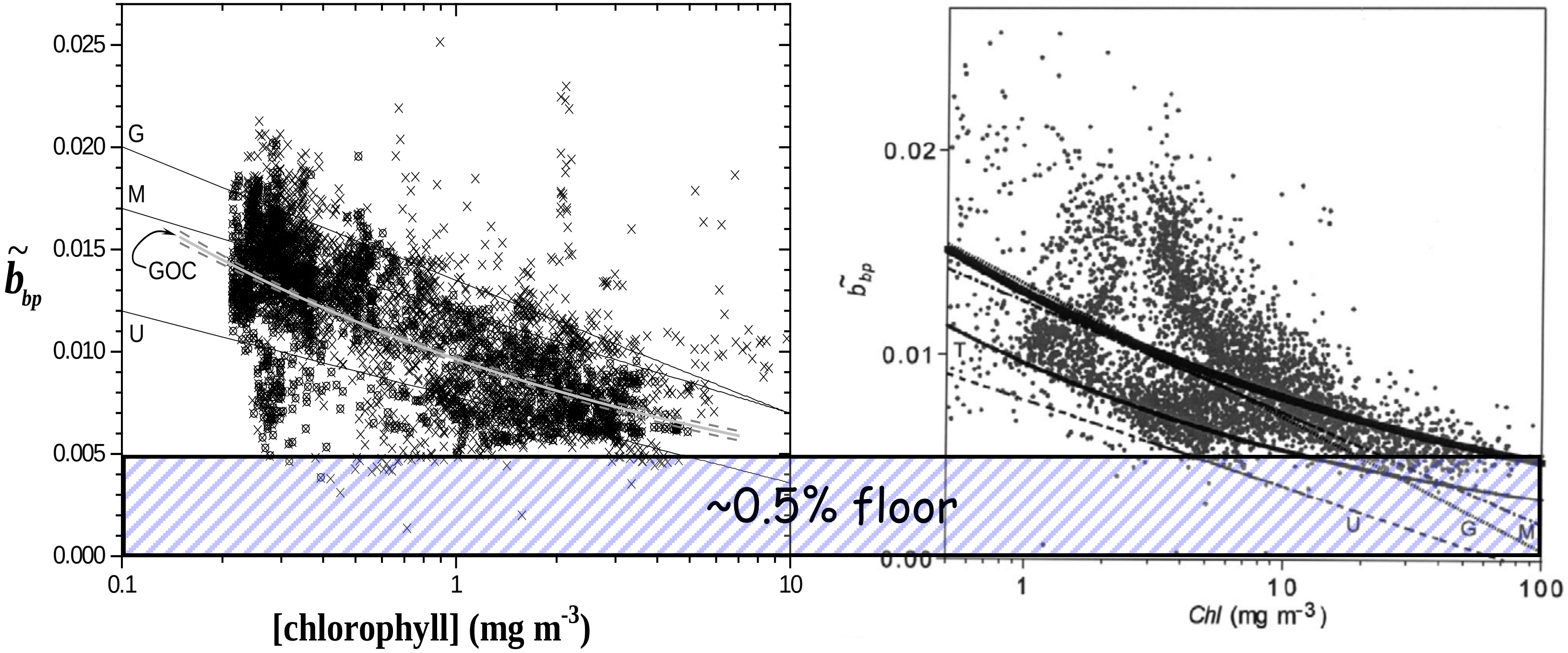

Twardowski et al. 2001

Sullivan et al. 2005

Phytoplankton b_b/b

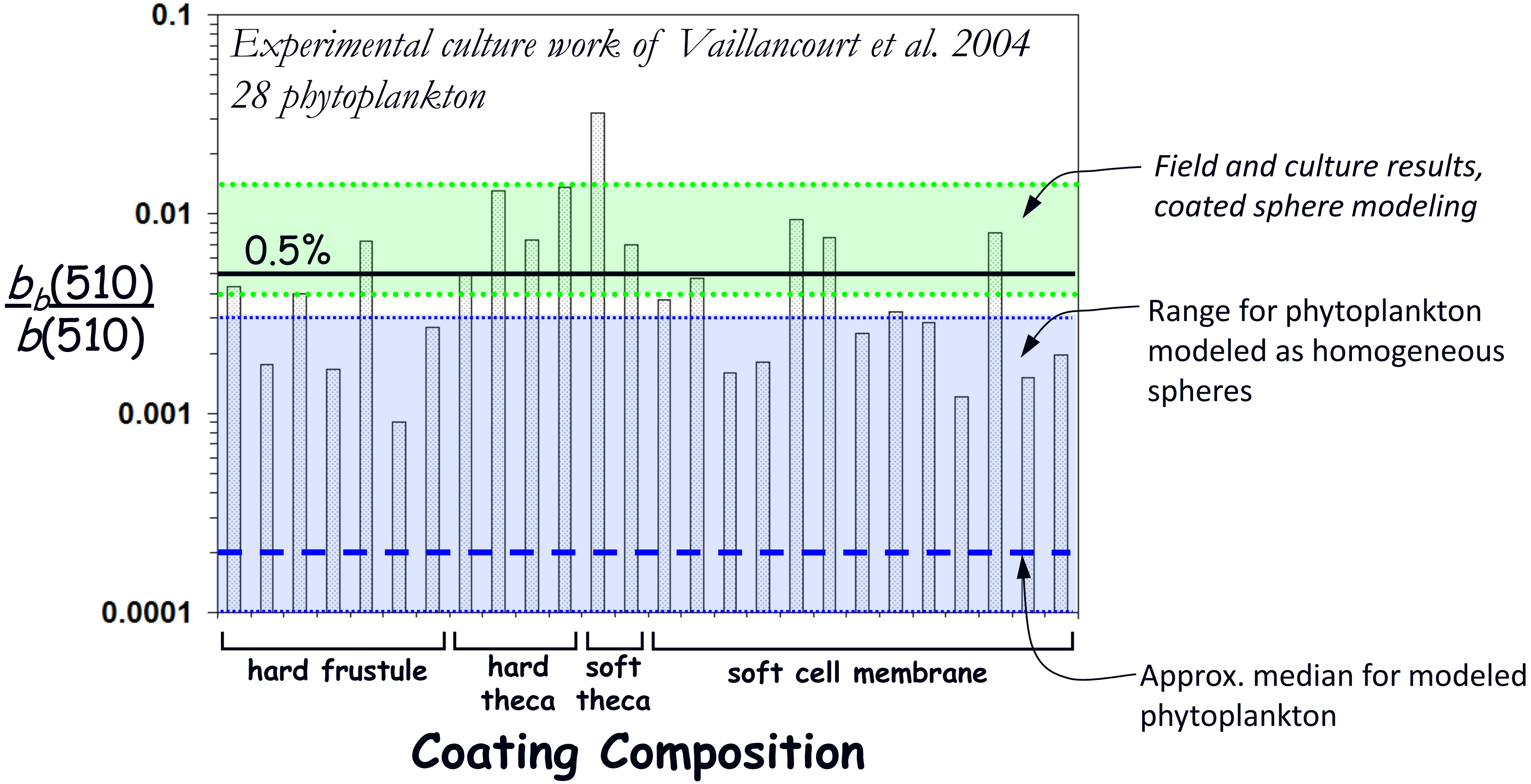

Phytoplankton likely do make a significant direct contribution to b_{bp}

Akashiwo Layer in Monterey Bay

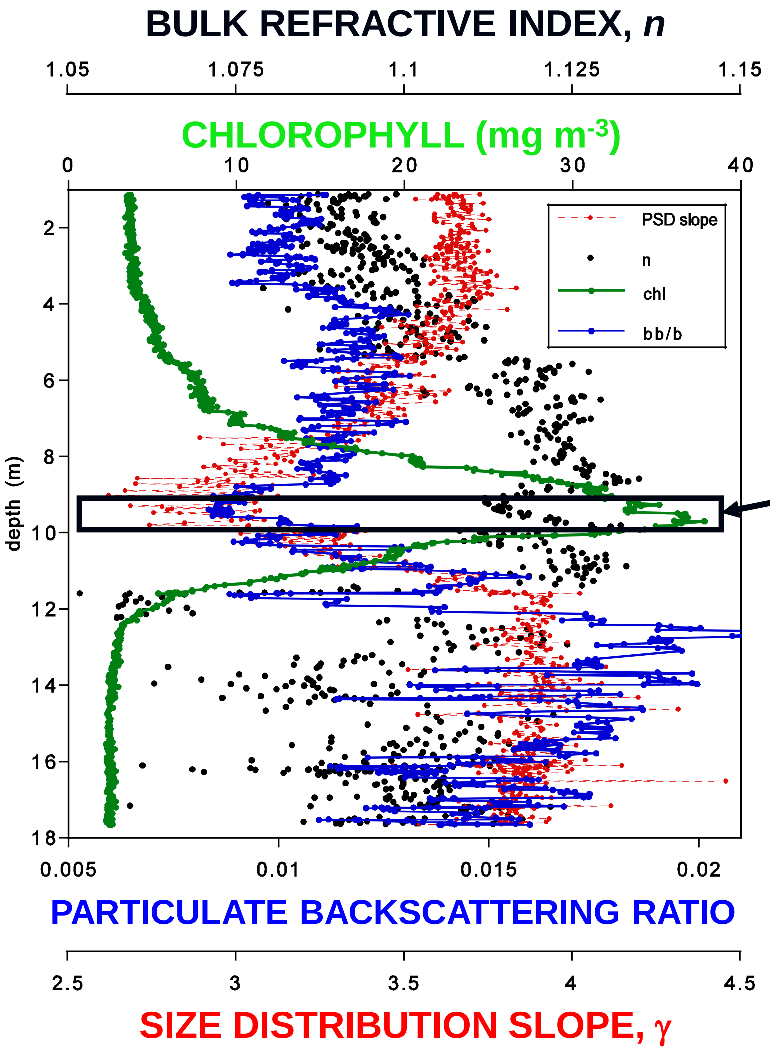

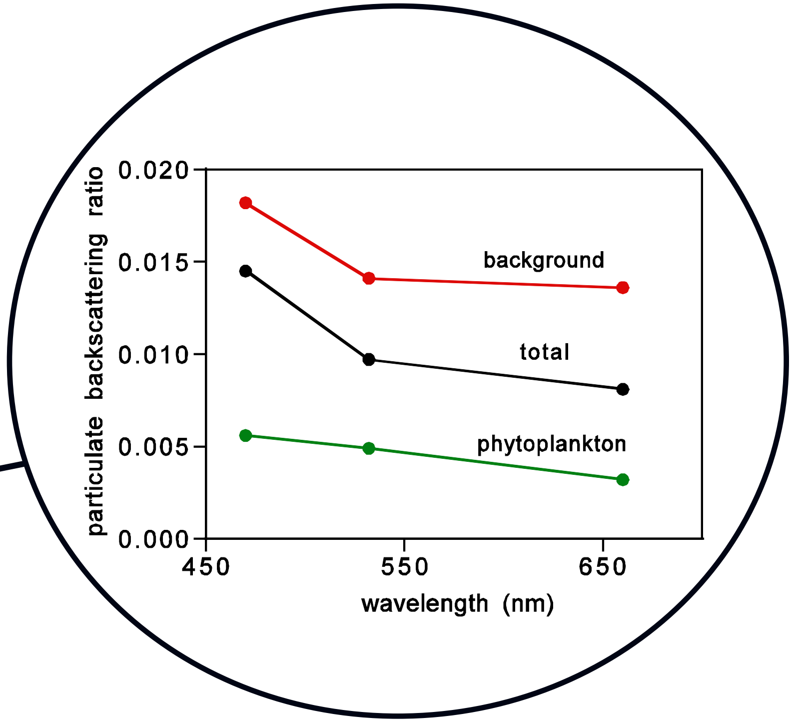

Akashiwo et al.

$b_{bp}(532) / b_p(532) \approx \underline{0.005}$

~$\underline{20\%}$ of $b_{bp}(532)$

Sullivan and Donaghay (unpubl)

Anomalous dispersion

Spectral and angular scattering intensity of a particle is principally dependent on:

- size relative to λ
- complex refractive index relative to the medium $(n - in')$

Anomalous dispersion describes how particle absorption alters the refractive index spectrum,

i.e., if you change a_p, you will change b_p, b_{bp}

Synechocystis

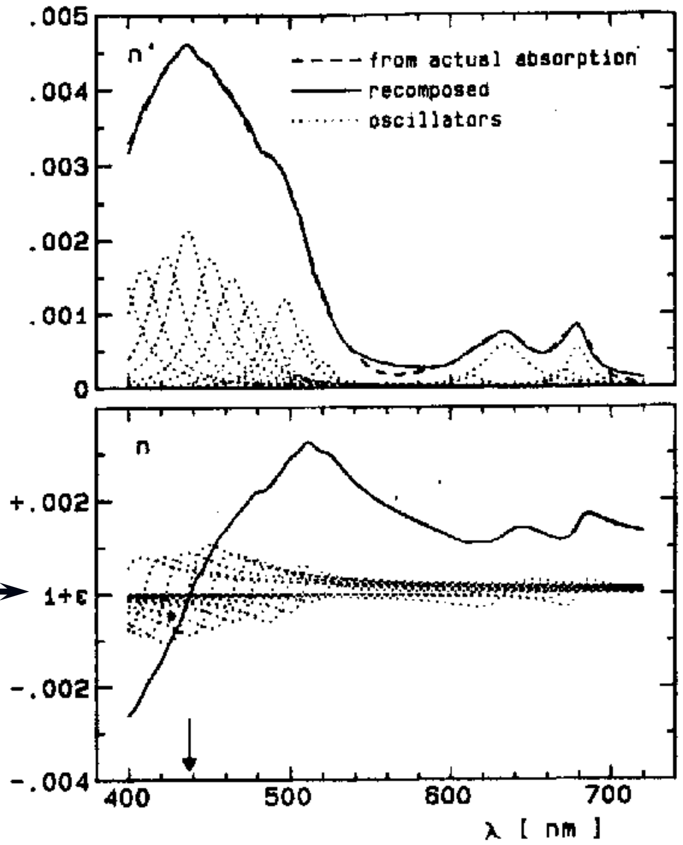

Stramski et al. 1988

around absorption peak

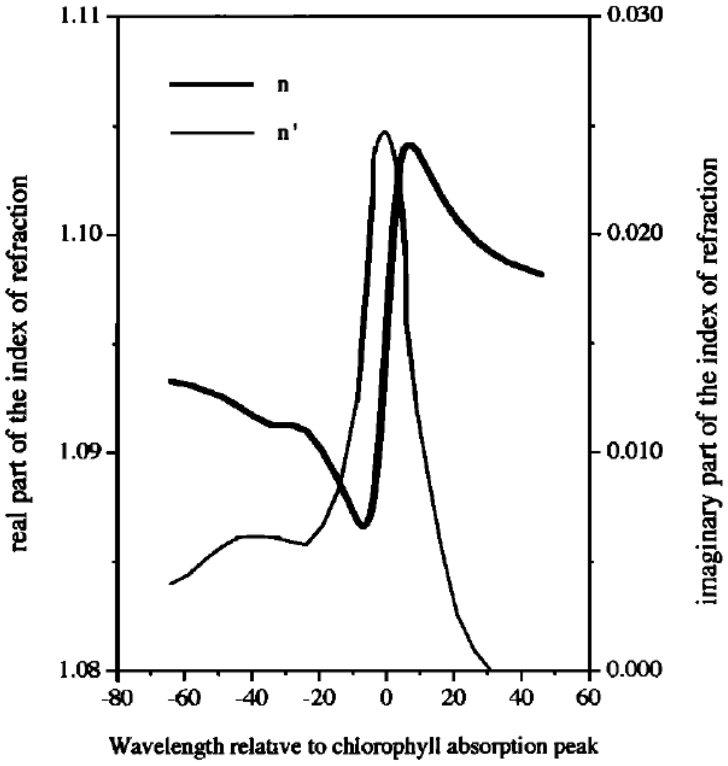

Zaneveld and Kitchen 1995

Spectral scattering by particles

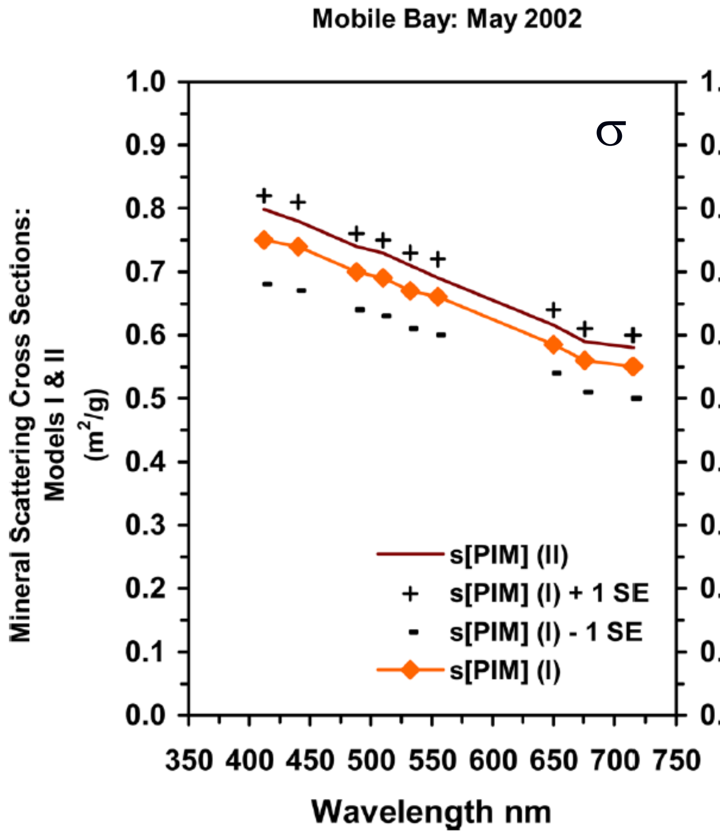

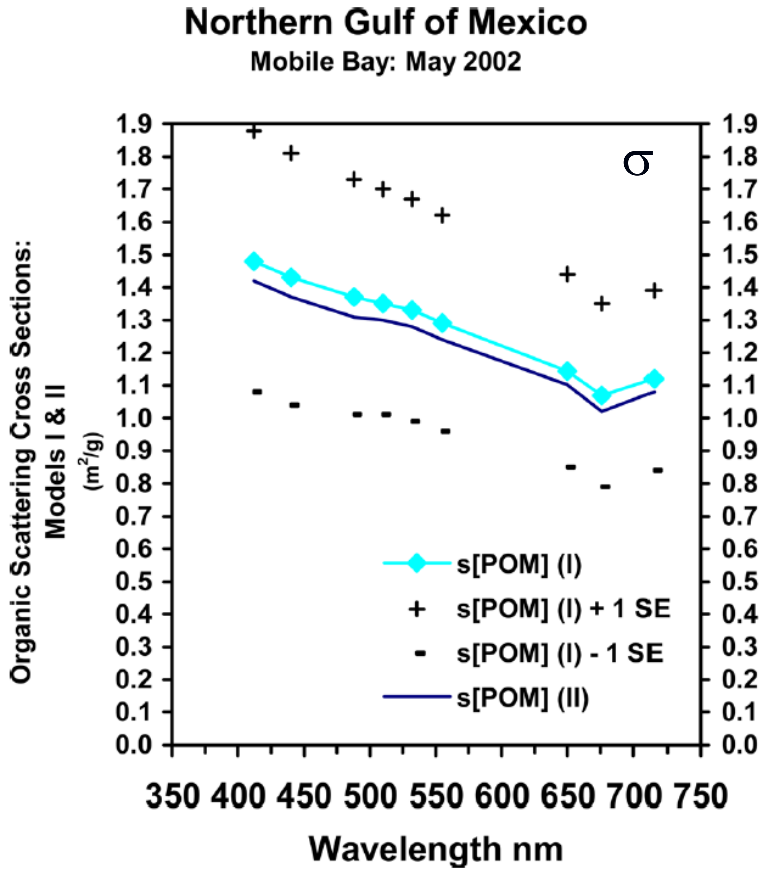

$b_p = \sigma$ PIM

$b_p = \sigma$ POM

Stavn and Richter 2009

Spectral backscattering ratio by particles

For size distribution described by power law, with relatively low absorption, theory predicts spectrally independent b_{bp}/b_p....
(e.g. Twardowski et al. 2001)

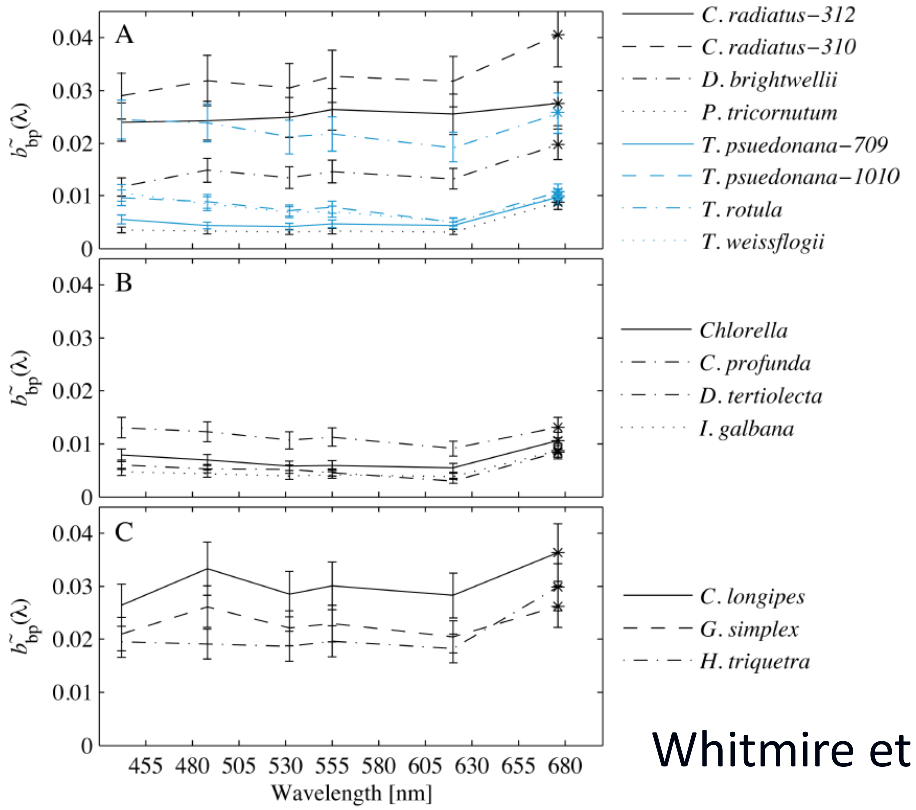

Whitmire et al. 2009

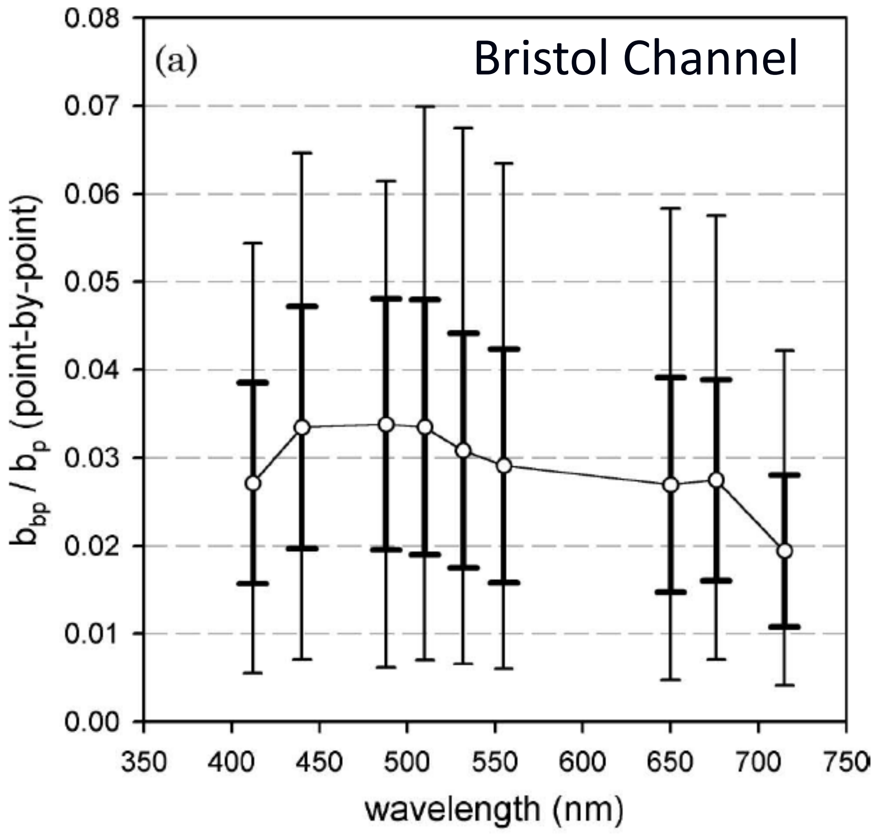

McKee et al. 2009

Models for computing particle scattering

- Rayleigh
- Lorenz-Mie (coated sphere, multi-layer sphere)
- van de Hulst anomalous diffraction approximation
- Geometric optics (IGOM, RBR)
- Discrete dipole approximation (DDA)
- Finite difference, time-domain (FDTD)
- Pseudo-spectral time-domain (PSTD)
- T-matrix (invariant imbedding, multiple sphere, extended boundary condition, many body iterative…)

Each has restrictions: size ranges, *n*, shape and symmetries

Phase functions of randomly oriented asymmetric hexahedra (mineral-mimicking)

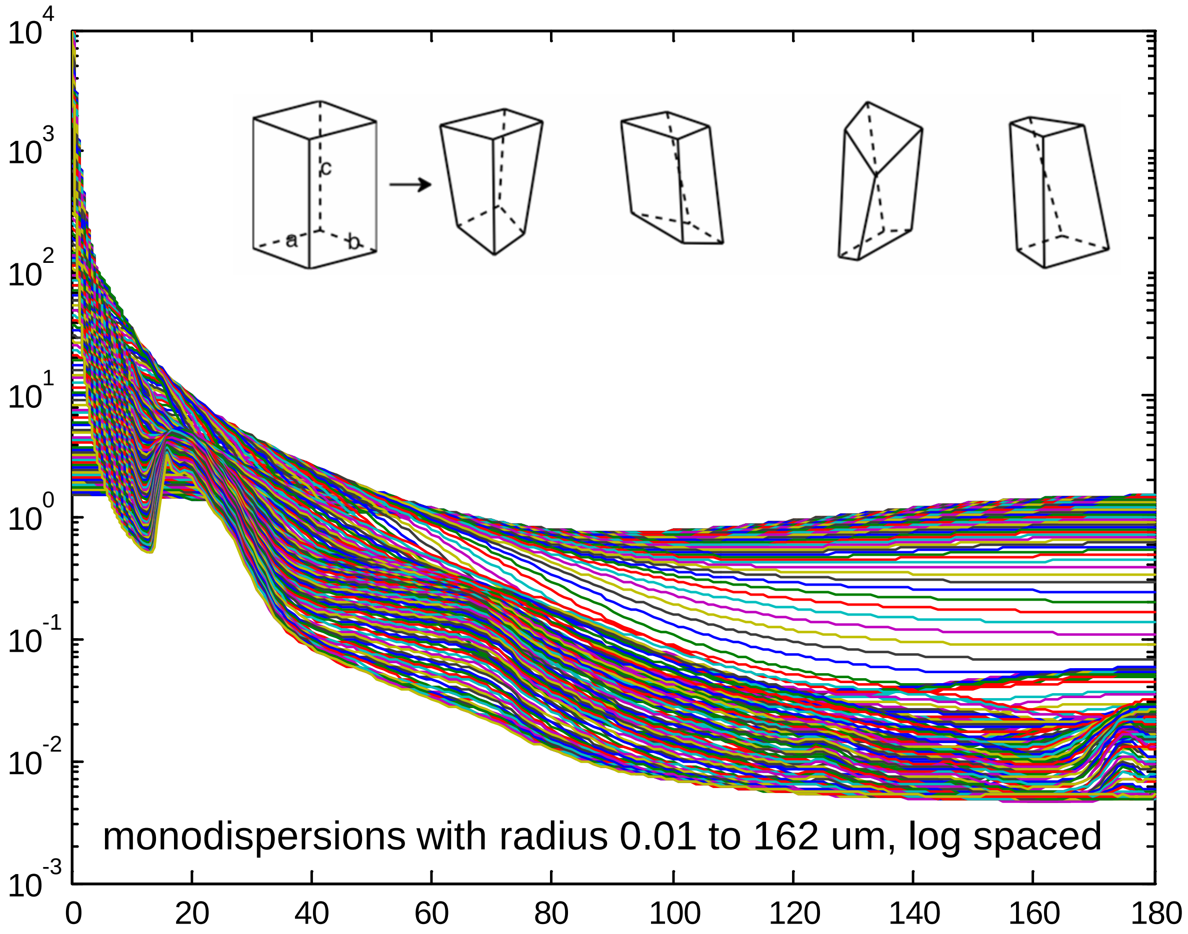

Discrete Dipole Approx (**DDA**)

and

Improved Geometrical Optics Model (**IGOM**)

Twardowski et al. (2012)

Bubbles

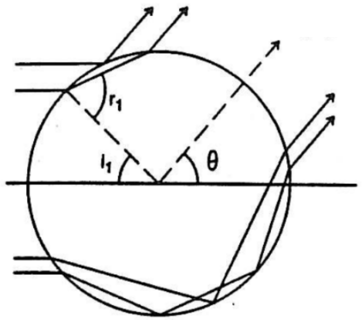

single bubble theory

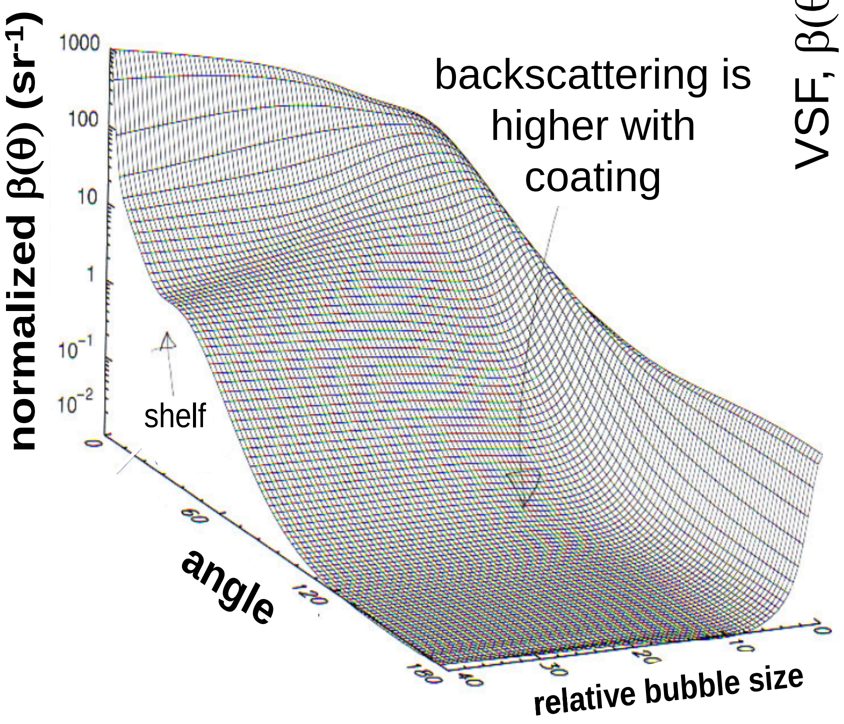

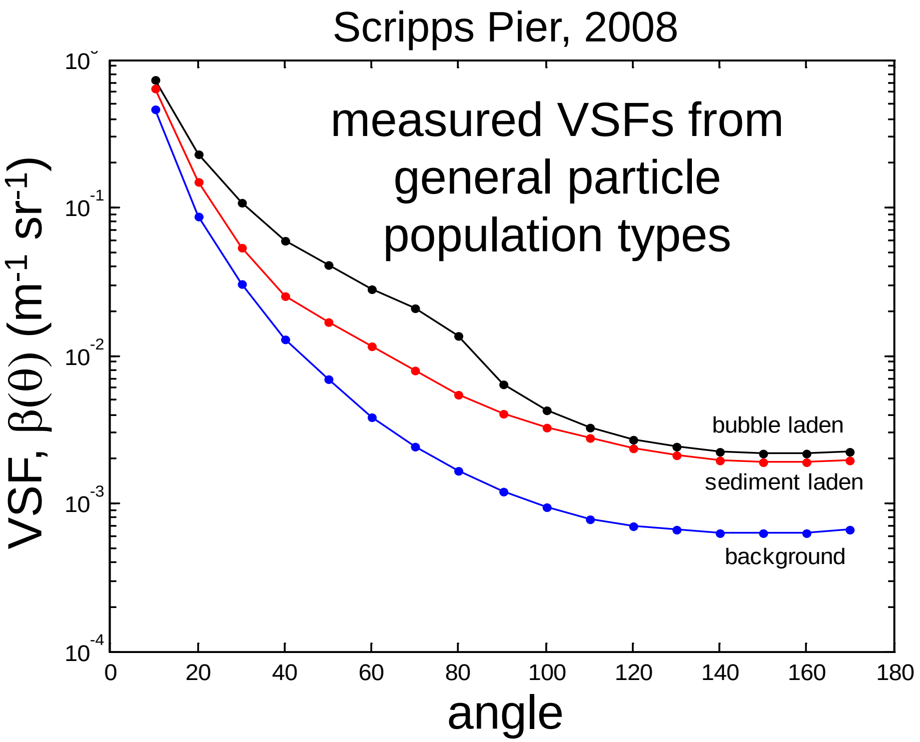

- Different particle populations exhibit different VSF shapes
- Theoretical bubble VSFs verified with *in situ* measurements
- Currently scattering is the only method of resolving small bubbles in seawater

Polarized scattering: effects of bubbles

S12/S11: degree of linear polarization

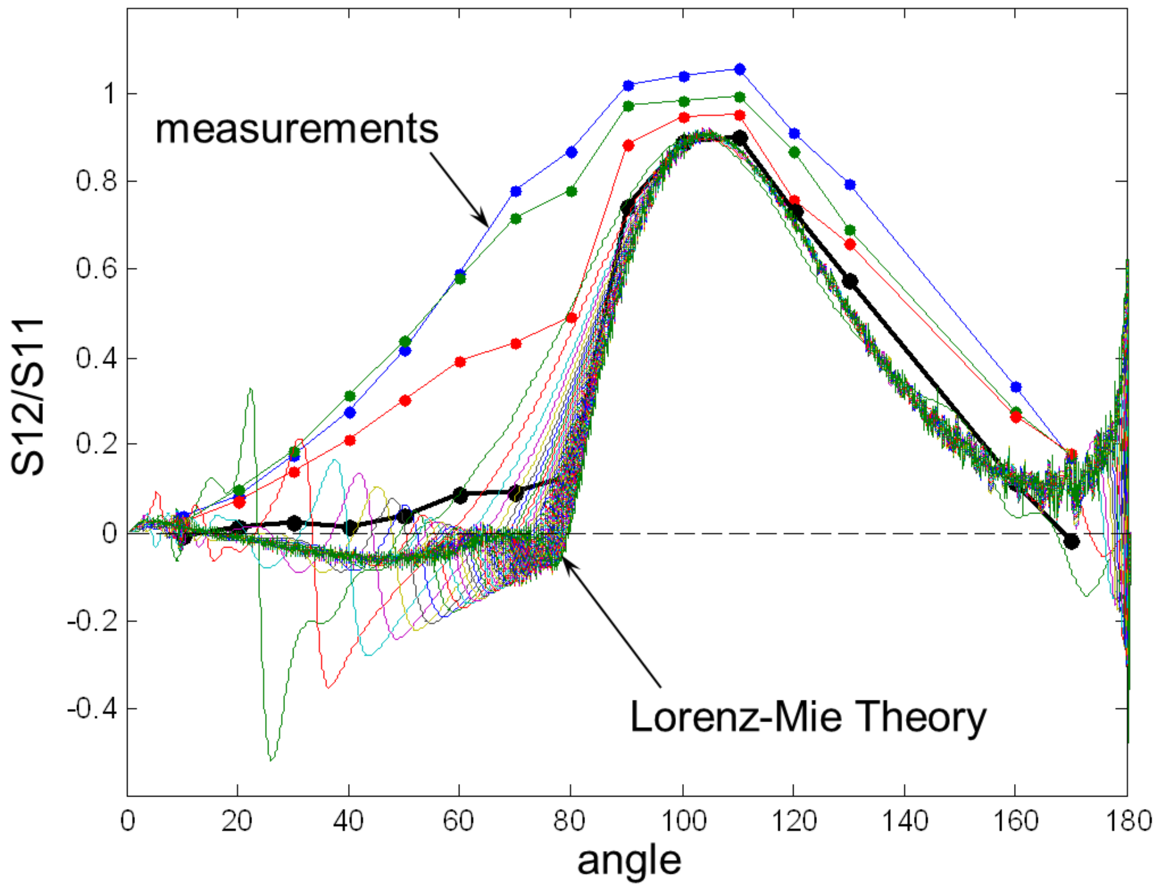

Twardowski et al. (unpubl)

VSF measurement detail

VSF measurement detail

<u>$\beta(\theta)$ *measurements are always resolved over a range of angles*</u>

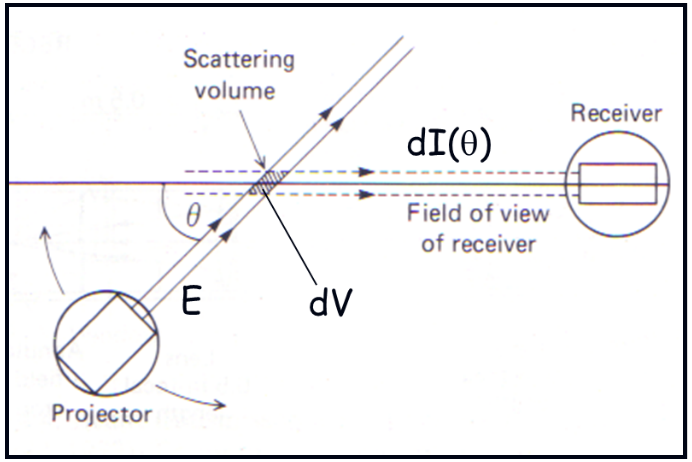

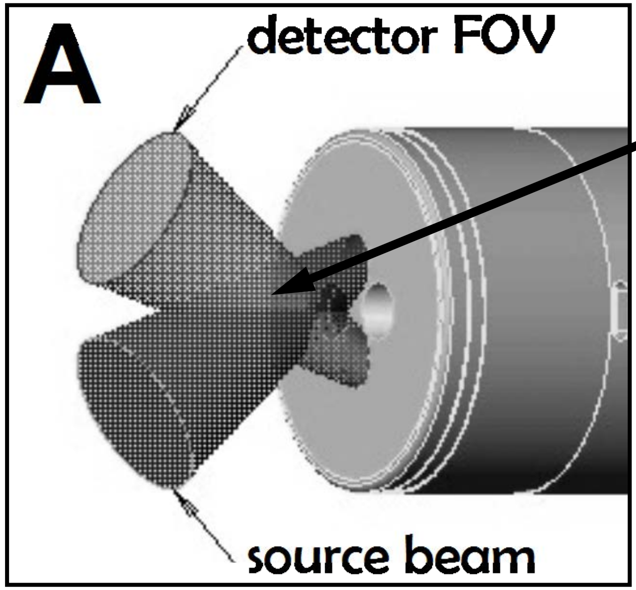

Overlapping volume defines W(θ)

W(θ) weighting function

$\bar{\theta}$ centroid angle

$$\bar{\beta}(\bar{\theta}, \Delta\theta) = \int_0^{\pi} \beta(\theta) W(\theta)\, d\theta$$

Example of WET Labs ECO geometries

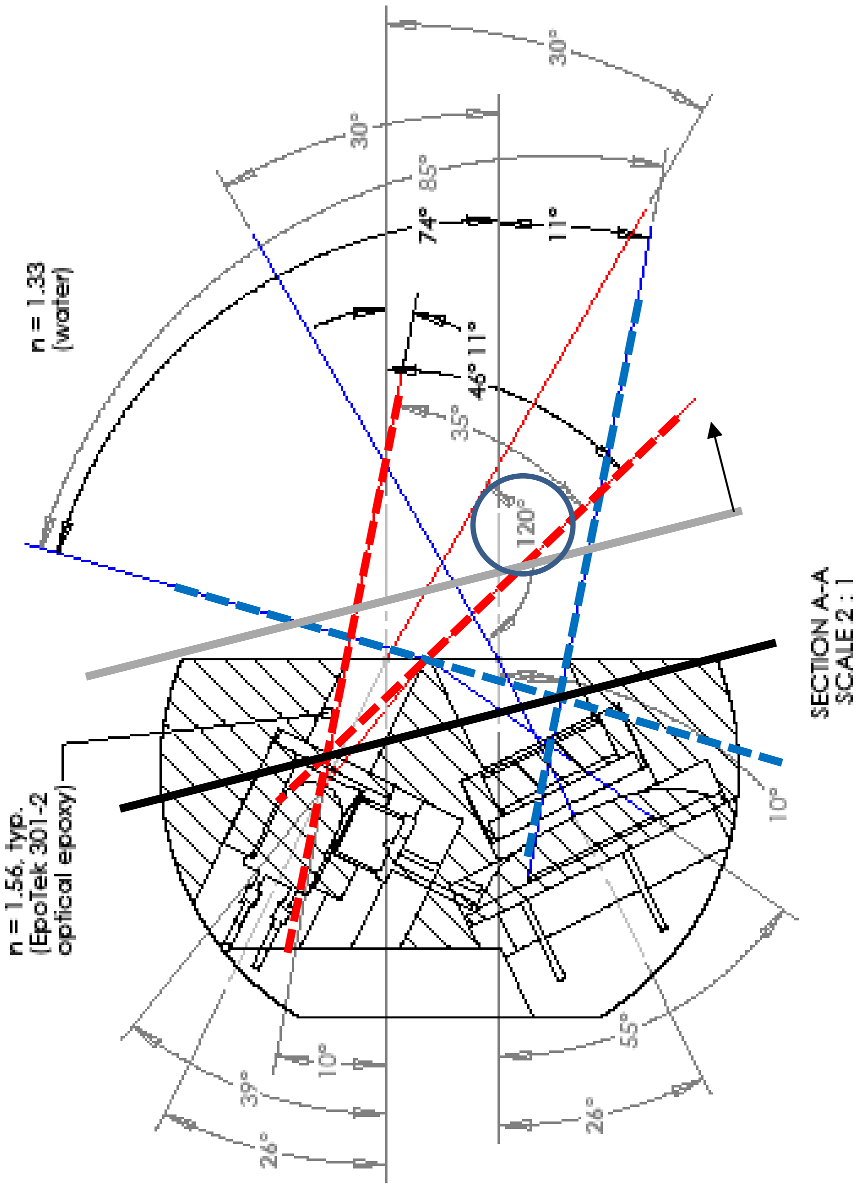

ECO-BB geometry

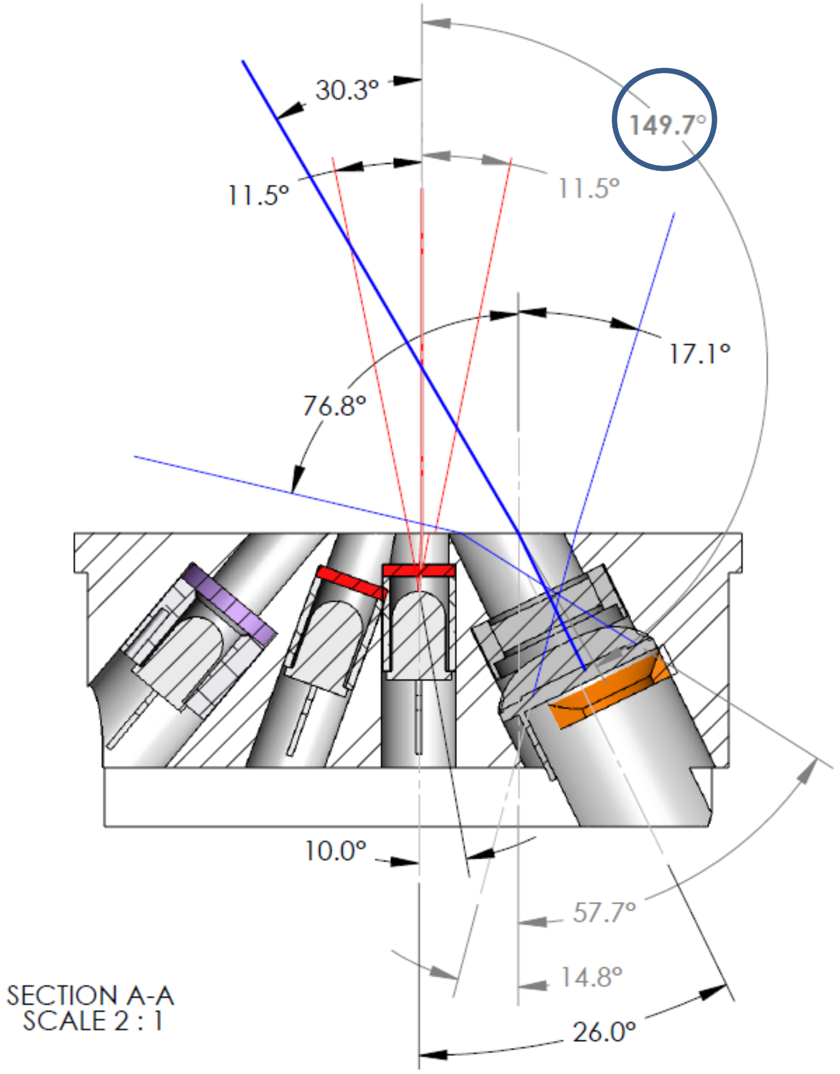

ECO-VSF geometry
(150°)

WET Labs MCOMS

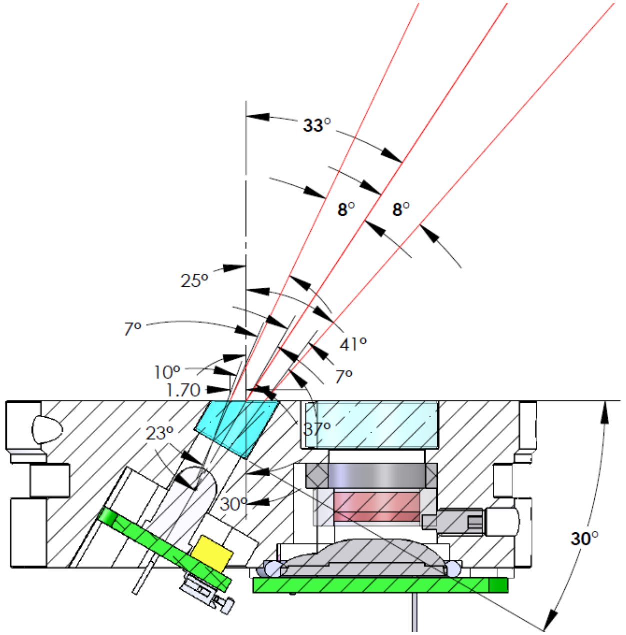

SECTION A-
SCALE 2 :

These angles are approximate.

- The detector has an epoxy dome that has some lensing effect.
- The filter loses efficiency as angle increases.

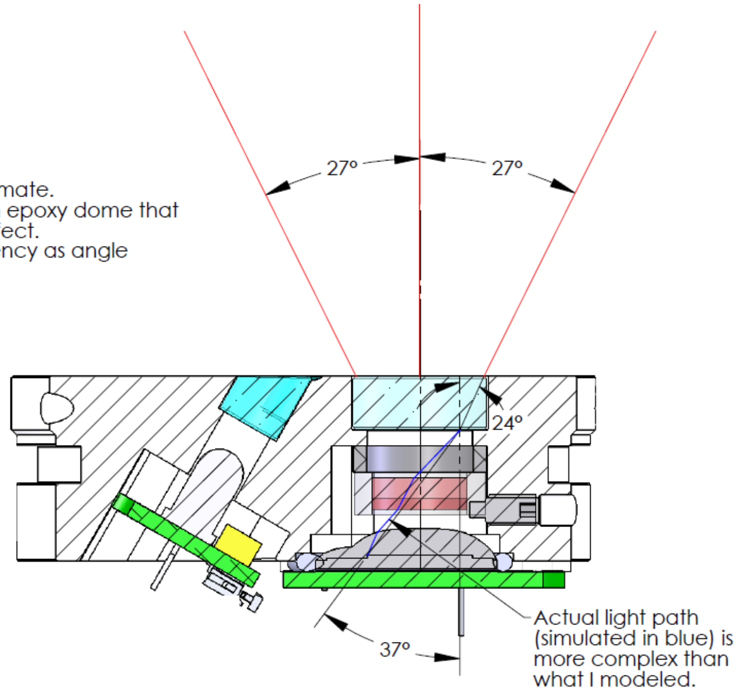

SECTION B-B
SCALE 2 : 1

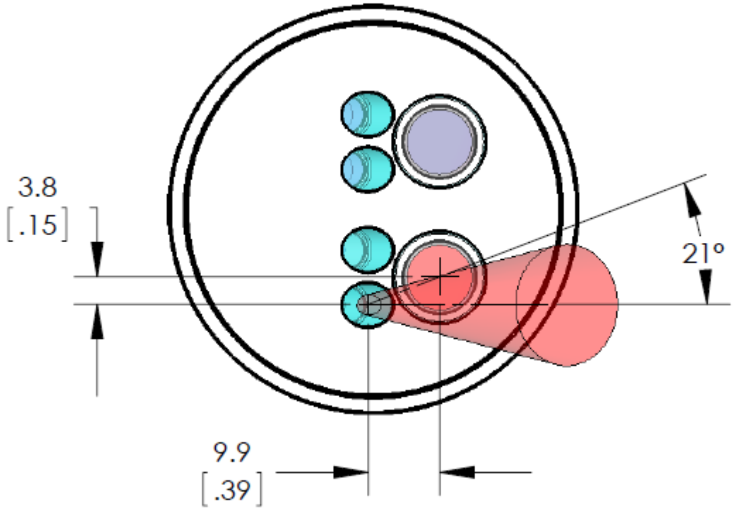

Determining W(θ)

Experimentally (Maffione and Dana 1997) – the plaque method
Analytically (Sullivan et al. 2013) – the "virtual plaque" method

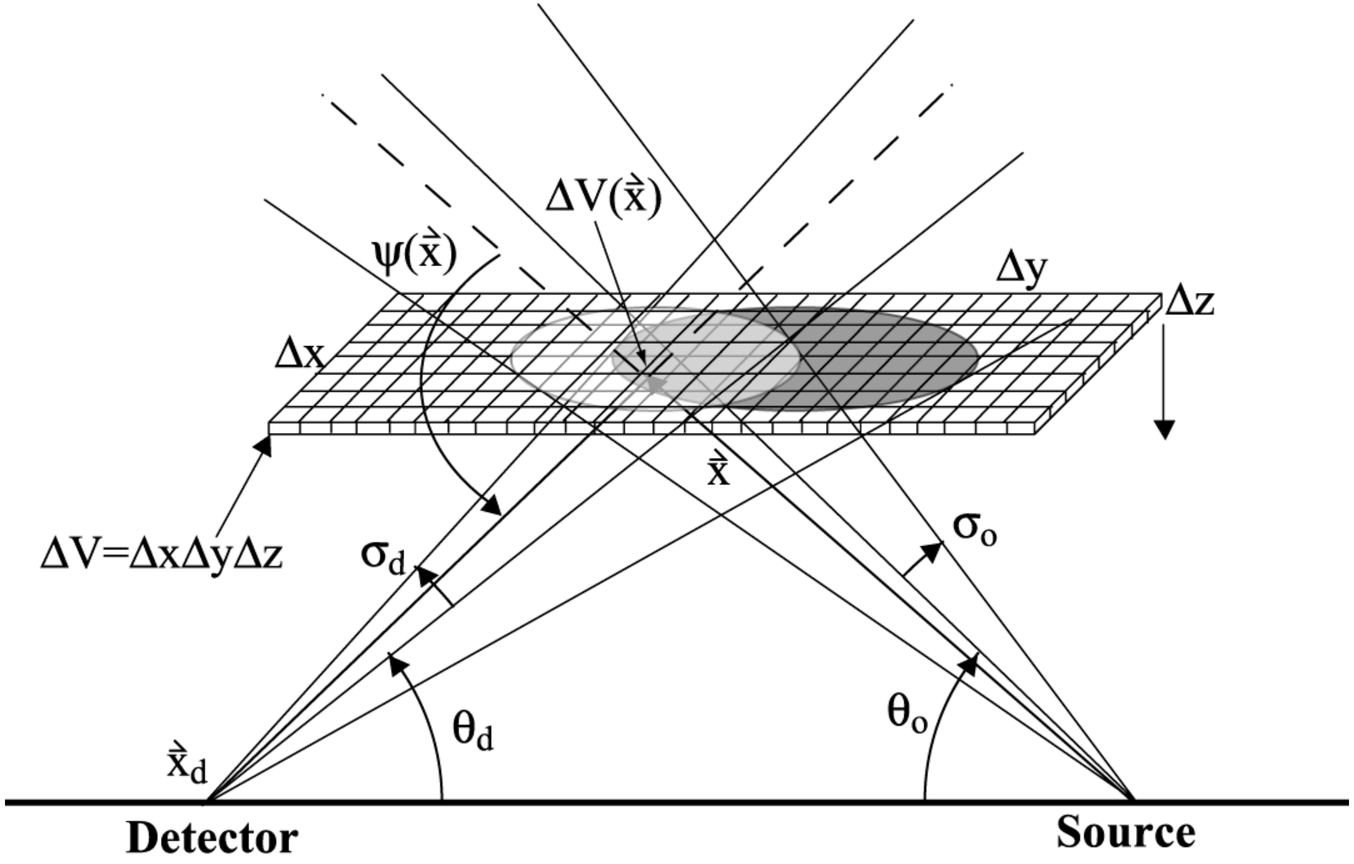

VIRTUAL METHOD

- Step virtual plaque through sample volume
- Determine area where source and detector beam images overlap for each z step
- Calculate power returned to detector at each dV in the overlapping area (note there is no consideration of VSF in doing this)
- Assign θ to each dV
- Compile results (i.e., fill θ bins) to derive weighting function

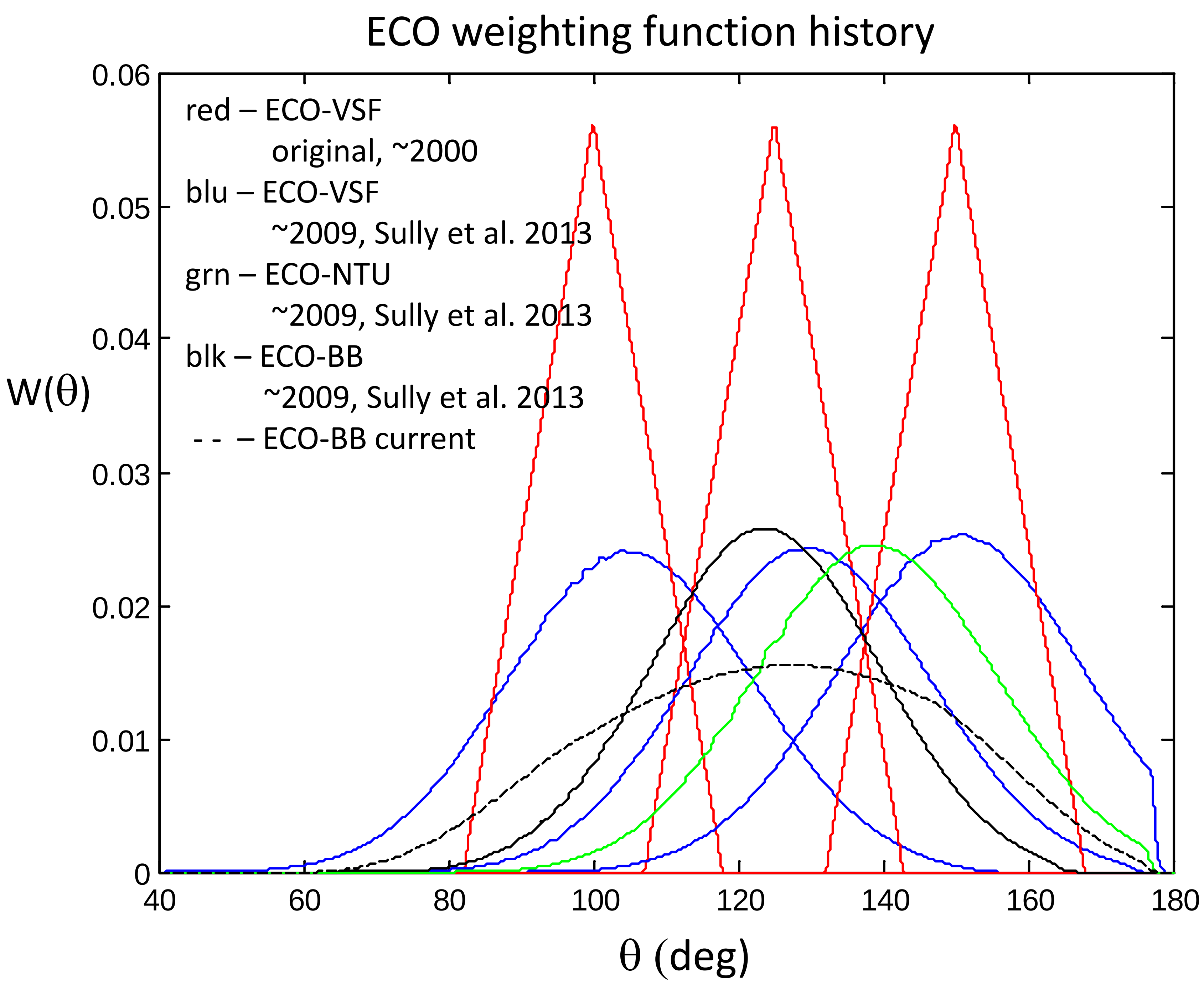
ECO weighting function history
red – ECO-VSF
original, ~2000
blu – ECO-VSF
~2009, Sully et al. 2013
grn – ECO-NTU
~2009, Sully et al. 2013
blk – ECO-BB
~2009, Sully et al. 2013
- - – ECO-BB current
W(θ)
θ (deg)
0.06
0.05
0.04
0.03
0.02
0.01
0
40
60
80
100
120
140
160
180

Calibration: Step 1

Compute phase function of easily modeled particle solution (e.g., microspherical beads) and convolve with W(θ)

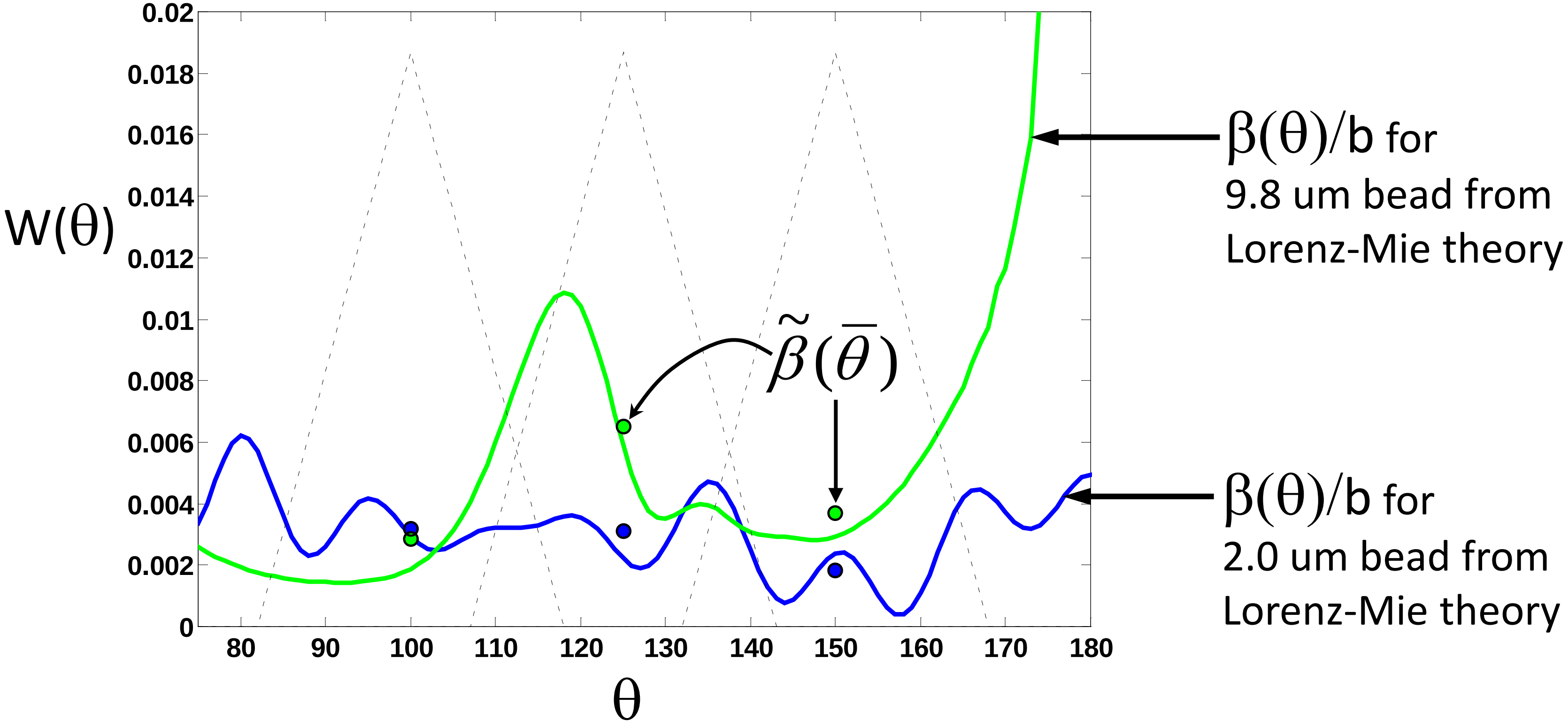

***use a Rayleigh scatterer (*d* < λ) for best results**

Calibration: Step 2

Place sensor in the solution with known phase function and measure raw digital counts and *b* (with ac9)

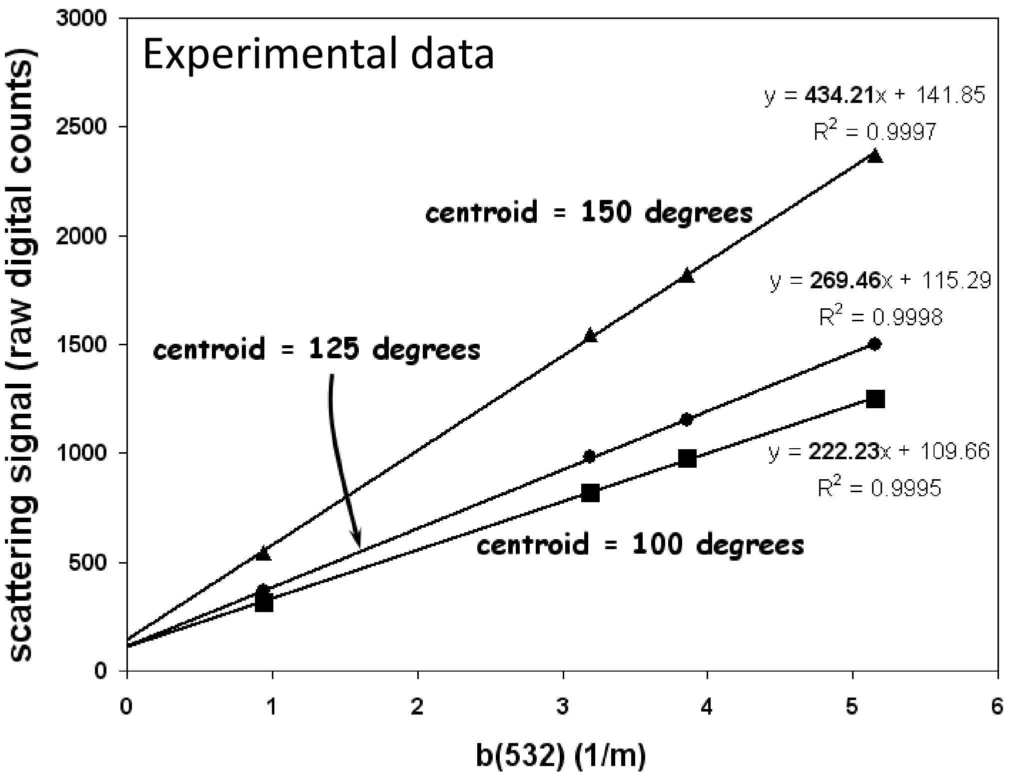

Intercepts are nonzero because
1) scattering sensor dark counts
2) ac9 is not calibrated precisely
3) insufficient water purity

<u>these do not matter</u> because the slope is what you care about, i.e., the change in counts per change in *b*

Calibration: Step 3

<u>Compute scaling factor, SF</u>

experimental

$$SF = \frac{\beta(\bar{\theta})}{b}\frac{b}{counts} = \frac{\beta(\bar{\theta})}{counts}$$

theory

Calibration: Step 4

<u>Determine dark offset, DO</u>

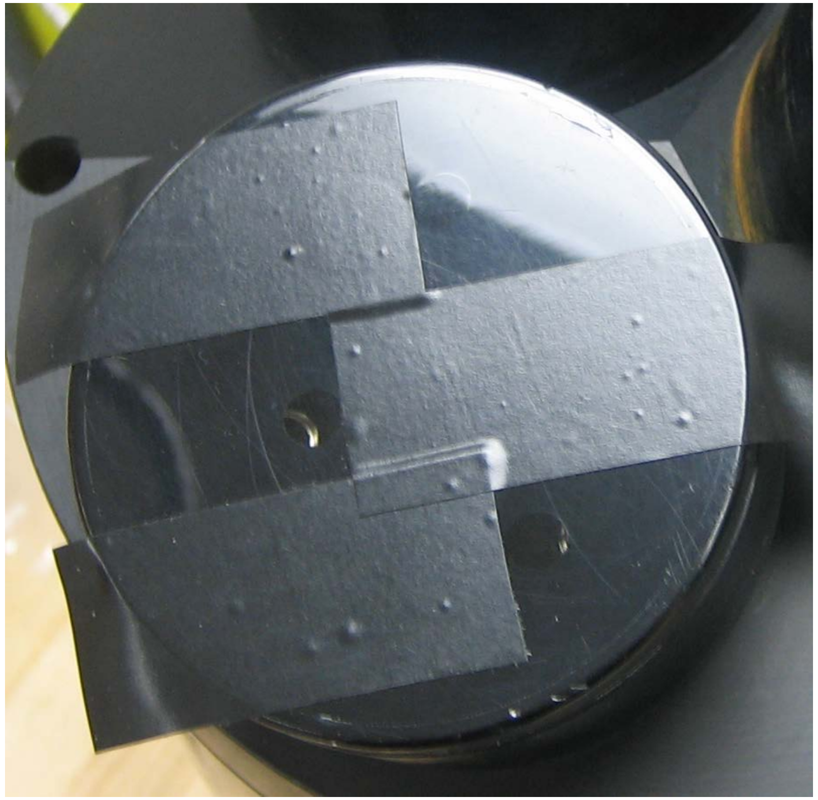

- -black tape over
  <u>detector only</u>
- -put in water to match
  refractive index
- -average time record
  (~30 s)

Applying the calibration

$$\beta(\overline{\theta}) = \text{scaling factor} \left(\text{raw counts} - \text{dark offset} \right)$$

Important…

- All $\beta(\theta)$ measurements are not equal due to instrument-specific $W(\theta)$
- Measurements of $\beta(\theta)$ in the field *will include water*. Water from highest quality purification systems is not close to being clean enough for calibations (pure water itself is several counts of signal)
- Ambient light rejection circuitry important for backscattering measurements

Correction for attenuation

Sometimes *required because light is attenuated on its way to and from the sample volume*

For bead calibration, scattering portion of attenuation is inherently corrected (close enough for ECOs…)

only need to correct for absorption when it is very high (> ~2 1/m)

$$\beta_{corr} = \beta_{meas} \exp(aL)$$

This is an approximation, valid when pathlength L is small

When pathlength is not small: MASCOT
(Multi-Angle SCattering Optical Tool)

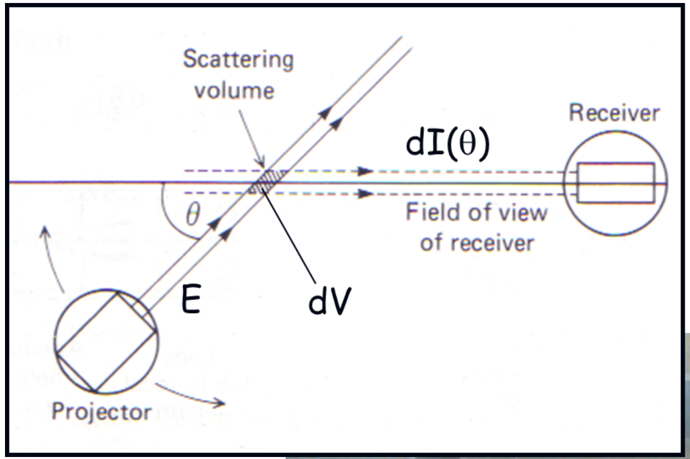

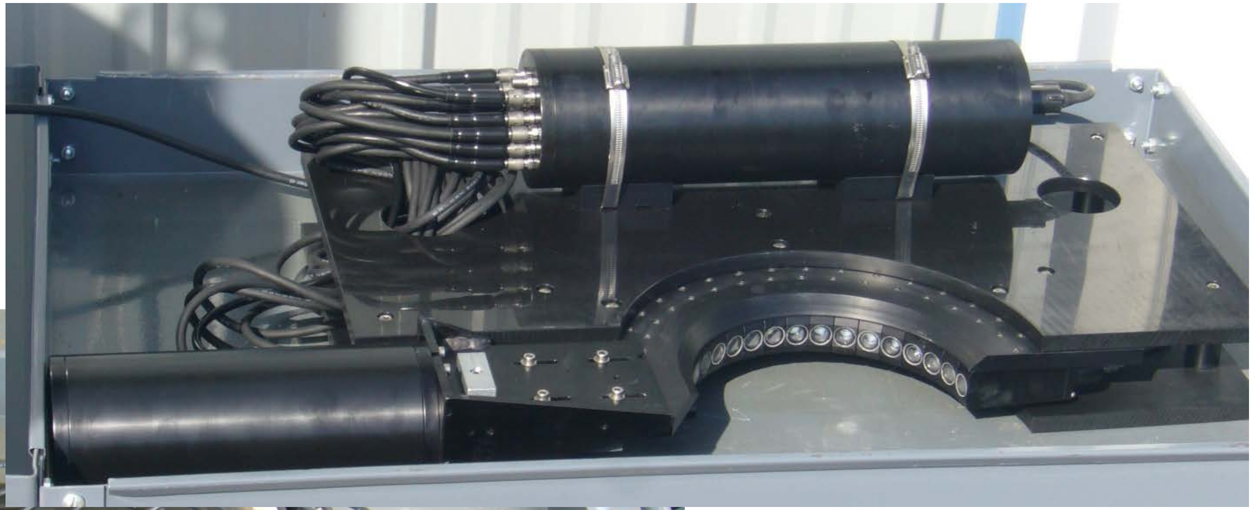

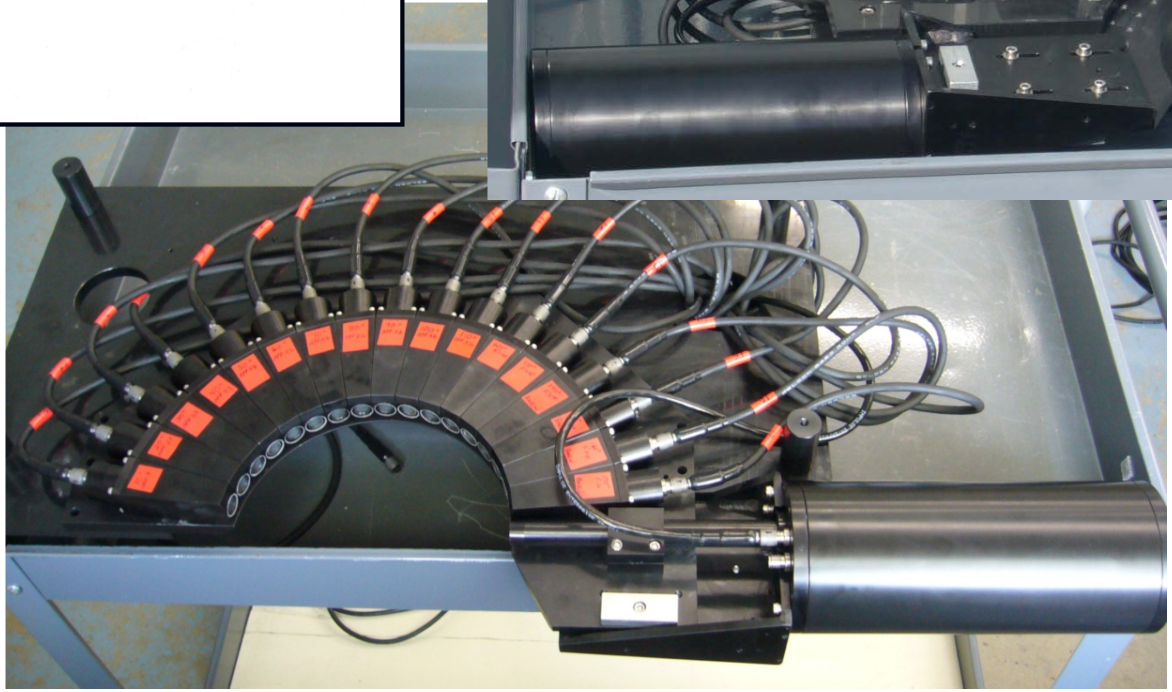

Full correction for attenuation

$$\beta(\overline{\theta}_i) = \frac{R_{cal}}{R_m}[\Phi_i - D_i] f_i e^{L[b_p \varepsilon + a_{pg} + a_w]}$$

R – source references

ε – fraction of scattering that is not included in the measurement

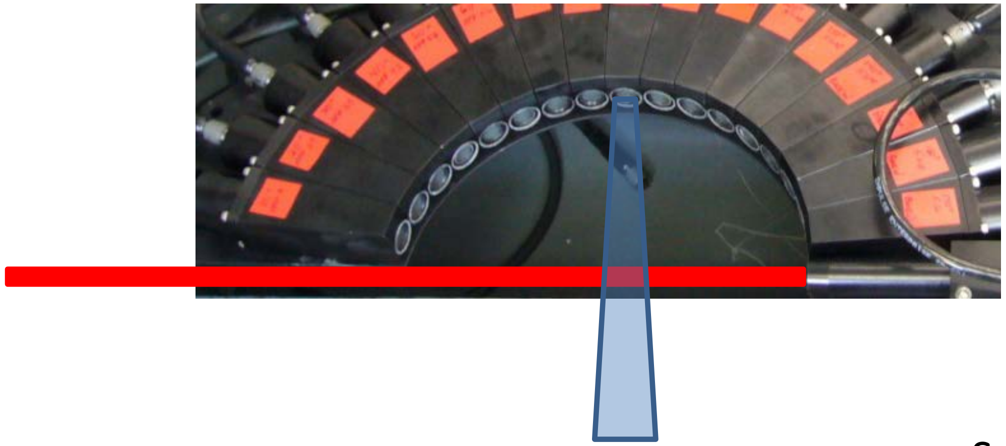

L ~ 20 cm

See Twardowski et al. (2012) for full details

Obtaining backscattering coefficients with β at limited θ

With a single $\beta(\theta)$ in the backward hemisphere

$$b_{bp} = \chi(\theta) 2\pi \beta_p(\theta)$$

Much discussion over which θ and which χ to use:

- Oishi (1990): **120°**
- Maffione and Dana (1997): **140 °**
- Boss and Pegau (2001): **117 °**
- Sullivan and Twardowski (2009): **118 °**

For most accurate current protocol, see Sullivan et al. (2013)

Deriving total scattering (*b*) from *a* and *c*: WET Labs ac-9 and ac-s

ac-s

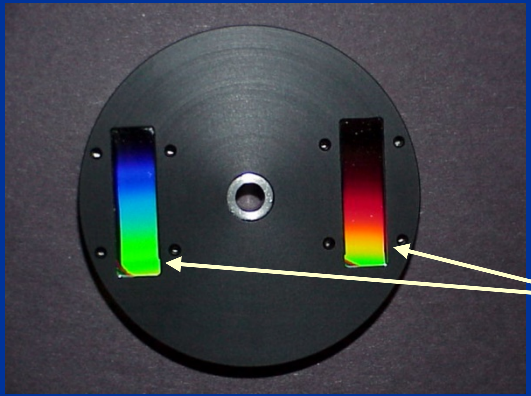

filter wheel

ac-9 has 9 individual interference filters

Linear Variable Filters (LVFs)

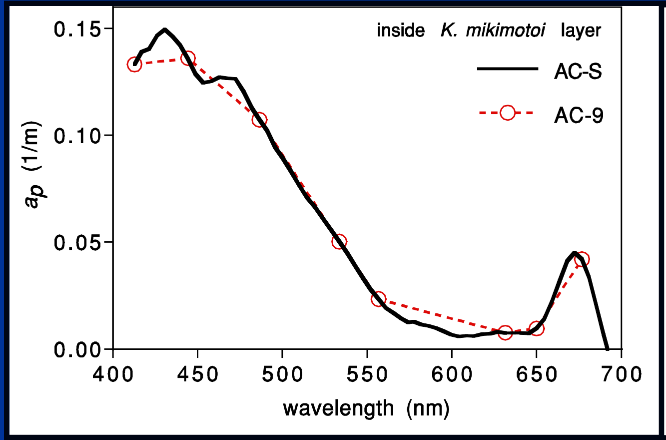

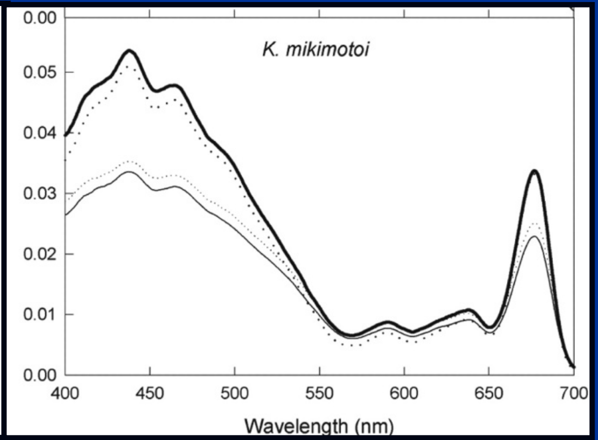

Sullivan and Donaghay (2004)
Irish fjord

Stahr and Cullen (2003)
In culture

c_{pg}, a_{pg}, a_g, c_p, a_p, b_p from dual ac's

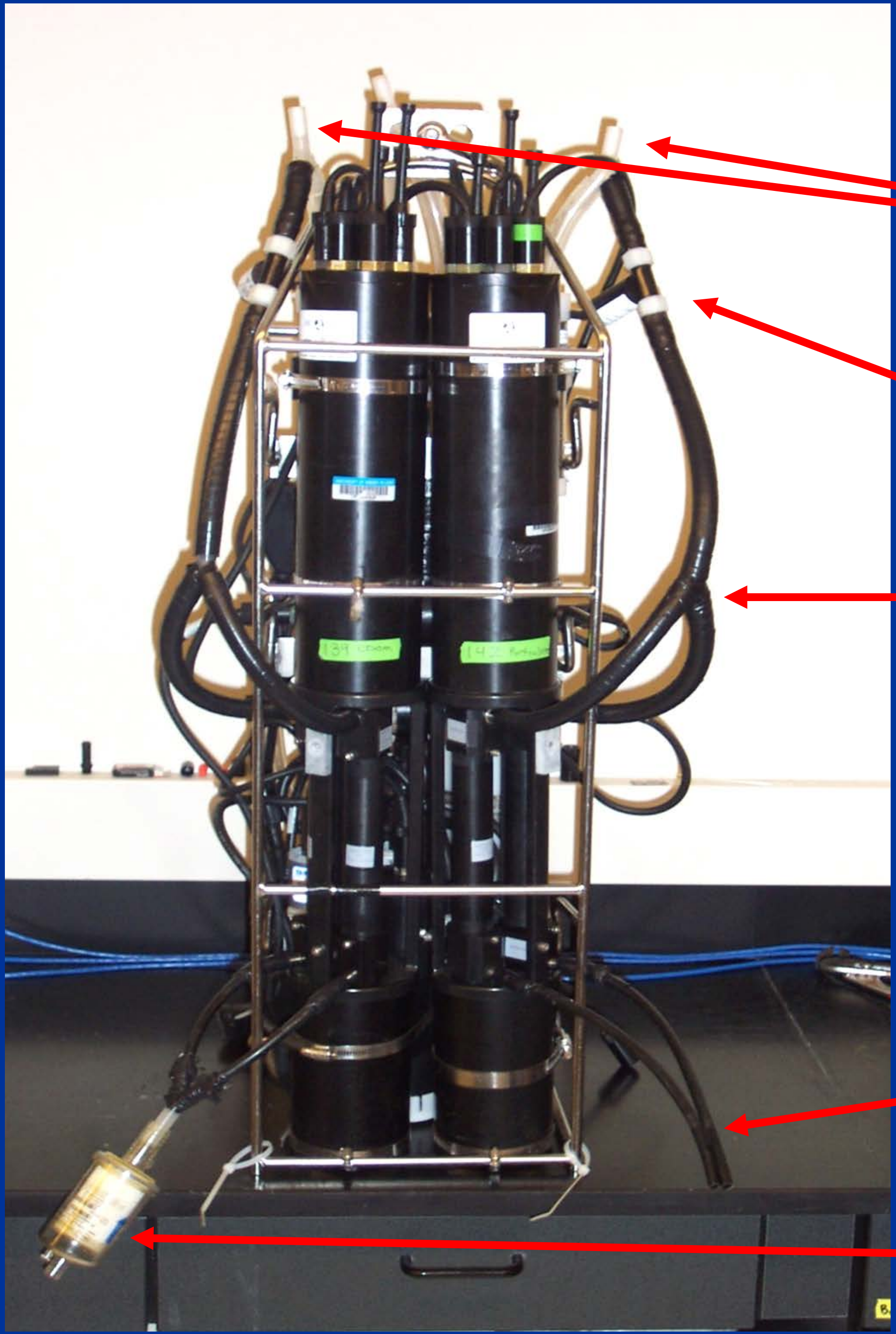

degassing "Y's"
(pumps below Y's)

in-line flow sensor

"Y" on outtakes

"smooth" flow paths

unfiltered (separate intakes)

0.2 µm pre-filter (using Y intake)

Anatomy of a beam attenuation meter (transmissometer)

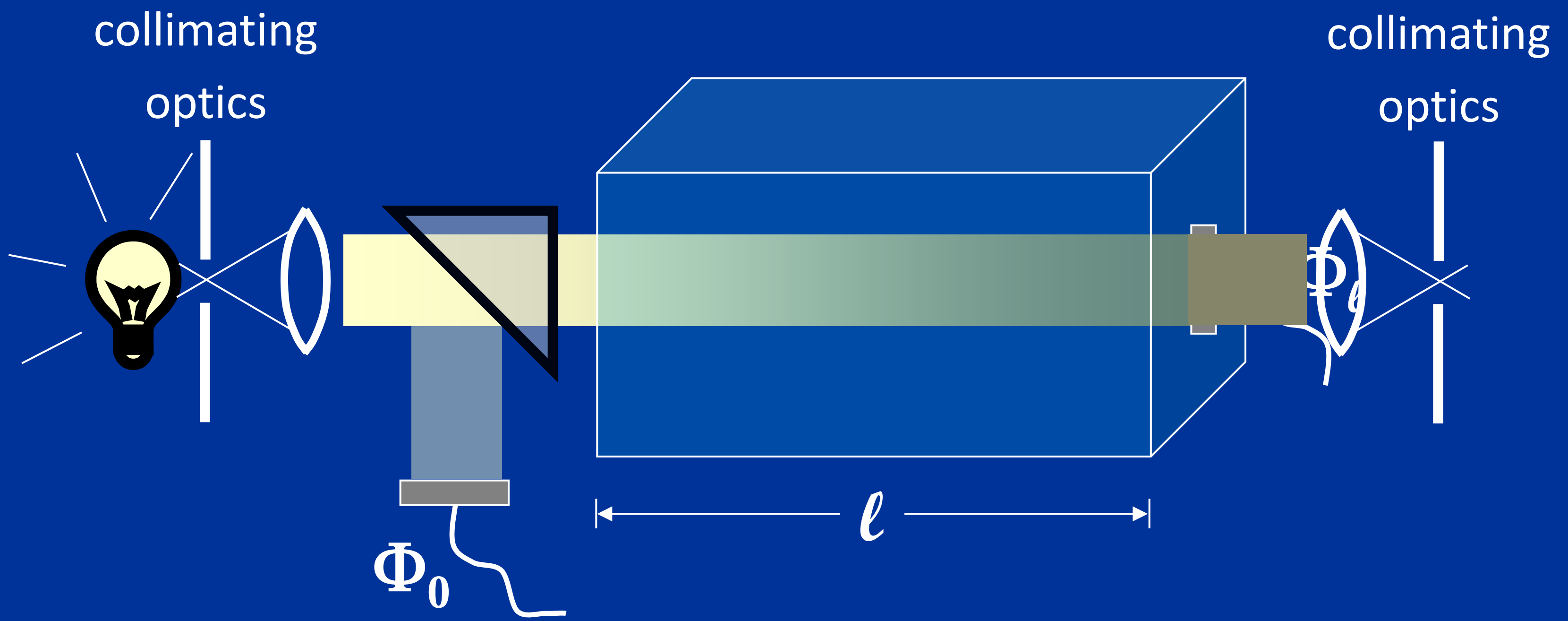

Problem: some scattered light also reaching detector

The theoretically ideal attenuation meter has an acceptance angle of ~0° but at 0° no light is received – need to compromise

Beam attenuation errors from near-forward scattered light

Table 1. Configuration specifications on beam attenuation meters

Instrument	beam source	beam width	acceptance angle (degrees)	pathlength (cm)
AlphaTracka	LED	15 mm	0.86	5
Sequioa LISST	solid state diode laser	6 mm	0.018, 0.036	5
WETLabs ac9	collimated incandescent bulb	10 mm	0.93	25
WETLabs cstar	L			

Instrument design must make compromises in acceptance angle, θ_a :

- Size
- S:N, accuracy
- T ulence at <0.1°

Errors dependent on both

optical geometry

AND

natural shape of VSF

Remember…

volume scatt

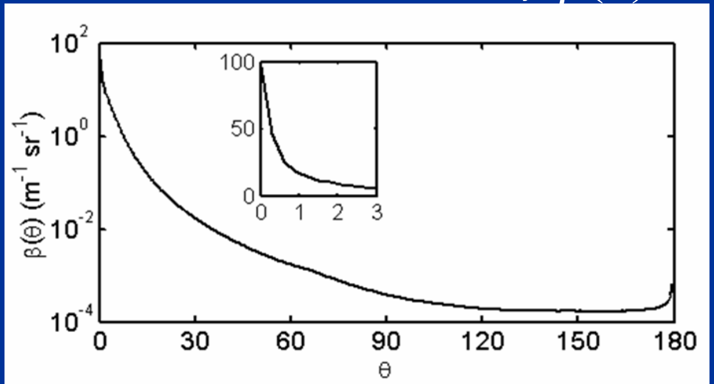

	tected
<0.1°	few percent?
0.7°	15-25%
0.93°	19-30%
1.5°	25-37%
1.9°	28-42%

based on Petzold VSFs

Accuracy

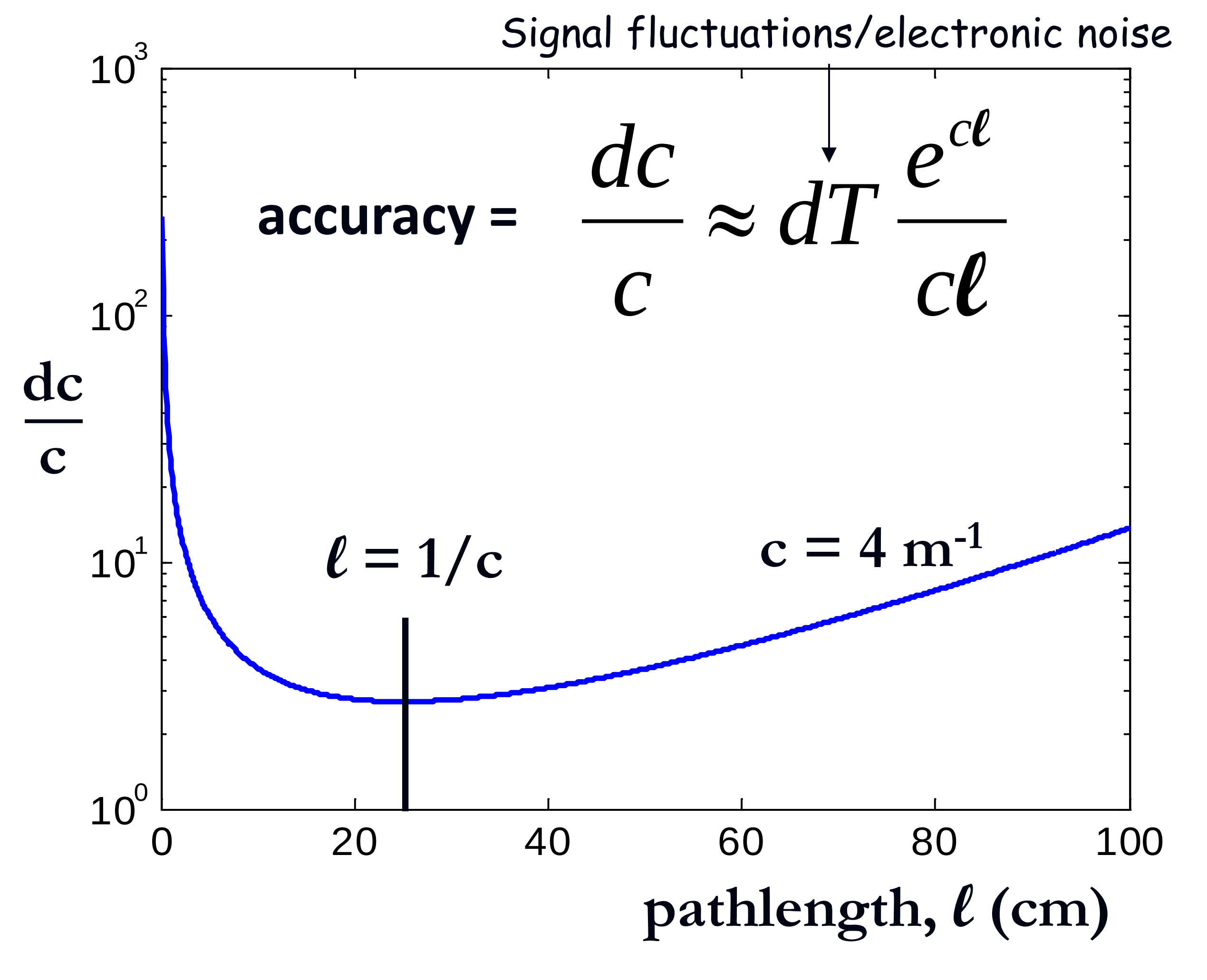

Accuracy is optimized when dc/c is minimized

Minimum occurs when

$c\ell \approx 1$

Choose pathlength accordingly…

Reflective tube method for absorption

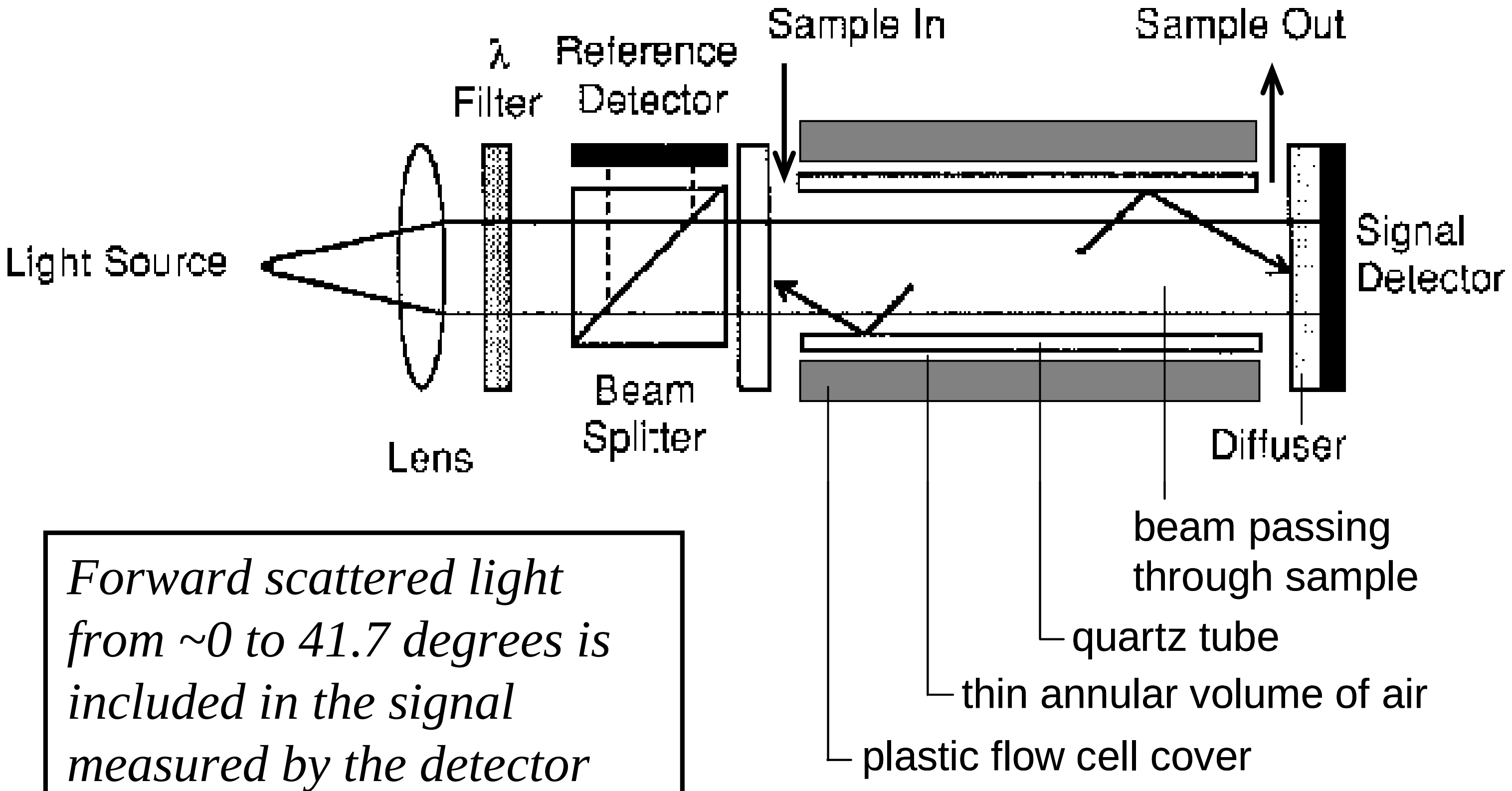

Forward scattered light from ~0 to 41.7 degrees is included in the signal measured by the detector

from Zaneveld et al. (1992)

Scattering error with reflective tube absorption

- Scattered light from ~41°-180° not measured
  - error usually ~15-22% of *b* and there are correction schemes (see Zaneveld et al. 1994)

There is a weighting function, W(θ) that defines the scattering error:

$$error = 2\pi \int_{0^o}^{180^o} W(\theta)\beta(\theta)\sin(\theta)d\theta$$

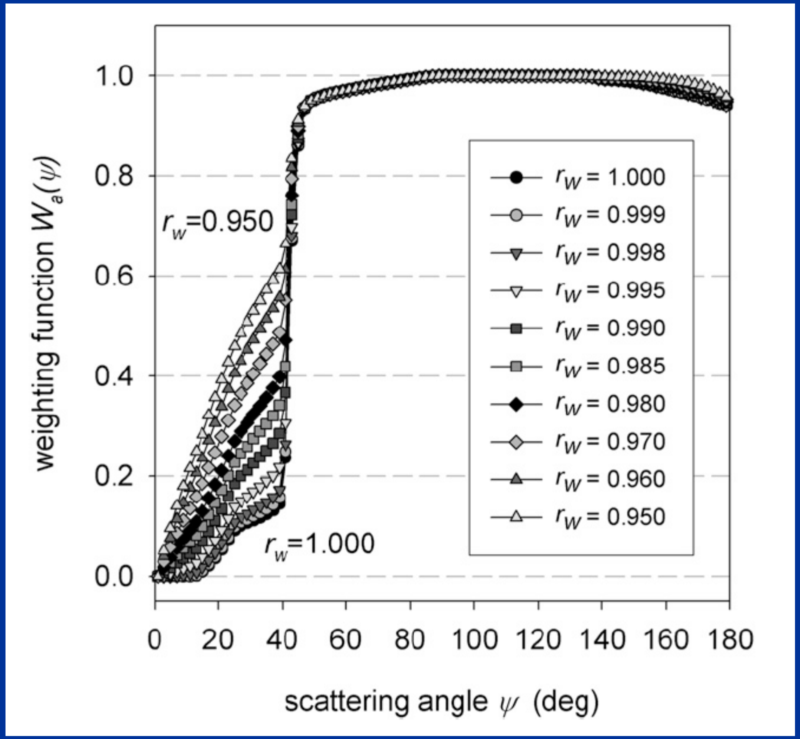

Can find *r* value that provides closest results to PSICAM (R. Rottgers)

- Found 97% to 98% (Stockley et al., in prep)
- Variability possibly attributed to aging ac device tubes

McKee et al. (2013)

Measuring total scattering, *b*

Remember…

$$\boxed{b = 2\pi\int_0^{\pi}\sin(\theta)\beta(\theta)d\theta}$$

Modeling

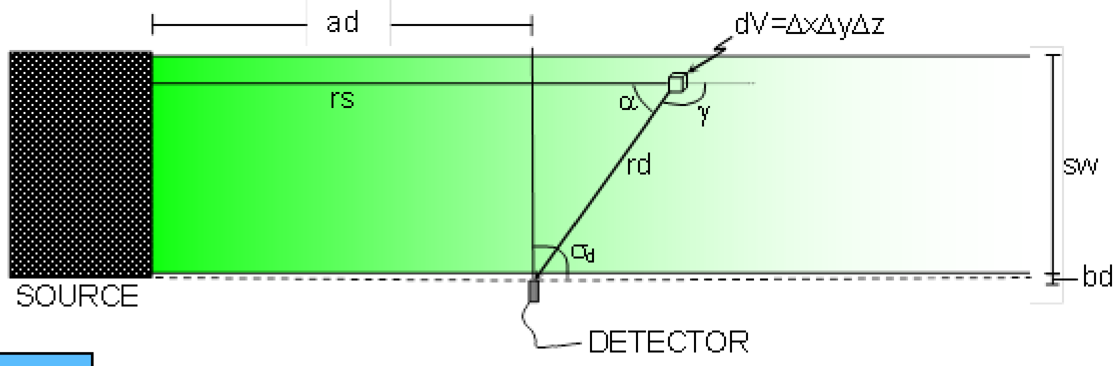

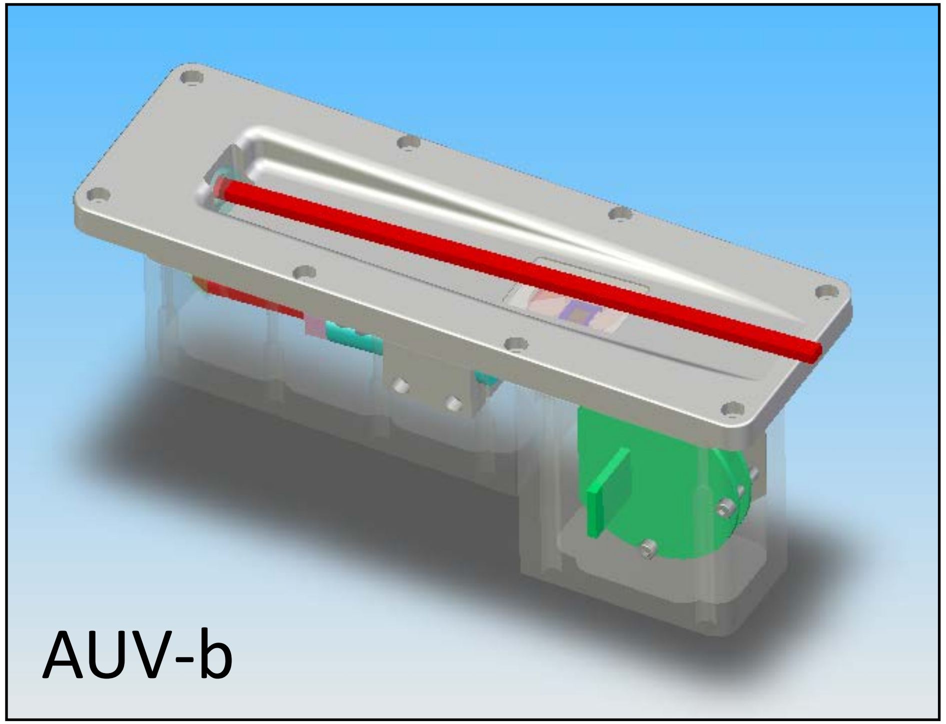

Twardowski et al. (unpub, 2006-2010)

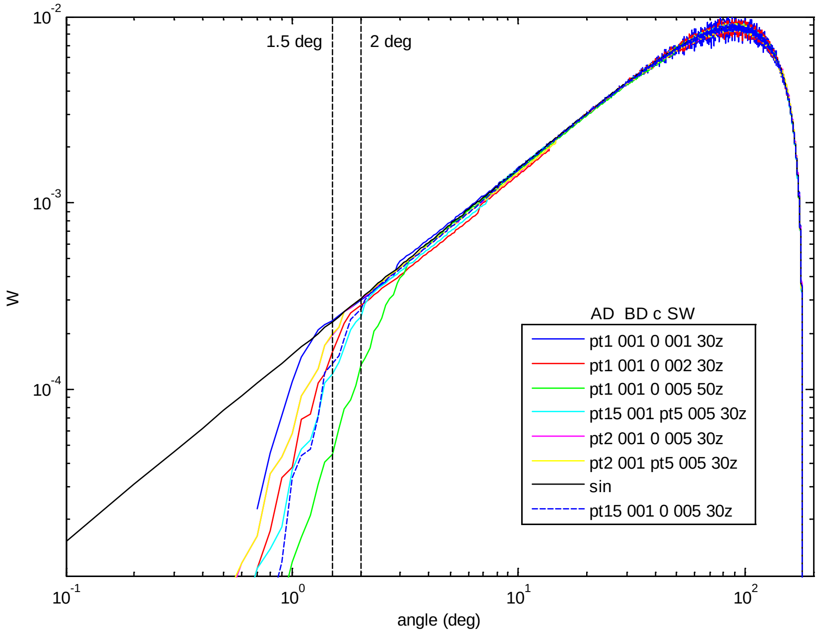

Very close to sin(θ) weighting function

Combination bb-b meter

Fry and Twardowski
NSF project

Interpretation and Application

General paths for application

Analytical: from first principles

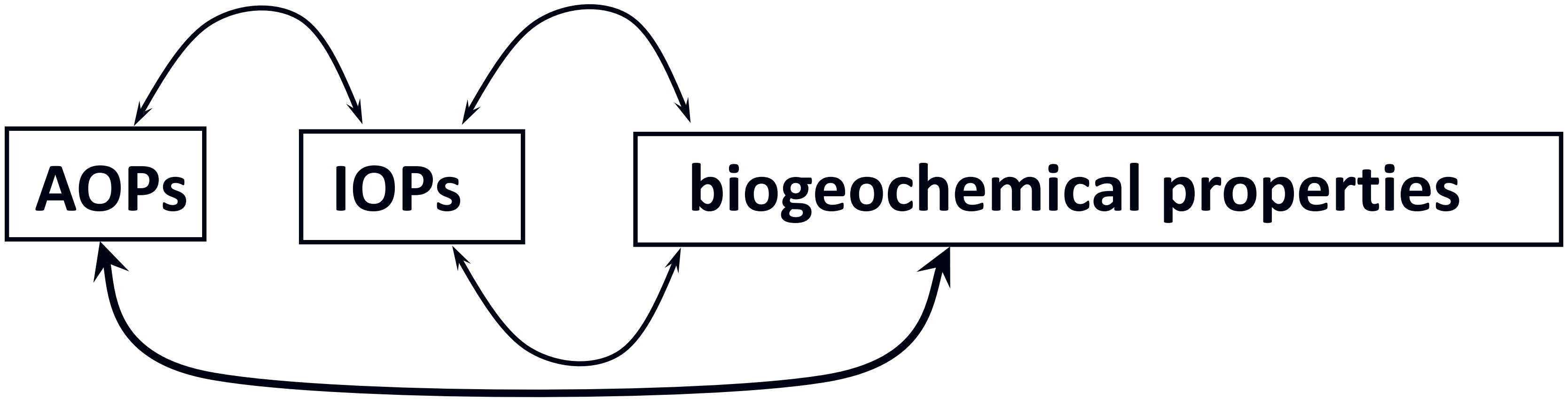

Empirical: statistical correlations

Usually empirical methods are based on some theoretical principle, and "analytical" methods usually must include some empiricism.

Scattering as a proxy for biogeochemical properties

A common example → Beer's Law: <u>IOP = ε[conc]</u>

<u>Some biogeochemical properties that influence optical properties:</u>

chlorophyll, phytoplankton pigments, particle size, particle density, particle composition, particle shape, particle concentration, total particle mass (TSM, SPM), POM/C, DOM/C, biomass, humic substances, hydrocarbons, $CaCO_3$,…

<u>*However*</u>: pools of particulate and dissolved matter can be highly variable and complex in composition, especially in coastal regions, usually confounding simple relationships.

Links Between IOPs & Biogeochemicals

- Chlorophyll
- POC
- TSM
- DOM, DOC
- Phytoplankton pigments
- Size distribution
- Bulk refractive index
- Sewage
- Hydrocarbons
- …

Table 1. Some biogeochemical properties derived from optical properties.

Biogeochemical property	Optical Property	Example Reference(s)
Particulate Organic Carbon (POC)	1) c_p or b_p	Peterson 1978; Gardner et al. 1993, 2001; Loisel and Morel 1998; Bishop 1999; Bishop et al. 2002; Claustre et al. 1999, 2000; Mishonov et al. 2003
	2) b_{bp}	Stramski et al. 1999; Balch et al. 1999
Total Suspended Matter (TSM)	1) c_p or b_p	Peterson 1978; Gardner et al. 1993, 2001; Walsh et al. 1995; Prahl et al. 1997
	2) turbidity	Fugate and Friedrichs 2002
Dissolved Organic Matter or Carbon (DOM, DOC)	1) a_g	Pages and Gadel 1990; Vodacek et al. 1997
	2) Fluorescence	Coble et al. 1993; Ferrari et al. 1996; Klinkhammer et al. 2000
DOM composition[a]	1) a_g, spectral shape	Carder et al. 1989; Blough and Green 1995
	2) Fluorescence, multi-spectral shapes	Coble 1996; Del Castillo et al., 1999; McKnight et al. 2001
Chlorophyll	1) a_p	Bricaud et al. 1998; Claustre et al. 2000
	2) Fluorescence	e.g., Yentsch and Menzel 1963; Claustre et al. 1999
Phycobiliproteins	Fluorescence	Cowles et al. 1993; Sosik et al. 2002
Phytoplankon pigment ratios	a_p, spectral shape	Trees et al. 2000; Eisner et al. 2003
Proteins	Fluorescence	Coble et al. 1993; Mayer et al. 1999
Hydrocarbons	Fluorescence	e.g., Holdway et al. 2000
Particle size distribution	1) c_p, spectral shape	Morel 1973; Boss et al. 2001
	2) $\beta(\theta)$	Brown and Gordon 1974; Zaneveld et al. 1974; Agrawal and Pottsmith 2000
Particulate refractive index	1) $\beta(\theta)$	Brown and Gordon 1974; Zaneveld et al. 1974
	2) $c_p(\lambda)$, b_{bp}, and b_p	Twardowski et al. 2001
Sewage	Fluorescence	Petrenko et al. 1997
Nitrate	UV absorption	Johnson and Coletti 2002

[a]For example – ratio of dissolved humic acid to fulvic acid, DOM molecular size distribution, DOM aromaticity, DOM source

Twardowski et al. (2005)

How is c_p (or b_p or b_{bp}) linked to particles?

Q_c is attenuation efficiency

$$\boxed{c_p = \frac{N}{V}\pi r^2 Q_c(r,n)}$$

$$\boxed{F(r) = \frac{dN}{dr} = r^{-s}}$$

First order approximation of natural size distribution, *F(r)*

COMBINE

$$\boxed{c_p = \pi \int_{r_{\min}}^{r_{\max}} Q_c(r,n) F(r) r^2 dr = \pi \int_{r_{\min}}^{r_{\max}} Q_c(r,n) r^{2-s} dr}$$

c_p for a population of spheres

Widely varying natural size distributions and refractive indices, *n*, are the main reason why c_p-TSM, c_p-POC etc relationships vary

<u>See reviews</u>: Morel and Bricaud 1986 and Morel 1991

How is c_p (or b_p or b_{bp}) linked to particles?

$$c_p = \pi \int_{r_{\min}}^{r_{\max}} Q_c(r,n) F(r) r^2 dr$$

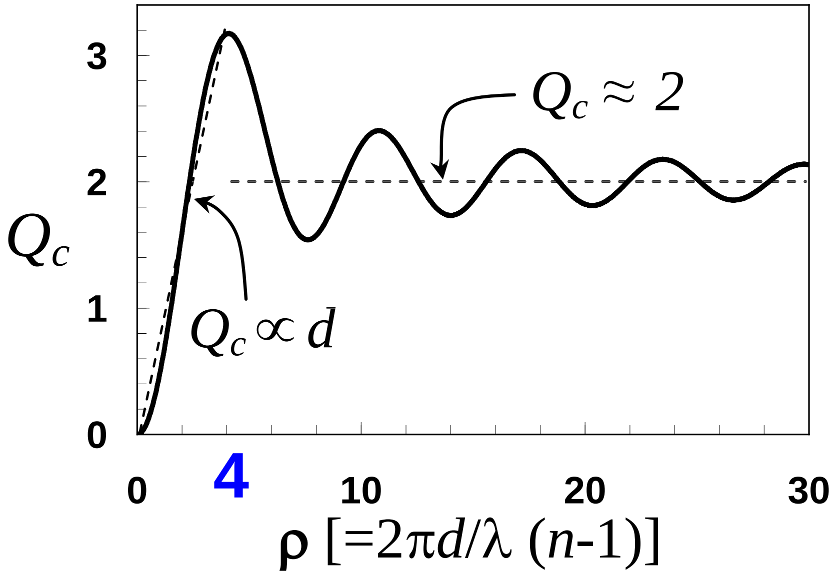

Can be modeled well for spheres with van de Hulst approximation

$$c_p \propto \begin{cases} \sum_{i=1}^{N} d_i^3, & \rho < 4 \xrightarrow{\propto} \text{total particle volume } \textbf{(TPV)} \\ \sum_{i=1}^{N} d_i^2, & \rho > 4 \xrightarrow{\propto} \text{total surface area } \textbf{(TSA)} \text{ OR total cross-sectional area } \mathbf{(\sum G)} \end{cases}$$

Example:
c_p and TSM

Reasonable correlations for each regression, but slopes are different for different water masses

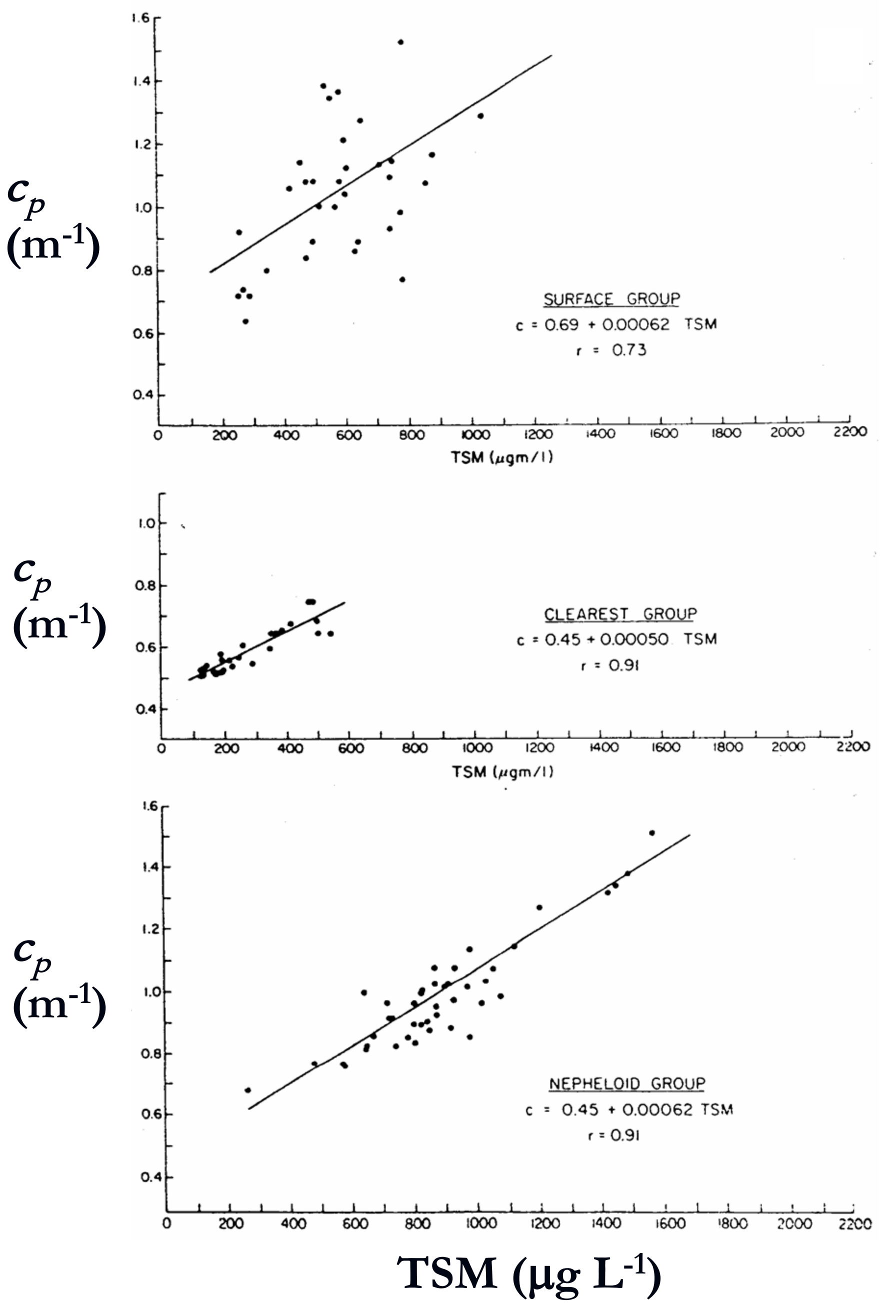

Peterson 1977

c_p and TSM: Long Island Sound

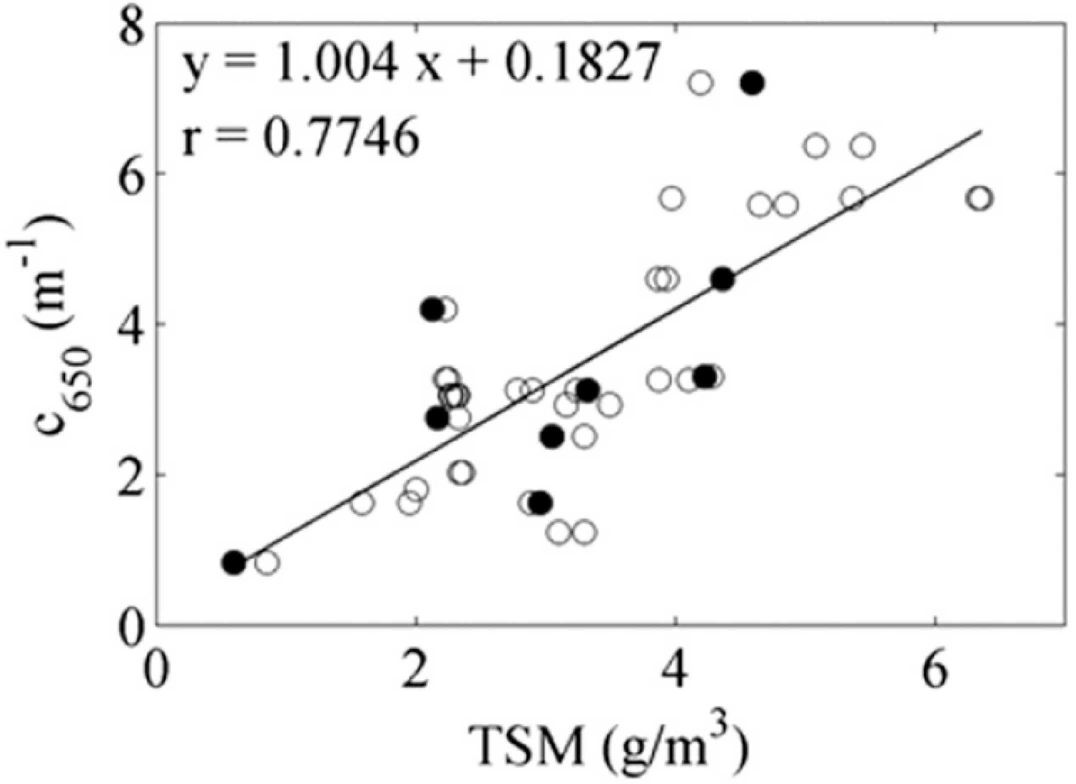

Groundwater et al. (2012)

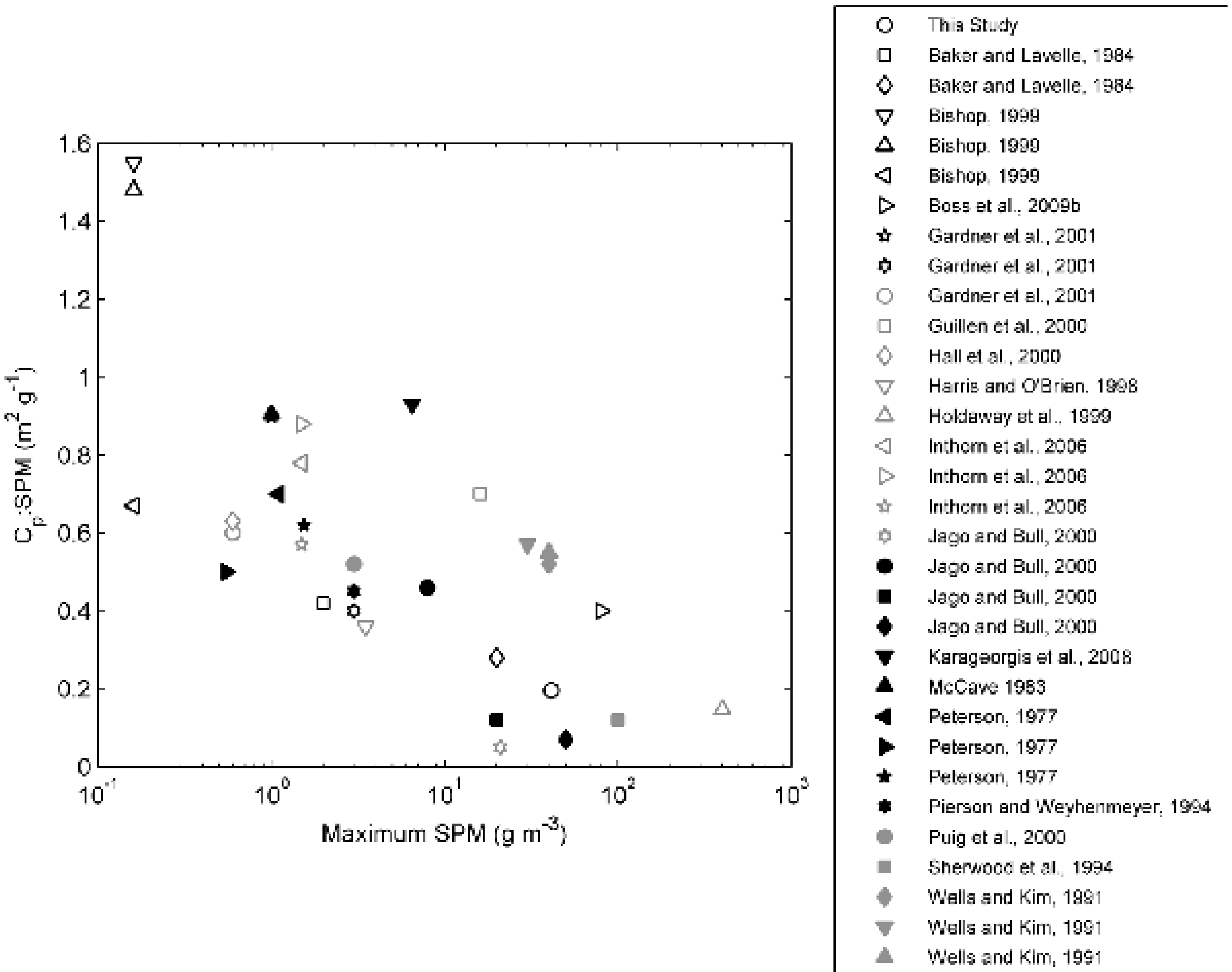
1.6
1.4
1.2
1
0.8
0.6
0.4
0.2
0
C_p:SPM ($m^2\ g^{-1}$)
10^{-1}
10^0
10^1
10^2
10^3
Maximum SPM ($g\ m^{-3}$)
This Study
Baker and Lavelle, 1984
Baker and Lavelle, 1984
Bishop, 1999
Bishop, 1999
Bishop, 1999
Boss et al., 2009b
Gardner et al., 2001
Gardner et al., 2001
Gardner et al., 2001
Guillen et al., 2000
Hall et al., 2000
Harris and O'Brien, 1998
Holdaway et al., 1999
Inthorn et al., 2006
Inthorn et al., 2006
Inthorn et al., 2006
Jago and Bull, 2000
Jago and Bull, 2000
Jago and Bull, 2000
Jago and Bull, 2000
Karageorgis et al., 2008
McCave 1983
Peterson, 1977
Peterson, 1977
Peterson, 1977
Pierson and Weyhenmeyer, 1994
Puig et al., 2000
Sherwood et al., 1994
Wells and Kim, 1991
Wells and Kim, 1991
Wells and Kim, 1991

Published slopes for TSM-c_p and POC-c_p

Table 1. Published biogeochemical-optical data.

reference	**location**	**TSM (μg-m/L) / c_p[a]**	**POC (μg-m/L) / c_p[a]**
Peterson (1977)	OR coast - nepheloid layer	1600	
	OR coast - clearest waters	2000	
	OR coast - surface	1600	
Mishonov et al. (2000)	Ross Sea		674
	NABE		319
	APFZ		455
Bishop et al. (1999)	N. Pacific		195
Gardner et al. (1992)	N. Atlantic	1020	378
Gardner et al. (2001)	NW Atlantic - pre-hurricane 1996, surface	1000	400
	NW Atlantic - pre-hurricane 1996, subsurface	1100	105
	NW Atlantic - post-hurricane 1996, surface	770	455
	NW Atlantic - post-hurricane 1996, subsurface	2500	135
	NW Atlantic - Spring 1997, surface	770	
	NW Atlantic - Spring 1997, subsurface	1700	
	NW Atlantic - Spring 1997, mid-water		1250
Walsh et al. (1995)	Eq. Pac April, 1992	451	
	Eq. Pac October, 1992	642	
Walsh (1990)	Gulf of Mexico	660	
Mishonov et al. (2003)	BATS		323
	NABE (revised from Mishonov et al. 2000)		303

[a] – wavelength typically 660 nm

TSM/c_p range:
~450-2500

POC/c_p range:
~100-1250

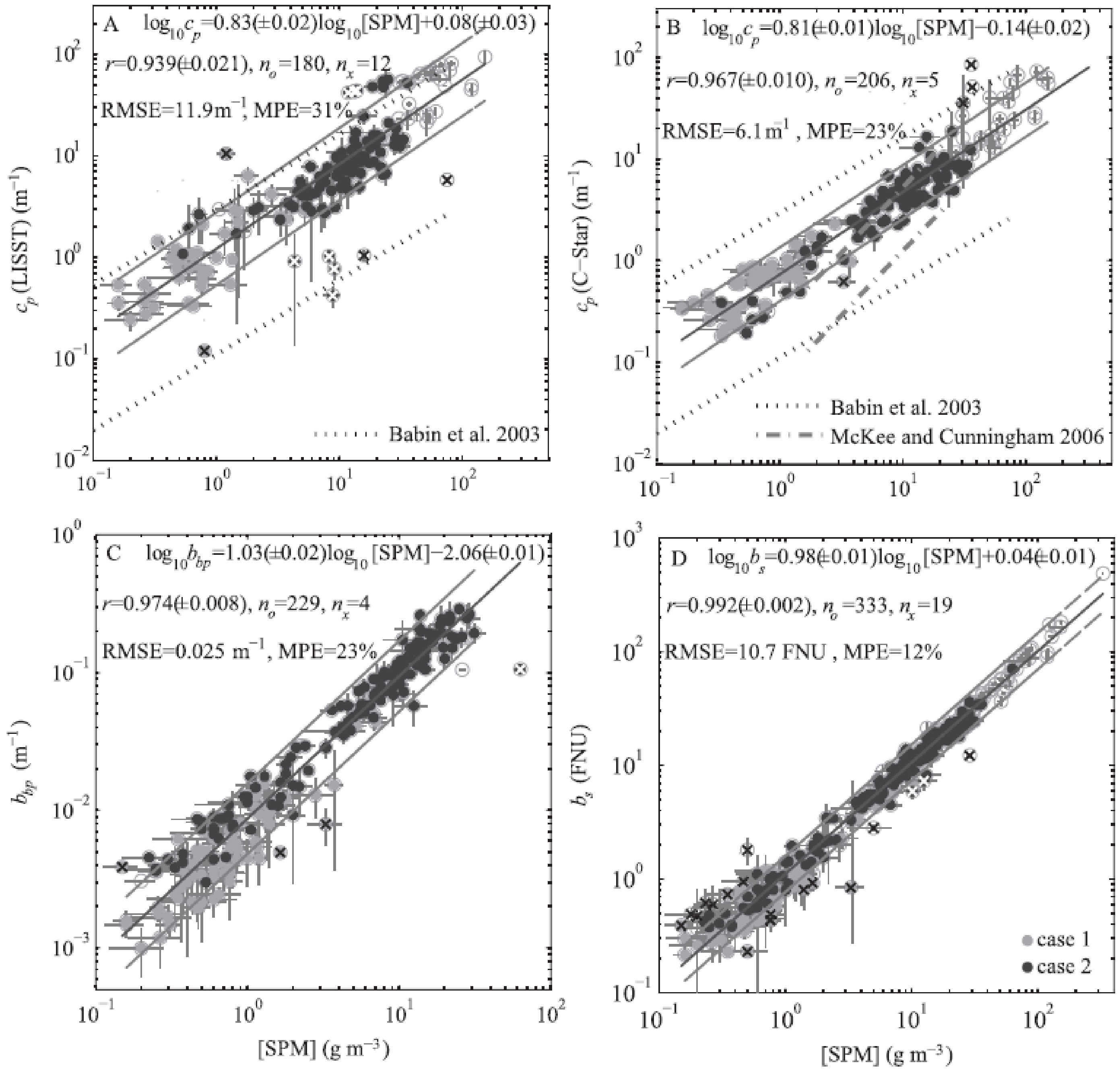

Neukermans et al. (2012)

c_p and POC: Mishonov and Gardner

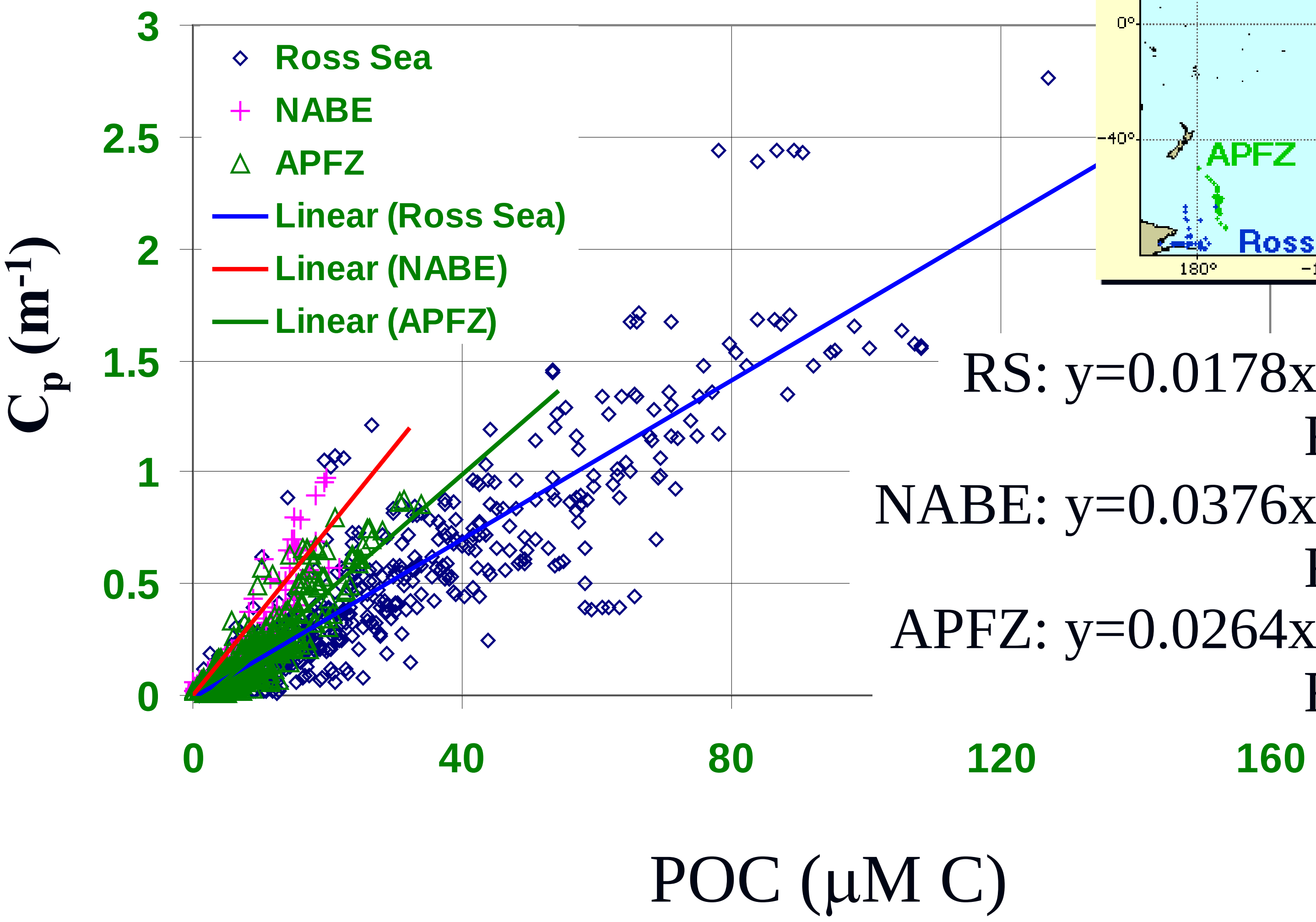

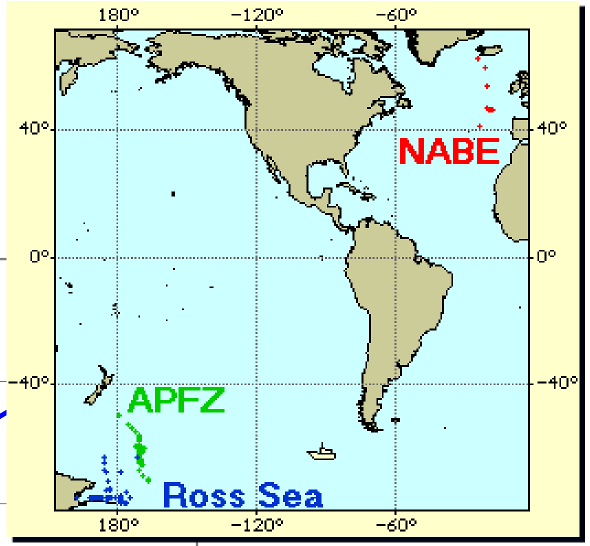

RS: $y=0.0178x - 0.0155$
$R^2=0.874$

NABE: $y=0.0376x - 0.0032$
$R^2=0.913$

APFZ: $y=0.0264x - 0.0649$
$R^2=0.982$

Mishonov and Gardner (TAMU)

Obtaining POC from $b_{bp}(510)$:

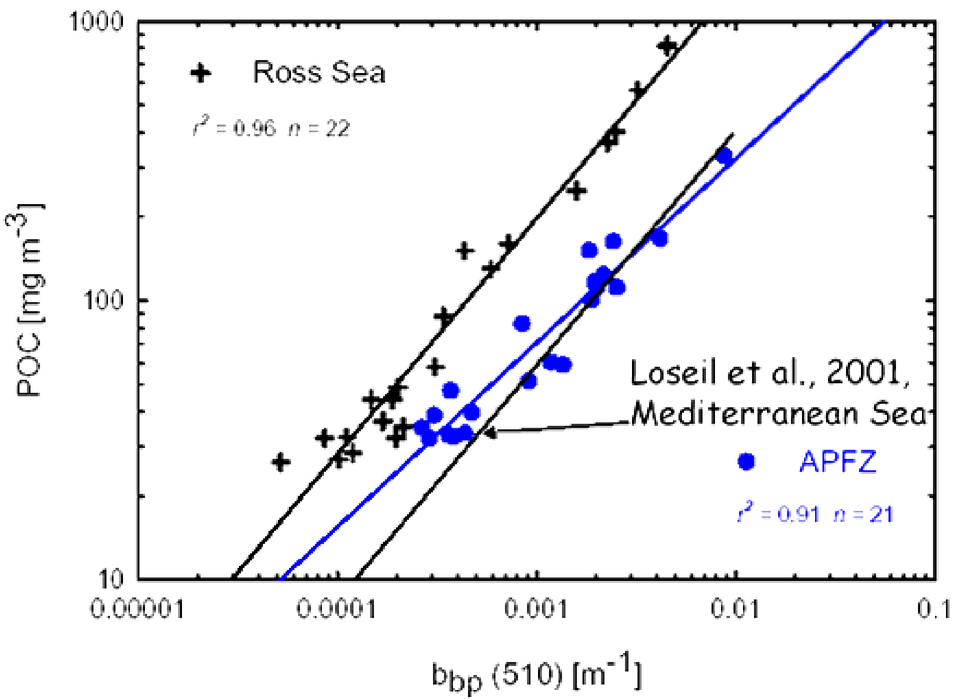

Stramski et al, 1999.

Likely causes for variability: b_{bp} computation, PSD, composition, Particles not accounted by POC method.

Obtaining POC from Beam-c (660):

SOLO float-
Carbon explorers:

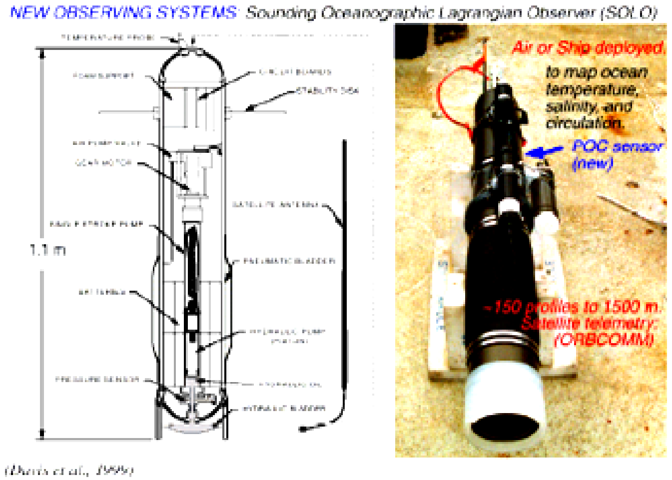

<u>Results:</u>

Two blooms of phytoplankton in North Pacific following dust deposition event (iron fertilization ?).

SeaWIFS [chl] and POC covary.

Notice co-variation of blooms and stratification and high chl/C ratios (vernal bloom ?).

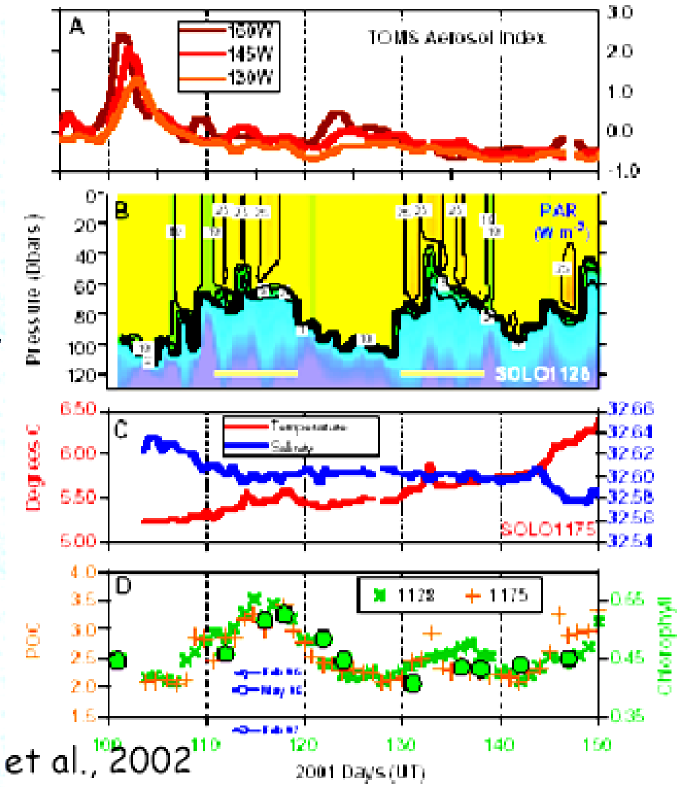

Bishop et al., 2002

Particle size distribution (PSD) slope and spectral attenuation

With a PSD modeled well by a power law (i.e., a "Junge" type PSD), a correlation is expected between the power law slope of $c_p(\lambda)$, γ, and the power law slope of the PSD, *s*:

$$s = 3 + \gamma$$

(Volz 1954, Morel 1973)

Or, more accurately when exact particle size limits are considered:

$$s = 3 + \gamma - 0.5\exp(-6\gamma)$$

(Boss et al. 2001)

Bulk particle refractive index model

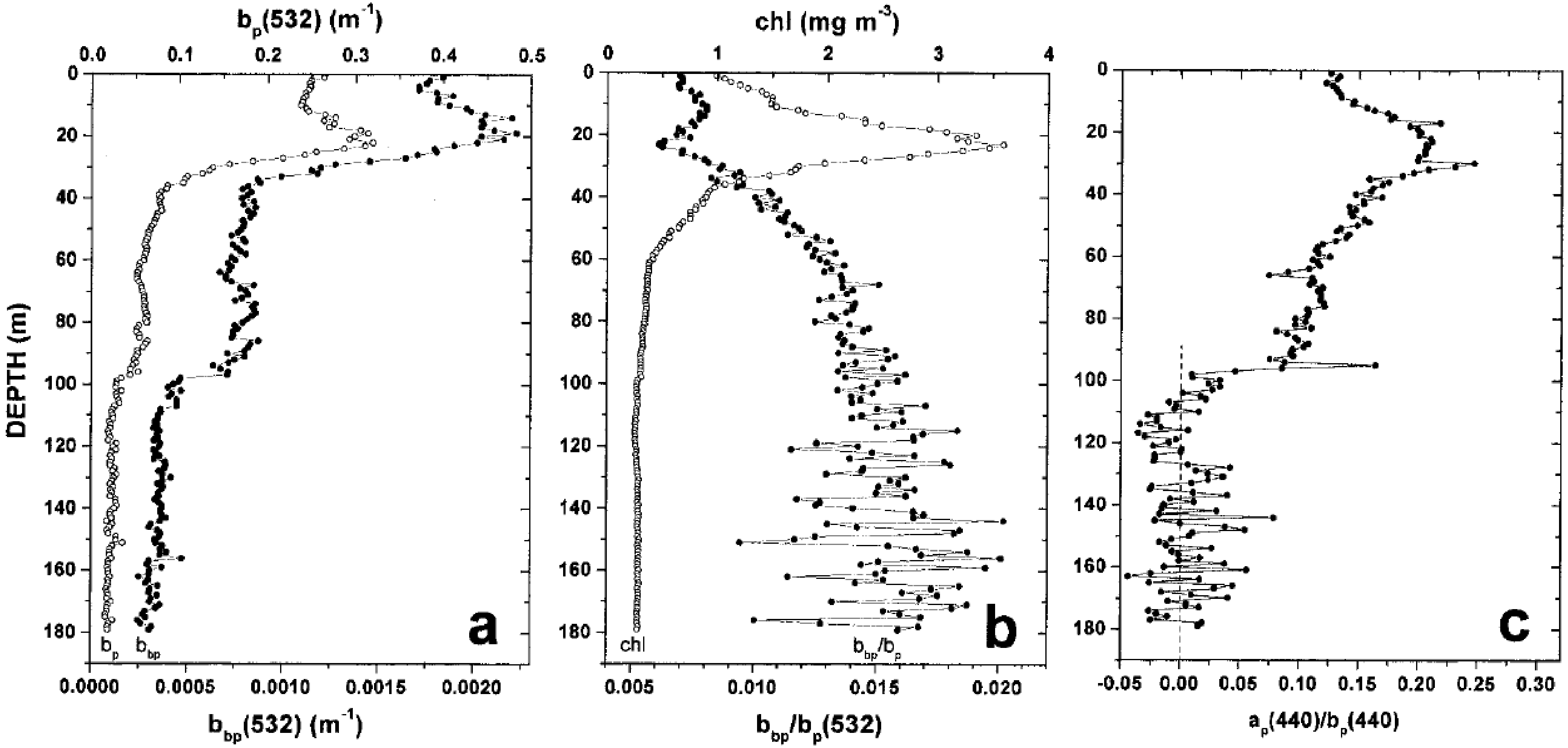

Field data from Gulf of California

Twardowski et al. (2001)

Bulk particle refractive index model

$$\hat{n}_p(\tilde{b}_{bp},\gamma) = 1 + \tilde{b}_{bp}^{\,0.5377+0.4867(\gamma)^2}[1.4676 + 2.2950(\gamma)^2 + 2.3113(\gamma)^4].$$

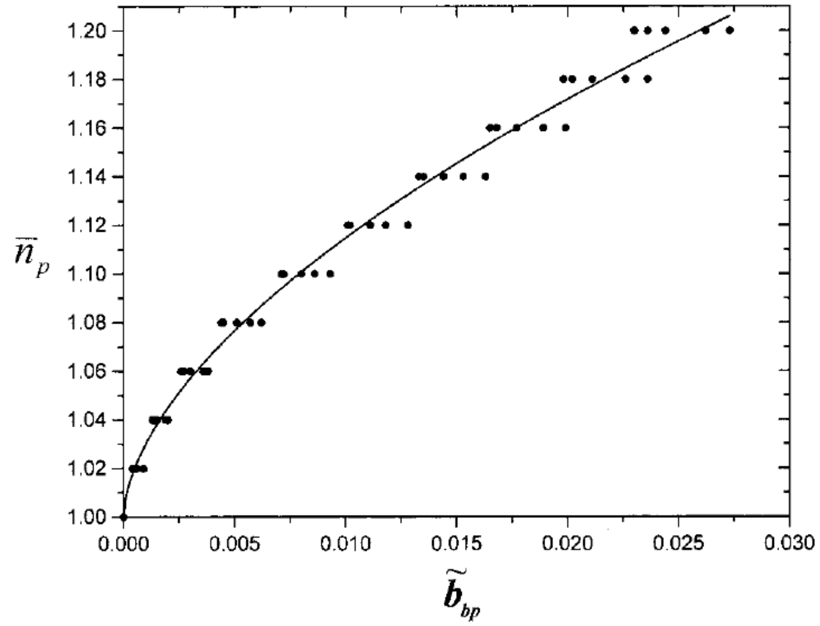

Figure 10. The relationship between bulk refractive index $\bar{n}_p$ and $\tilde{b}_{bp}$ for hyperbolic slopes ranging between 2.5 (0.25) 3.5 (data from Figure 1a replotted and fitted). For these ranges of ξ, $\bar{n}_p$ was a strong function of $\tilde{b}_{bp}$ (regression given in text, equation (14)).

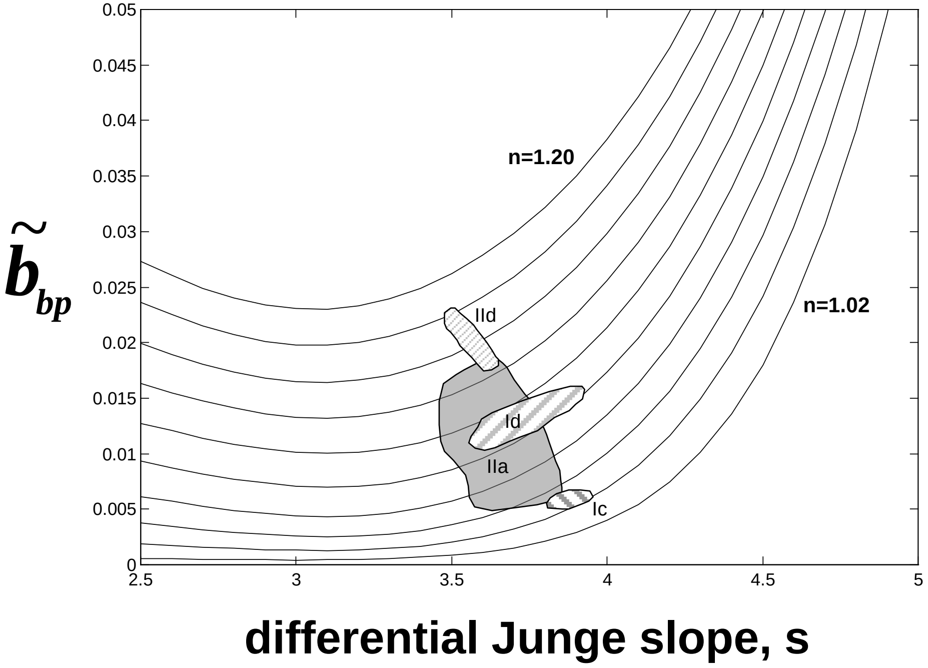

Ic – Case I, chlorophyll maximum
Id – Case I, deep water
IIa – Case II, south of midrift islands
IId – Case II, bottom water, north of midrift islands

Field data from Gulf of California

Based on Lorenz-Mie theory

Twardowski et al. (2001)

Can we use *n* and PSD models to improve SPM estimation?

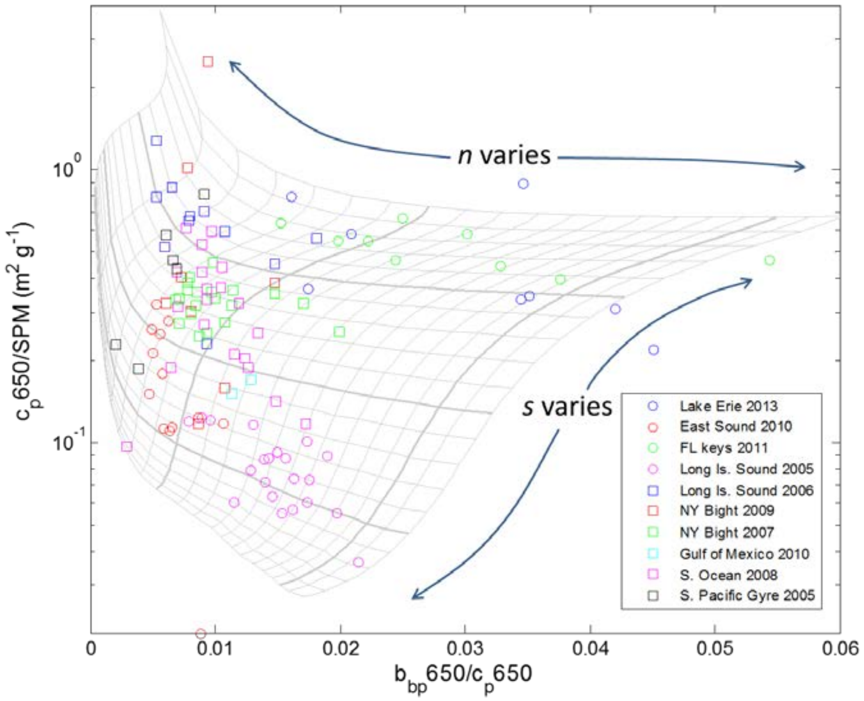

Field data (122 sample sites from 10 different global locations) overlying analytical model results.

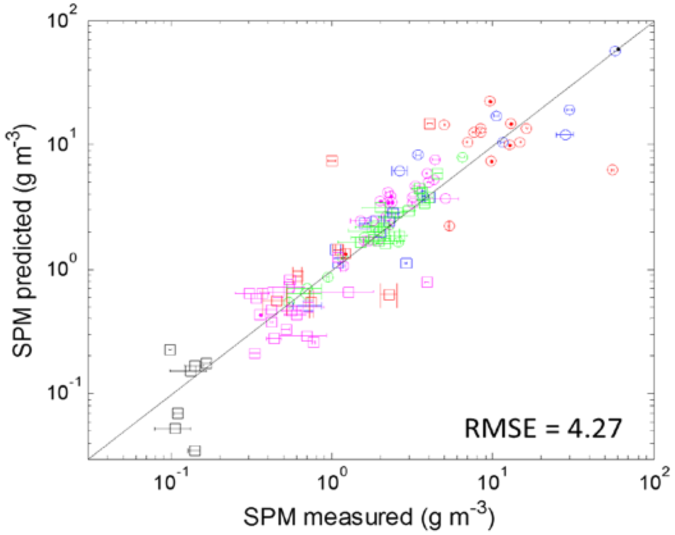

1) derive PSD slope *s* from the c_p slope (Boss et al. 2001),
2) use measured b_{bp}/c_p and derived *s* to solve for c_p/SPM with the model,
3) divide measured c_p by the derived c_p/SPM = SPM.

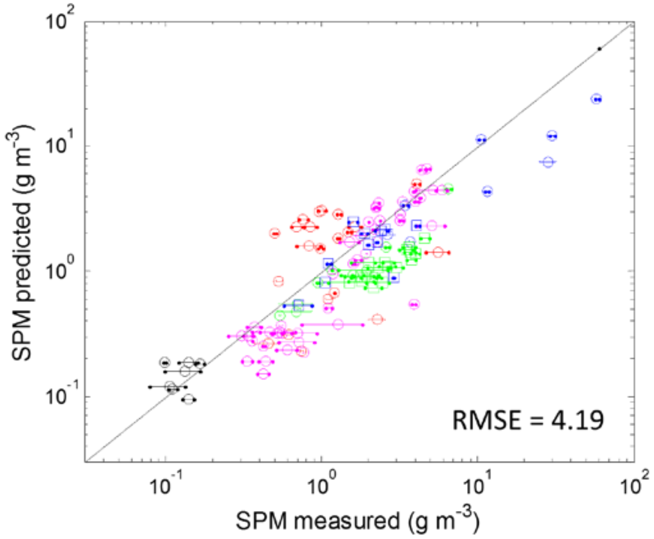

empirical state-of-the-art: SPM predicted from a Type II linear regression between measured SPM and c_p, plotted versus measured SPM, i.e., if one had *a priori* knowledge of the best linear fit

Twardowski et al. (2018)

VSF inversion

Scripps Pier, 2008

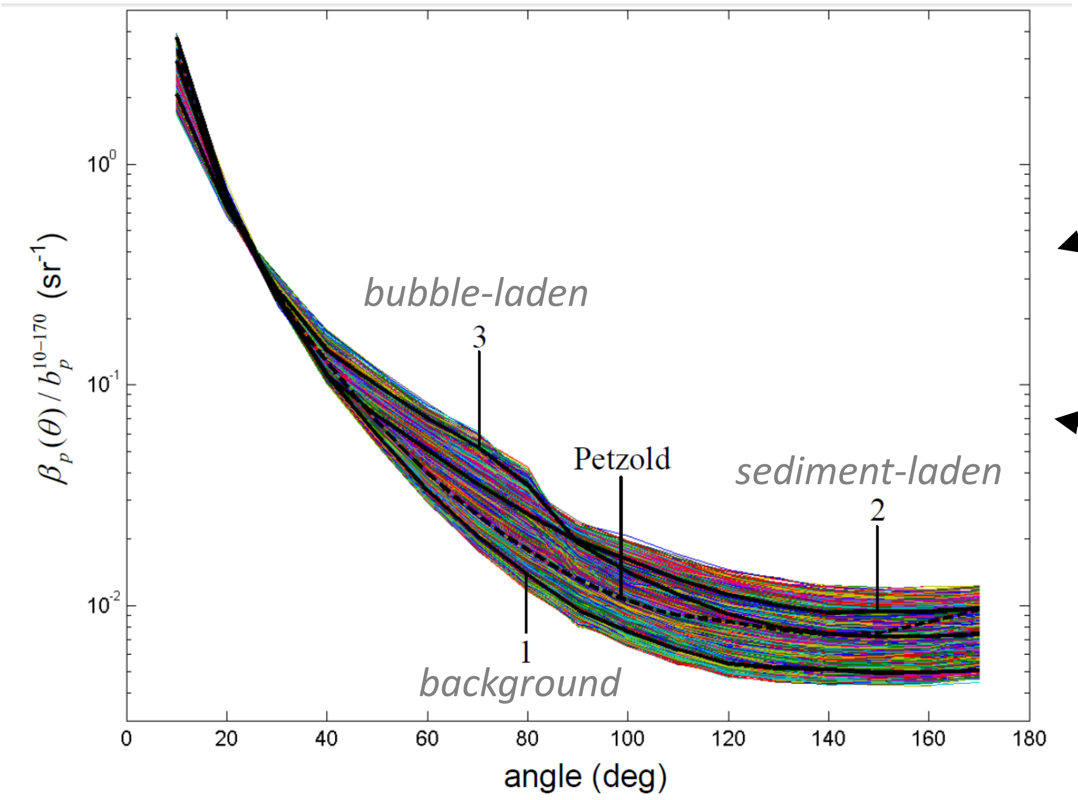

Fit to

measured

VSFs

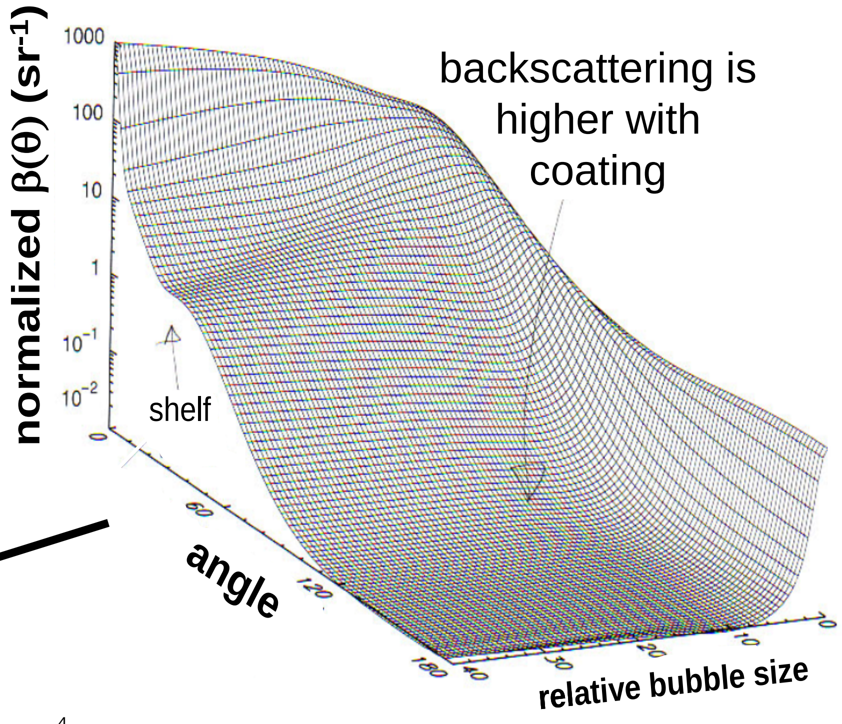

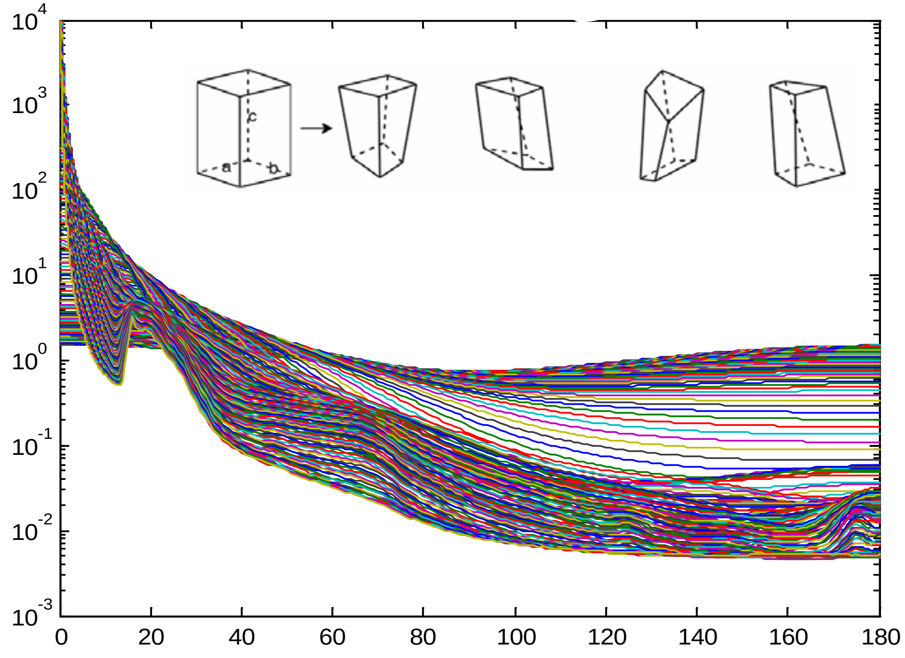


Scripps Pier

VSF inversion: large bubble subpopulation

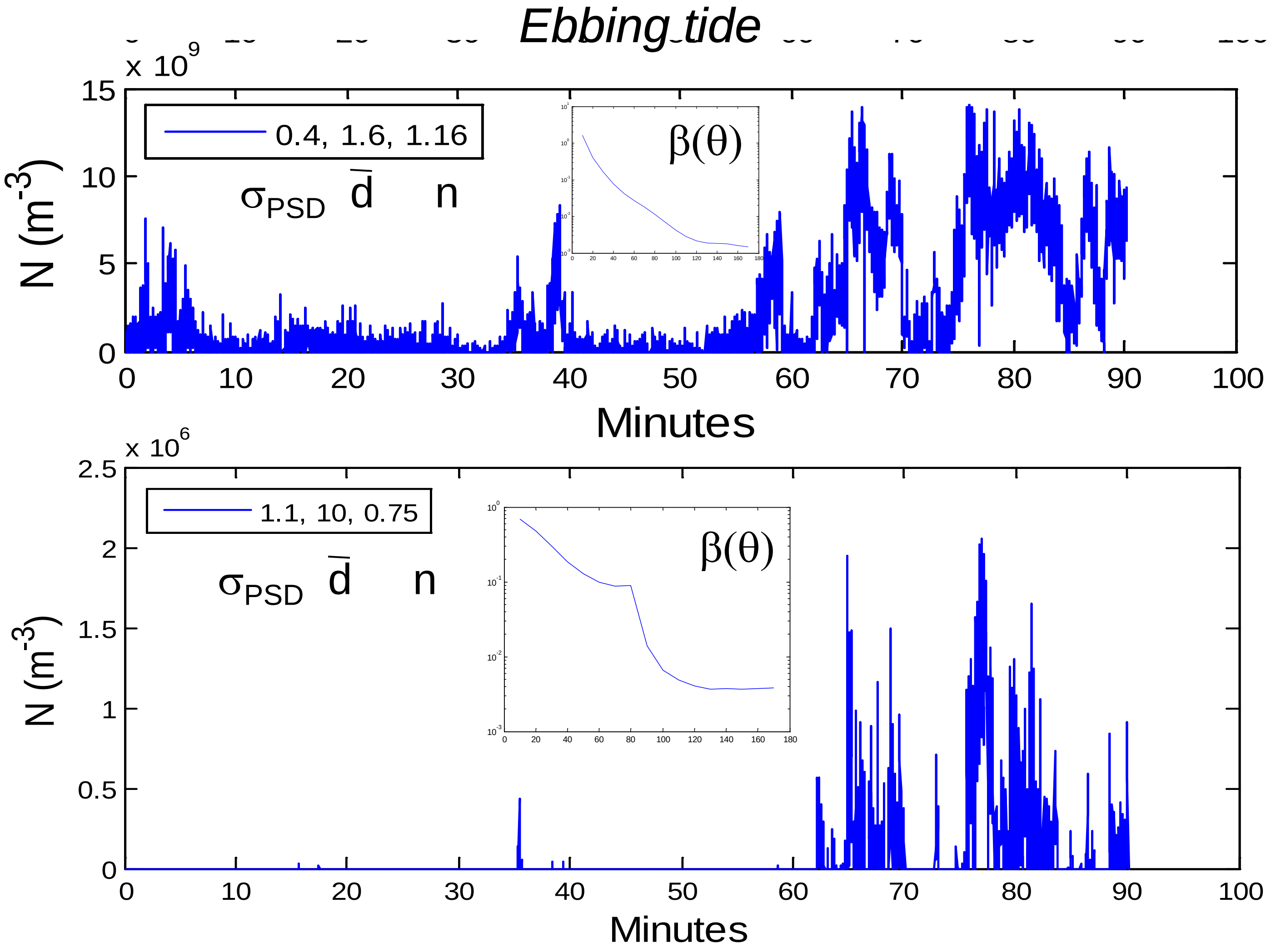

sediments

bubbles

Twardowski et al. (2012)

Bubbles resolved with optics and acoustics

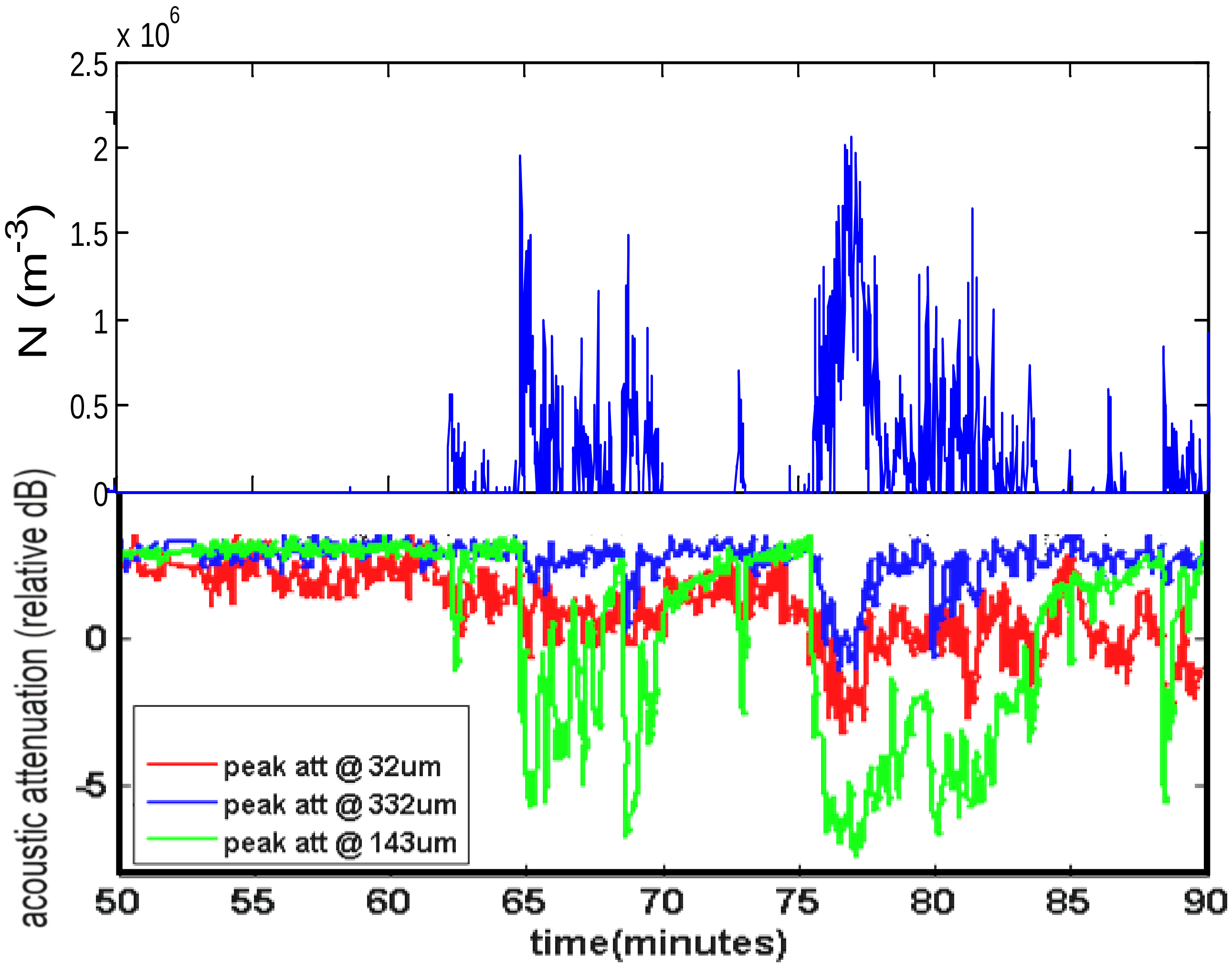

large bubble size class from inversion

acoustic signal from bubbles

Twardowski et al. (2012)

Surfactants are important for bubbles

Optics

Acoustics

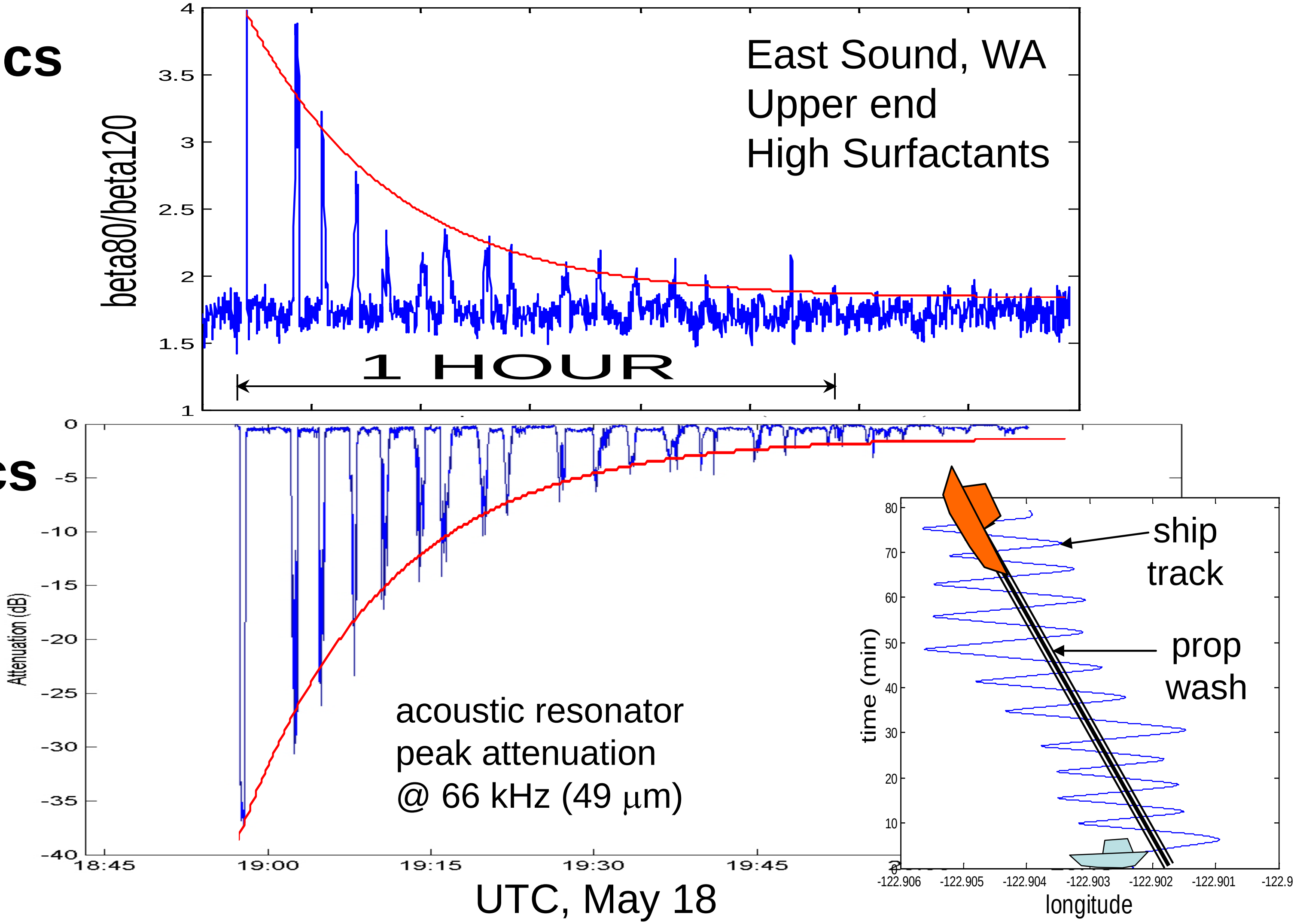

Particle orientation

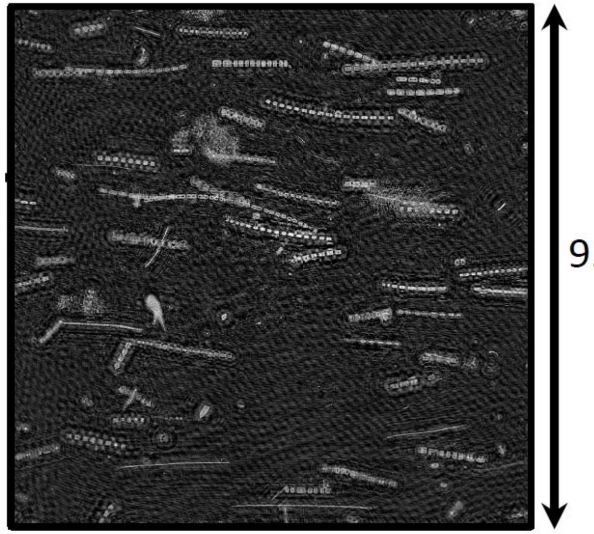

9.4 mm

Image from ~3.5 m depth showing horizontal orientation of diatom colonies (mostly *Ditylum brightwellii*) within a thin layer.

In situ holographic microscope

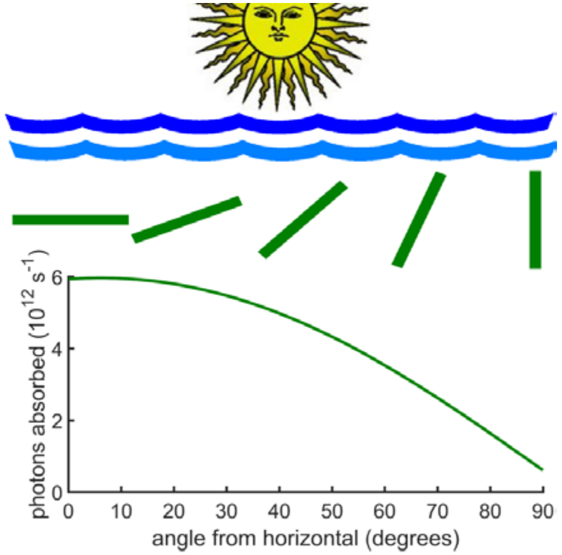

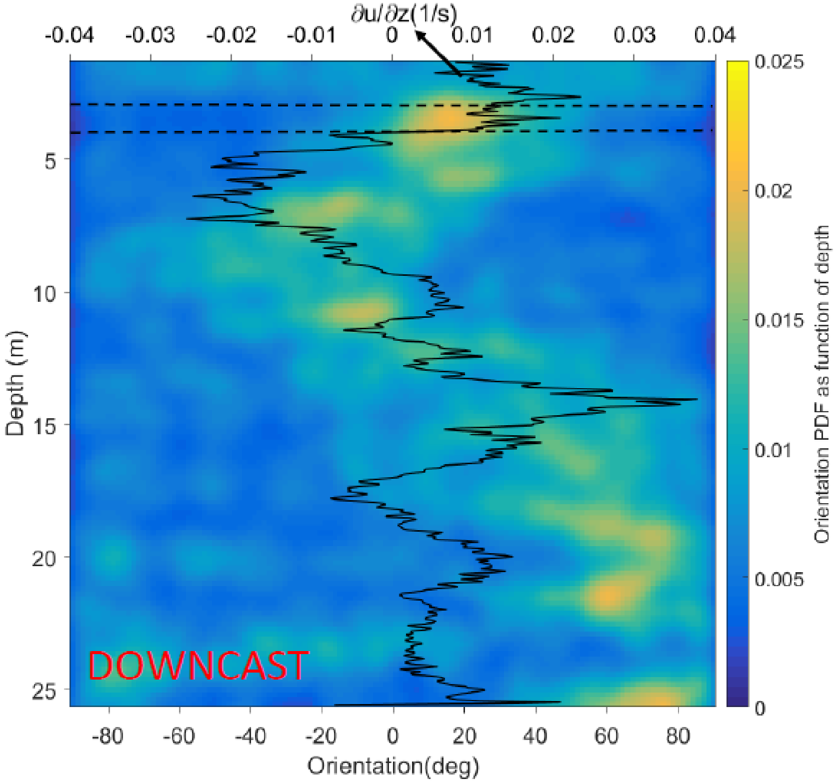

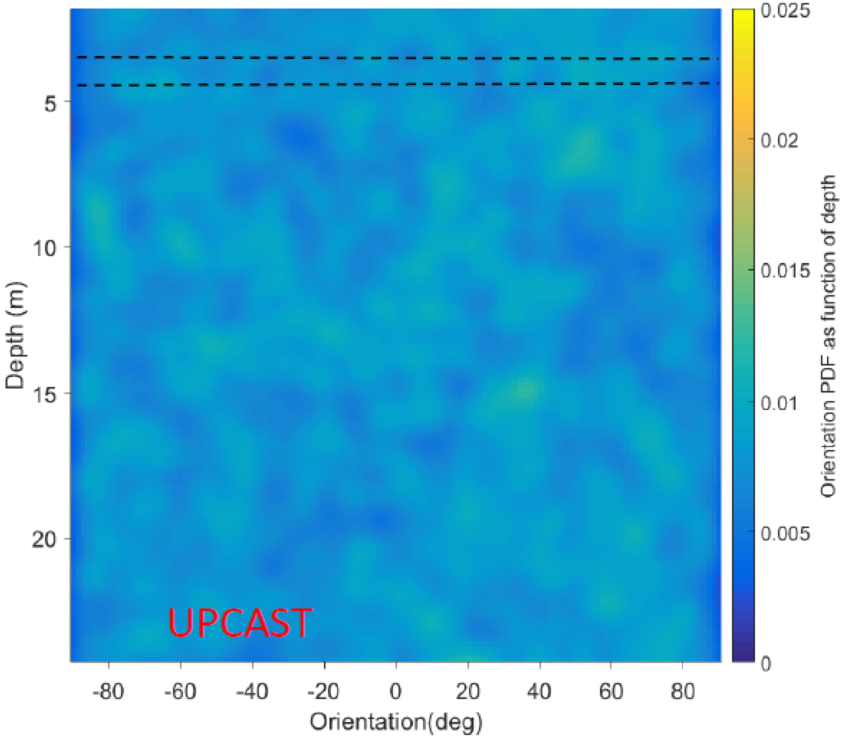

Nayak et al. (2017)
McFarland et al., in prep

Imaging

$$upward\ looking\ range = Z_i = \frac{1}{c-K}\left[-ln\left(\frac{C_L}{2M_0}\right)+\frac{bd}{4\pi\theta_0}\right]$$

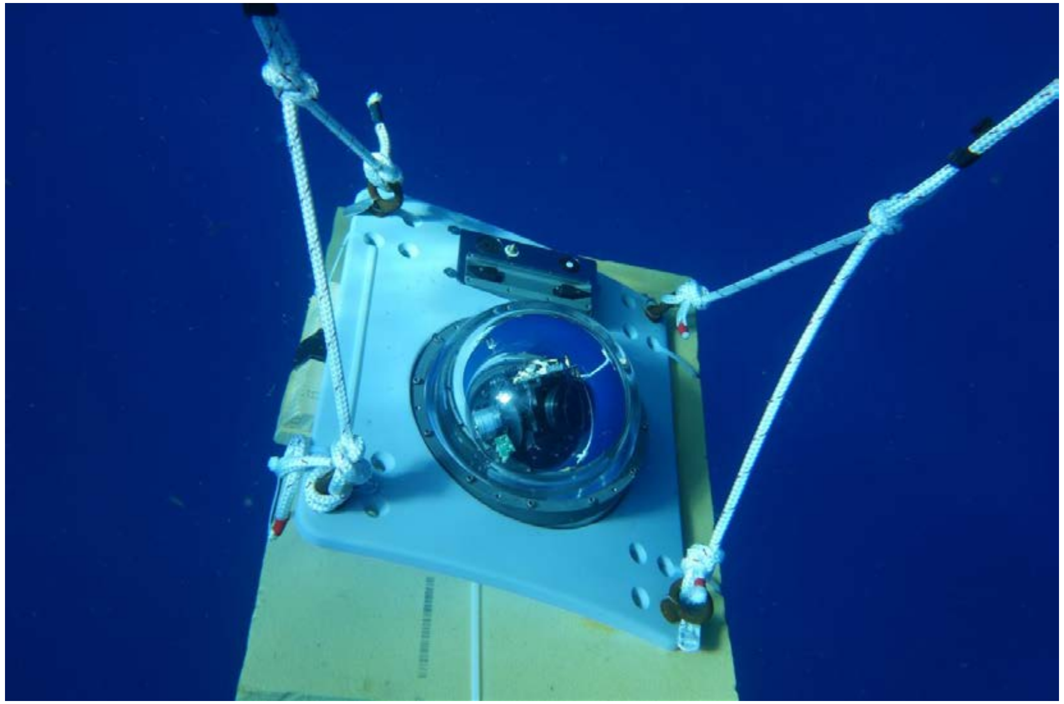

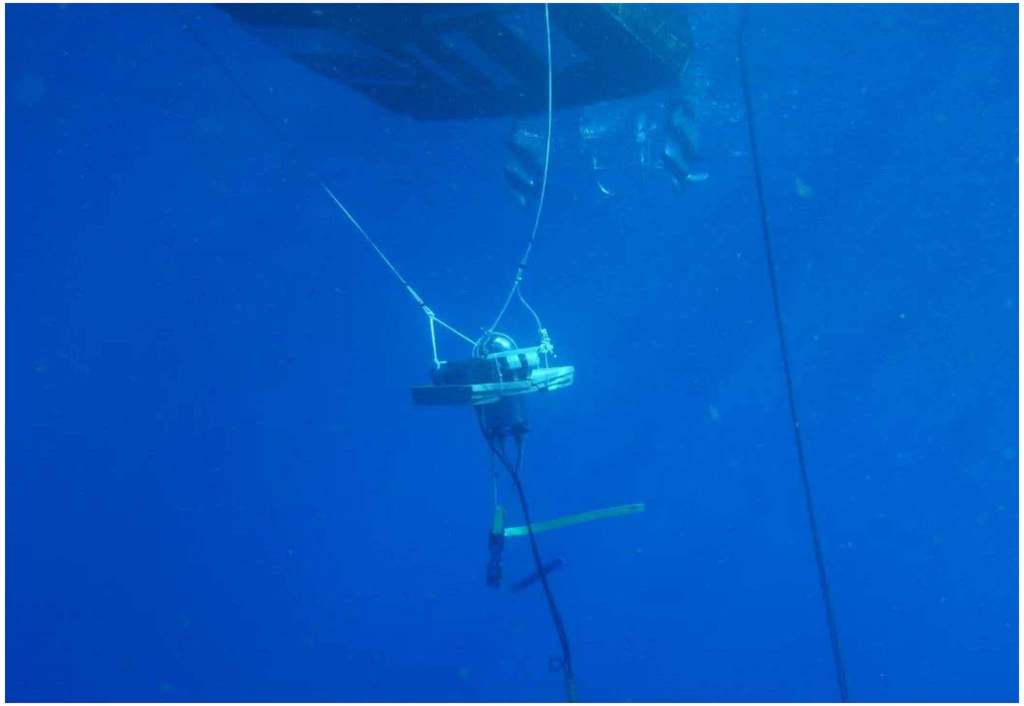

Twardowski (unpubl)

Relevance of VSF to ocean color

$$R_{rs}(0^-) = \frac{L_u(0^-)}{E_d(0^-)} \cong \Psi\left(\frac{b_b}{a+b_b}\right)$$

Gordon (1975)
Morel and Prieur (1975)

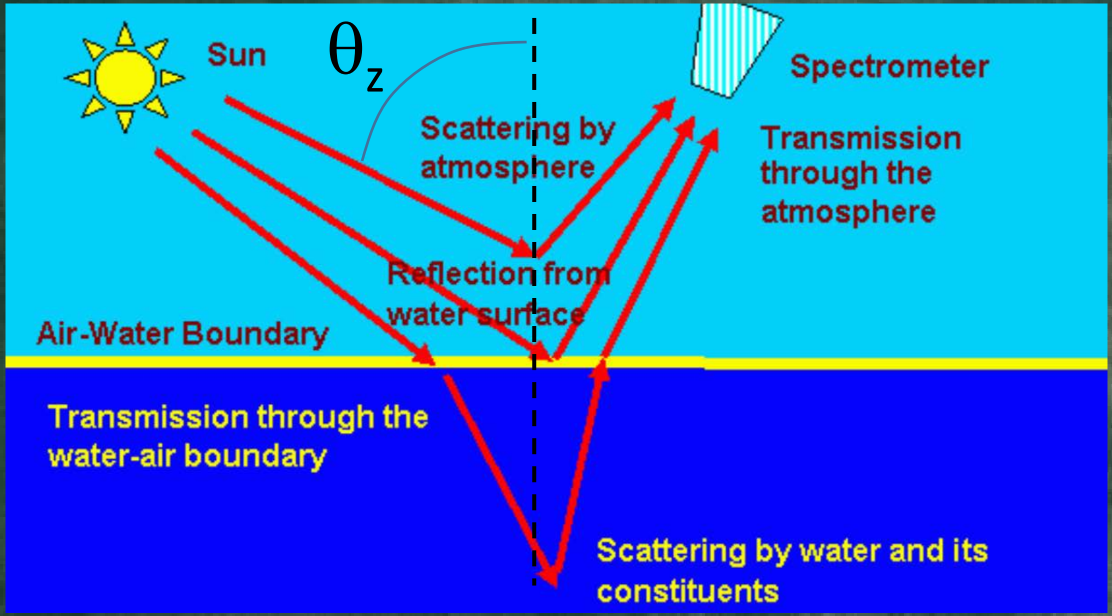

$L_w(\theta,\phi,\theta_z)$ → OCI Drift corrections → atmospheric correction → $L_{wN}(\pi, \theta_z = 0)$ → *Algorithms…*

BRDF LUT
(Morel et al. 2002)
THIS IS CONTROLLED
BY THE VSF

Explicit inclusion of the VSF in SA algorithms

$$\frac{L_u}{E_{od}} = \frac{\beta(\pi - \theta_z)}{a(1+\bar{\mu}_\infty^{-1}) + b_b - 0.05 b_f}$$

Zaneveld (1995)

$$\frac{L_u}{E_d} = \sec(\theta_z)\frac{\beta(\pi - \theta_z)}{c}\frac{\sec(\pi)}{\sec(\pi) - \sec(\theta_z)} e^{-cz\sec(\theta_z)}$$

Jerlov (1976)

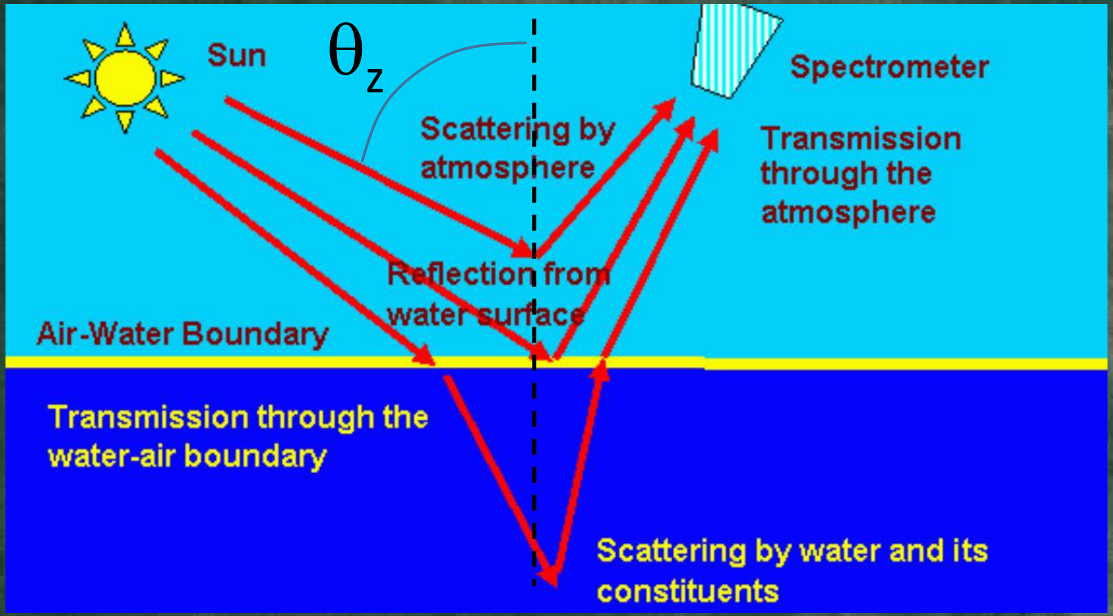

- Could directly apply VSF information from a PACE polarimeter
- Without polarimeter, could apply representative phase function basis vectors (similar to SA basis vector models summarized in Werdell et al)

Scattering angle distributions from space

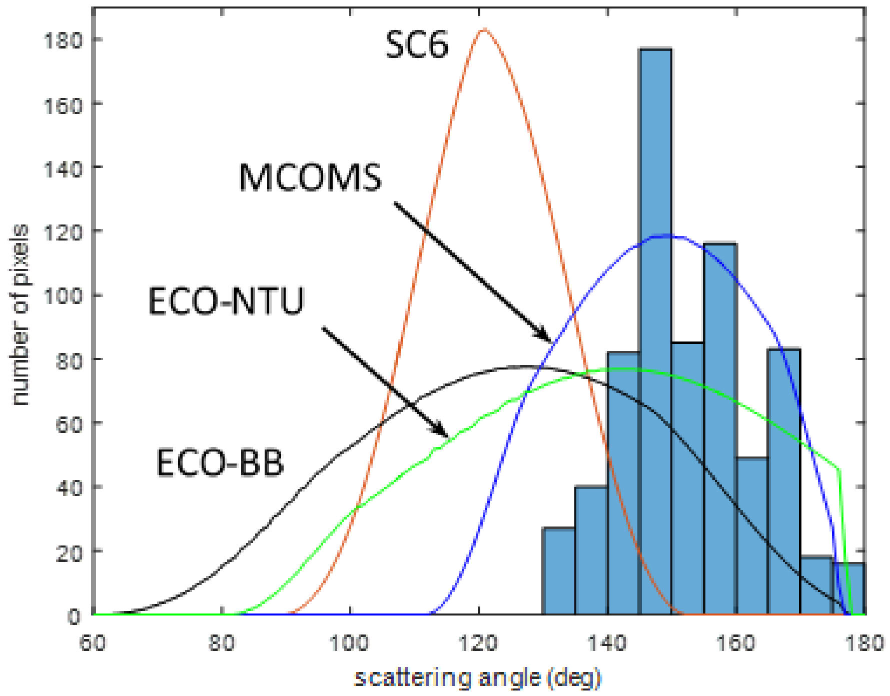

In-water single scattering angles from future PACE imager through an orbit

Analytical algorithm using VSF (ZTT)

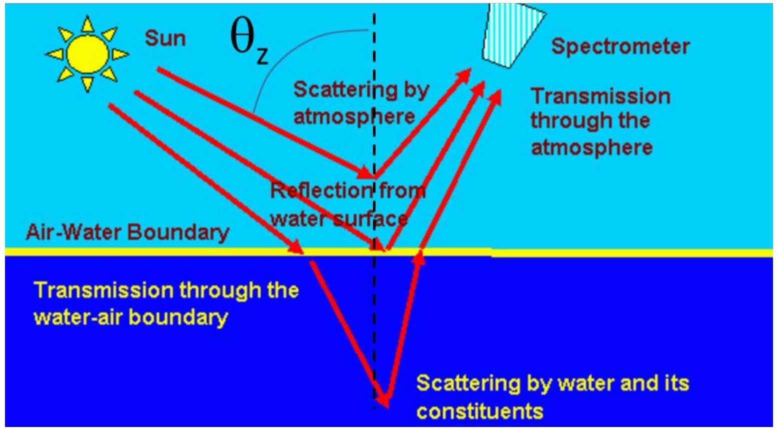

$$r_{RS}(\theta_s,\theta_v,\phi,V,a,b_b) \cong r_{RS,Raman}(\theta_s{}',a,b_b) + \frac{1}{\bar{\mu}_d\left(\theta_s',V,\frac{b_b}{a},\eta_{bb}\right)} \boxed{\frac{\beta(\gamma)}{b_b}} \left[\frac{a}{b_b}\left(1-\cos(\theta_v)\,\Psi_{K_{Lu}}(\theta_s{}')/\bar{\mu}_\infty\left(\frac{b_b}{a},\eta_{bb}\right)\right)+f_L(\theta_s,\theta_v,\phi)+\left(1-f_L(\theta_s,\theta_v,\phi)\right)\tilde{b}_b{}^{-1}\right]^{-1}$$

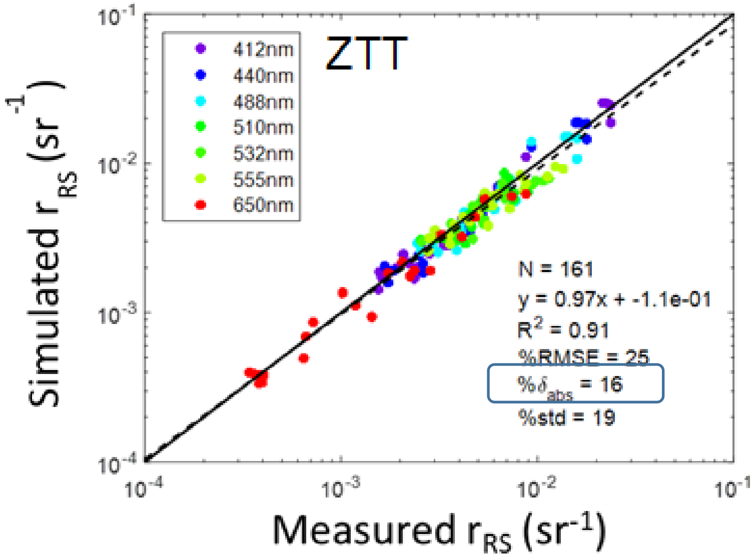

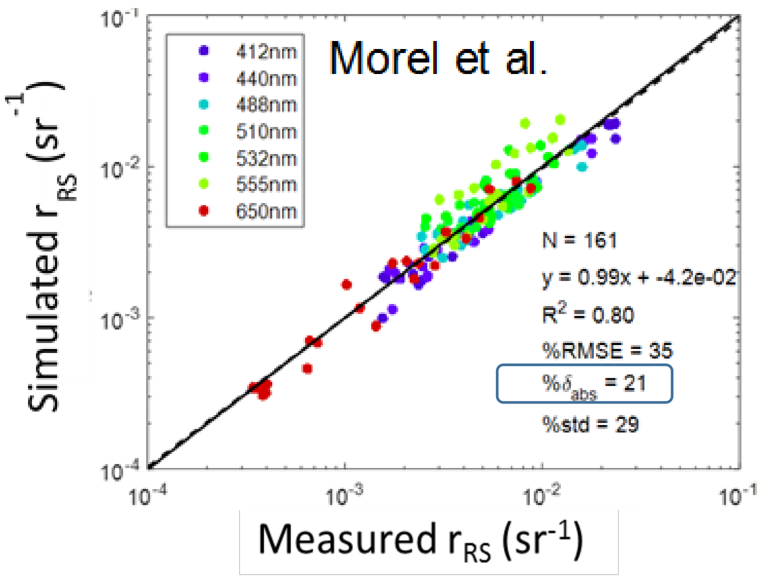

State-of-the-art LUT

constant β/b_b shape is assumed…

Twardowski and Tonizzo (in review)

SO MUCH TO DO…!

- Pure water: depolarization ratio (0.039, 0.051, 0.09 ….?)
- Pure seawater: effect of salts (only have Morel 1968 experiment)
- Spectral scattering:
  - hyperspectral bb
  - phase function shape
  - anomalous dispersion
- $\beta(180)$
- Scattering by nonspherical, complex particle populations
- Effect of scattering by nonrandomly oriented particles
- Anything to do with polarized scattering
- Ocean color algorithms from space that explicitly include VSF
- ….?